1987

A flow visualization study of laminar/turbulent transition in a curved channel.

Siedband, Marc A.

NAVAL POSTGRADUATE SCHOOL
Monterey, California

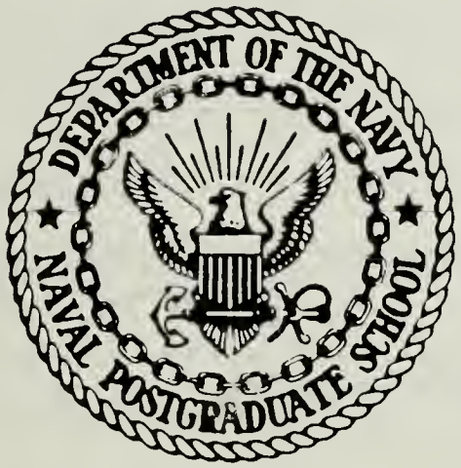

THESIS

A FLOW VISUALIZATION STUDY
OF LAMINAR/TURBULENT TRANSITION
IN A CURVED CHANNEL

by

Marc A. Siedband

March 1987

Thesis Advisor: Phillip M. Ligrani

Approved for public release; distribution is unlimited.

REPORT DOCUMENTATION PAGE

1a REPORT SECURITY CLASSIFICATION UNCLASSIFIED	1b RESTRICTIVE MARKINGS
2a SECURITY CLASSIFICATION AUTHORITY	3 DISTRIBUTION / AVAILABILITY OF REPORT Approved for public release; distribution is unlimited
2b DECLASSIFICATION / DOWNGRADING SCHEDULE	
4 PERFORMING ORGANIZATION REPORT NUMBER(S)	5 MONITORING ORGANIZATION REPORT NUMBER(S)
6a NAME OF PERFORMING ORGANIZATION Naval Postgraduate School 6b OFFICE SYMBOL (If applicable) Code 69	7a NAME OF MONITORING ORGANIZATION Naval Postgraduate School
6c ADDRESS (City, State, and ZIP Code) Monterey, California 93943-5000	7b ADDRESS (City, State, and ZIP Code) Monterey, California 93943-5000
8a NAME OF FUNDING / SPONSORING ORGANIZATION Propulsion Directorate 8b OFFICE SYMBOL (If applicable)	9 PROCUREMENT INSTRUMENT IDENTIFICATION NUMBER MIPR No. C-80019-F
8c ADDRESS (City, State, and ZIP Code) U. S. Army Aviation Res & Technology Activity-AVSCOM NASA-Lewis Research Center Cleveland, Ohio 45433	10 SOURCE OF FUNDING NUMBERS PROGRAM ELEMENT NO / PROJECT NO / TASK NO / WORK UNIT ACCESSION NO

11 TITLE (Include Security Classification)
A FLOW VISUALIZATION STUDY OF LAMINAR/TURBULENT TRANSITION IN A CURVED CHANNEL

12 PERSONAL AUTHOR(S)
Marc A. Siedband

13a TYPE OF REPORT	13b TIME COVERED	14 DATE OF REPORT (Year Month Day)	15 PAGE COUNT
Master's Thesis	FROM _____ TO _____	1987 March	126

16 SUPPLEMENTARY NOTATION

17 COSATI CODES			18 SUBJECT TERMS (Continue on reverse if necessary and identify by block number)
FIELD	GROUP	SUB-GROUP	Dean Vortices, Taylor-Gortler Vortices, Dean Number, Rectangular Curved Channel, Secondary

19 ABSTRACT (Continue on reverse if necessary and identify by block number)

Laminar/turbulent transition was studied as it occurs in a newly constructed curved channel of rectangular cross section. The channel is 1.27 centimeters high by 50.8 centimeters wide (0.5 in. x 20 in.), aspect ratio of 40 to 1, with a concave surface radius of curvature of 60.96 centimeters (24 in.). Mean velocities for air in the channel range from 1.40 to 3.89 m/sec, which corresponds to Dean number and hydraulic Reynolds number ranges of 167 to 461 and 2,231 to 6,173, respectively.

Flow visualization from a smoke wire shows changes in the behavior and appearance of a smoke trace illuminated in the radial plane with varying Dean number and varying channel location. In some cases, these smoke trace patterns show distortion similar to what would be expected

20 DISTRIBUTION / AVAILABILITY OF ABSTRACT XX UNCLASSIFIED/UNLIMITED ☐ SAME AS RPT ☐ DTIC USERS	21 ABSTRACT SECURITY CLASSIFICATION UNCLASSIFIED
22a NAME OF RESPONSIBLE INDIVIDUAL Phillip M. Ligrani	22b TELEPHONE (Include Area Code) (408) 646-3382 22c OFFICE SYMBOL 69Li

Item 18 Cont'd
Flow, Laminar Flow, Concave Curvature, Convex Curvature

Item 19 Cont'd
if pairs of counter-rotating vortices are present. A map of vortex stability as channel location and Dean number were varied was constructed from analysis of smoke trace photographs.

S N 0102-LF-014-6601

A Flow Visualization Study of Laminar/Turbulent Transition in a Curved Channel

by

Marc A. Siedband
Lieutenant Commander, United States Navy
B.S., United States Naval Academy, 1975

Submitted in partial fulfillment of the
requirements for the degree of

MASTER OF SCIENCE IN MECHANICAL ENGINEERING

from the

NAVAL POSTGRADUATE SCHOOL
March 1987

ABSTRACT

Laminar/turbulent transition was studied as it occurs in a newly constructed curved channel of rectangular cross section. The channel is 1.27 centimeters high by 50.8 centimeters wide (0.5 in. x 20 in.), aspect ratio of 40 to 1, with a concave surface radius of curvature of 60.96 centimeters (24 in.). Mean velocities for air in the channel range from 1.40 to 3.89 m/sec, which corresponds to Dean number and hydraulic Reynolds number ranges of 167 to 461 and 2,231 to 6,173, respectively.

Flow visualization from a smoke wire shows changes in the behavior and appearance of a smoke trace illuminated in the radial plane with varying Dean number and varying channel location. In some cases, these smoke trace patterns show distortion similar to what would be expected if pairs of counter-rotating vortices are present. A map of vortex stability as channel location and Dean number were varied was constructed from analysis of smoke trace photographs.

TABLE OF CONTENTS

LIST OF FIGURES

LIST OF SYMBOLS

Symbol	Meaning
A	Cross-sectional area of the channel
A_2	Cross-sectional area of the orifice
d	Channel height
d_w	Wire diameter
D	Pipe diameter
D_h	Hydraulic diameter
De	Dean number
K	Flow coefficient
L'	Development length for laminar flow
$\dot{m}$	Mass flow rate of air
P	Perimeter of the channel
P_1	Pressure 1-D upstream of the orifice
P_2	Pressure 1/2 D downstream of the orifice
P_{atm}	Atmospheric pressure
ΔP	Pressure change across the channel
ΔP_o	Pressure change across the orifice
Q	Volumetric flow rate
r_i	Radius of curvature of the convex channel surface
R	Gas constant for air
Re	Reynolds number, Ul/ν
Re_c	Reynolds number based on channel height, Ud/ν
Re_h	Reynolds number based on hydraulic diameter, UD_h/ν

Re_w	Reynolds number based on wire diameter, Ud_w/ν
Re_x	Reynolds number based on distance from start of curve, Ux/ν
T_1	Air temperature upstream of the orifice
U	Mean streamwise velocity
U_{max}	Maximum streamwise velocity
x	Distance from start of curve
Y	Expansion coefficient
Γ	Vortex circulation
ν	Kinematic viscosity of air
μ	Absolute viscosity
ϕ	Dimensionless parameter obtained from channel aspect ratio
ρ	Air density
ρ_1	Air density 1-D upstream of the orifice
ω	Vorticity

ACKNOWLEDGEMENT

The author wishes to express his appreciation to Professor Phillip M. Ligrani for his guidance throughout the execution of this project.

Special thanks are extended to model-makers Charles Crow and Willard Dames for their assistance in the assembly of the curved channel and various support equipment.

Finally, the author wishes to thank his wife Debbie and sons Michael and David for their encouragement and understanding during the course of this study.

This work was supported by the Propulsion Directorate, U.S. Army Aviation Research and Technology Activity - AVSCOM, located at the Lewis Research Center of NASA. Dr. Kestutis Civinskas is the program manager.

I. INTRODUCTION

A. BACKGROUND AND LITERATURE REVIEW

Since the early part of this century, it has been well known that fully developed laminar flow along a concave wall does not maintain a simple two dimensional (i.e. parabolic) velocity profile. Instead, a series of counter-rotating vortex pairs form as a result of varying centrifugal forces acting on the fluid particles. These vortices were first considered analytically by W.R. Dean in 1928 for flow in a narrow channel formed by two concentric cylinders [Ref. 1] and are similar to ones observed by Taylor and Görtler [Refs. 2, 3]. Figure 1 [Ref. 4] is a schematic of Dean vortices in a curved channel. These vortices are known to enhance heat transfer on curved channel surfaces for both laminar and turbulent flows. Understanding such flows is expected to lead to design improvements for heat exchangers and configurations used to cool gas turbine blades and vanes.

Vortex onset and development is dependent upon the magnitude of the curvature, as expressed by the Dean number, where $De = Re_c\sqrt{d/r_i}$. Here the channel Reynolds number is defined by $Re_c = Ud/\nu$, where U is the mean streamwise velocity, d is the channel height, r_i is the radius of curvature of the convex channel surface, and ν is the kinematic viscosity.

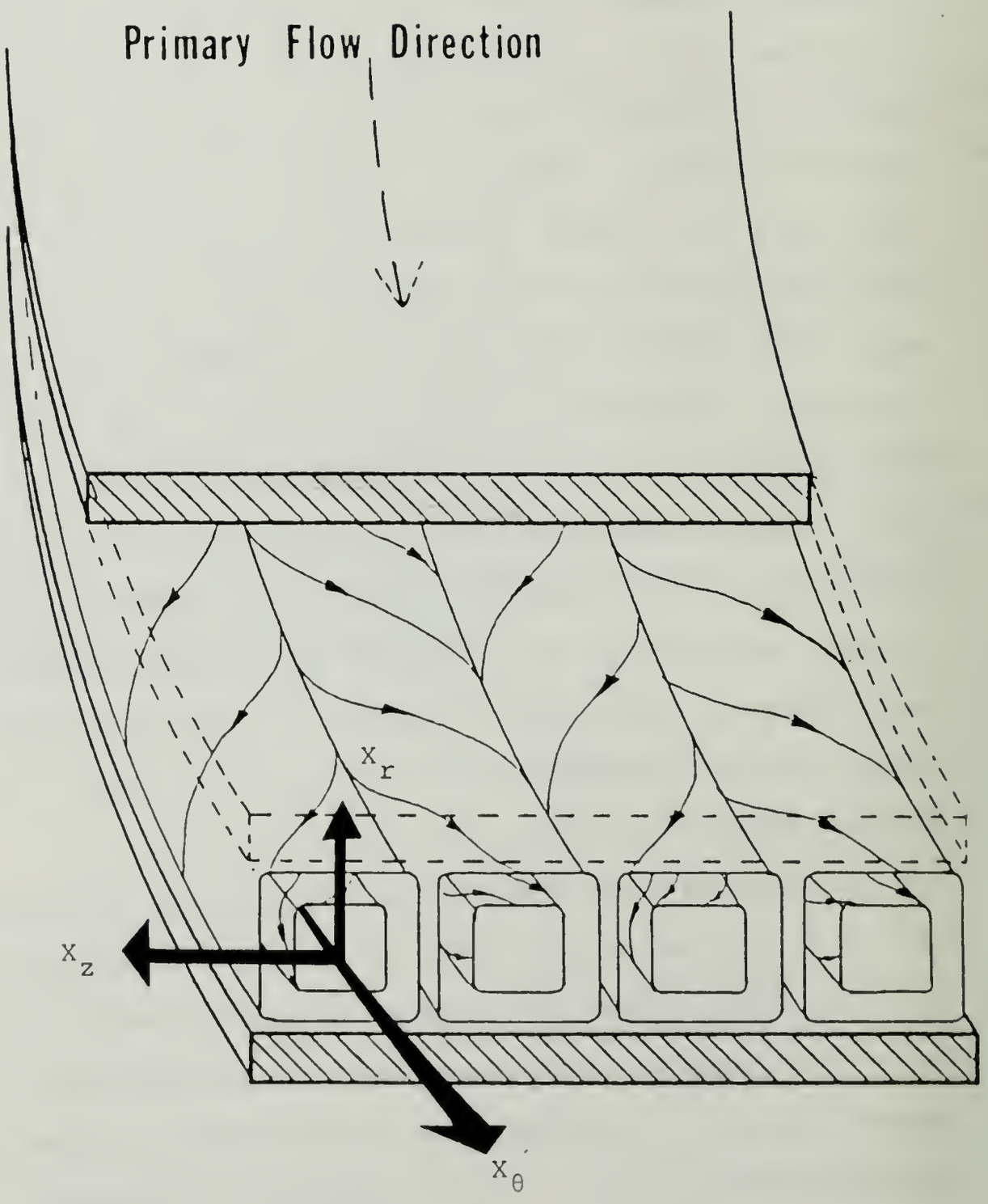

Figure 1. Schematic of Dean vortices in a curved channel.

For a rectangular channel curved in the streamwise direction, the flow at sufficiently low Dean numbers is entirely azimuthal. This is known as slug flow or Poiseuille flow. Above a critical Dean Number ($De > 36.6$), pure laminar flow becomes unstable and the secondary flow discussed above occurs. This is due to the fact that fluid particles in the center of the flow profile are travelling at higher velocities and are therefore subjected to higher centrifugal forces than those closer to the walls. The faster moving particles move outward toward the concave wall, forcing the fluid particles there to move inward toward the center of the channel where velocities are higher. The process repeats itself and the Dean vortices form. (The critical Dean number and the Dean numbers discussed below are the result of computer simulations using the Navier-Stokes equations being performed at Stanford University.) As the Dean number is raised further ($De > 45$), the vortices oscillate at low frequency (large wavelength) as they travel in the streamwise direction. The wavelength becomes smaller up to a Dean number of about 75. At even higher Dean numbers ($75 < De < 500$ to 600), unpublished simulation results (presently unconfirmed by experiments) show that these vortices have an oscillatory, rocking type of motion as they are convected. Ultimately, these complex secondary flow fields break down into turbulent flow.

A brief history of earlier research into the flow and heat transfer characteristics of flow in a curved channel can be found in reference 4. The presence of Dean vortices in a

curved channel of aspect ratio 40 was confirmed at the Naval Postgraduate School by R. McKee in 1973 [Ref. 5]. Modifying McKee's channel and modeling it as a pair of infinite parallel plates with the outer wall heated and the inner wall adiabatic, M. Durao and J. Ballard [Refs. 6, 7] studied the effect of Dean vortices on heat transfer for laminar flows in straight and curved rectangular channels. Research continued in 1981 by R. Holihan, Jr. [Ref.4] for laminar transition flows, S. Daughety [Ref. 8] for turbulent flows, and J. Wilson [Ref. 9] for transition and turbulent flows. Each of these studies used McKee's apparatus, which was modified each time to improve the accuracy of the results. In 1985, using a new curved channel designed for even more precise measurements, heat transfer studies by G. Galyo [Ref. 10] were conducted for turbulent flow.

Kelleher, Flentie, and McKee [Ref. 11] reported results of velocity surveys and flow visualization for the secondary flow in a curved channel half the size of the facility used in the current study. Velocity profiles were presented for Dean numbers of 79.2, 94.9, and 113.5. Flow visualization was performed using an aerosol mist (DOP) for Dean numbers of 69.3 and 77.2. It was shown that the velocity profiles on the convex side of the channel mid-plane were 180 degrees out of phase with those on the concave side. Also shown was the fact that the vortices covered the full width of the channel from

the convex to the concave wall and that channel geometry and not the Reynolds number controlled vortex size.

The numerical simulations of the Navier-Stokes equations for Taylor-Görtler vortices performed by Finlay, Keller, and Ferziger [Ref. 12] describe changes in the vortex pattern which occur as the Dean number and wave number are varied. Also obtained are the vortex strengths and growth rates of the Taylor-Gortler vortices. In addition to the results discussed in paragraph 3 above, this study also provided evidence of a small pair of secondary vortices developing adjacent to the convex wall for De = 80.0 and De = 100.0.

B. OBJECTIVES

The first objective of this investigation was to design and implement the operation of a sufficiently large curved rectangular duct to perform high quality flow visualization studies of Dean vortices. The test facility was to have the same aspect ratio (40 : 1) as previous investigations [Refs. 4 through 10], but with all dimensions scaled up by a factor of two. The aspect ratio is defined as the channel spanwise dimension divided by the channel height.

After the channel was in operation, the objectives were:

1. to obtain information on the flow behavior at various Dean numbers and various streamwise and spanwise locations within the curved channel,
2. to study the development of fluid path lines produced by a smoke wire as they are distorted and convected by the flow, and
3. to produce stability maps for laminar-to turbulent transition and vortex development.

The purposes of the results of the study are:

1. to obtain better understanding of fluid mechanics phenomena which affect heat transfer in a channel where streamwise curvature and strong secondary flows are present, and
2. to provide a basis of comparison and validation for computer simulations using the Navier-Stokes equations with appropriate boundary conditions.

C. THESIS ORGANIZATION

Subsequent to the introduction, this thesis describes the experimental facilities, detailing the specifications and characteristics of each component. Next, experimental techniques are discussed, including channel operation, flow visualization, photography, and measurement and calibration methods. Finally, experimental results and conclusions are presented.

II. EXPERIMENTAL FACILITIES

A. CURVED CHANNEL

A schematic of the curved channel test facility is shown in Figure 2. Figures 3 and 4 are front and side views of the actual channel.

The lip at the entry of the inlet section is constructed of quarter circumference sections of six inch outside diameter pipe. Following this is the 25.4 cm by 50.8 cm (10 in. x 20 in.) rectangular inlet section, consisting of a honeycomb followed by three screens stretched across the inlet channel cross section. The screens were pulled taut prior to tightening the flange bolts. This ensured that the screens were flat and perpendicular to the flow direction. The aluminum honeycomb is 3.81 cm (1.5 in.) deep (streamwise direction) and consists of hexagonal cells approximately 0.635 cm (0.25 in.) across. The fiberglass window screen has a square weave with about 0.159 cm (0.0625 in.) between strands. These items are intended to reduce spatial non-uniformities of the air entering the nozzle, resulting in more stable laminar flow. Distance between each screen or between the honeycomb and the next screen is approximately 10 cm (4 in.), following suggestions on design rules for small low speed wind tunnels provided in reference 13.

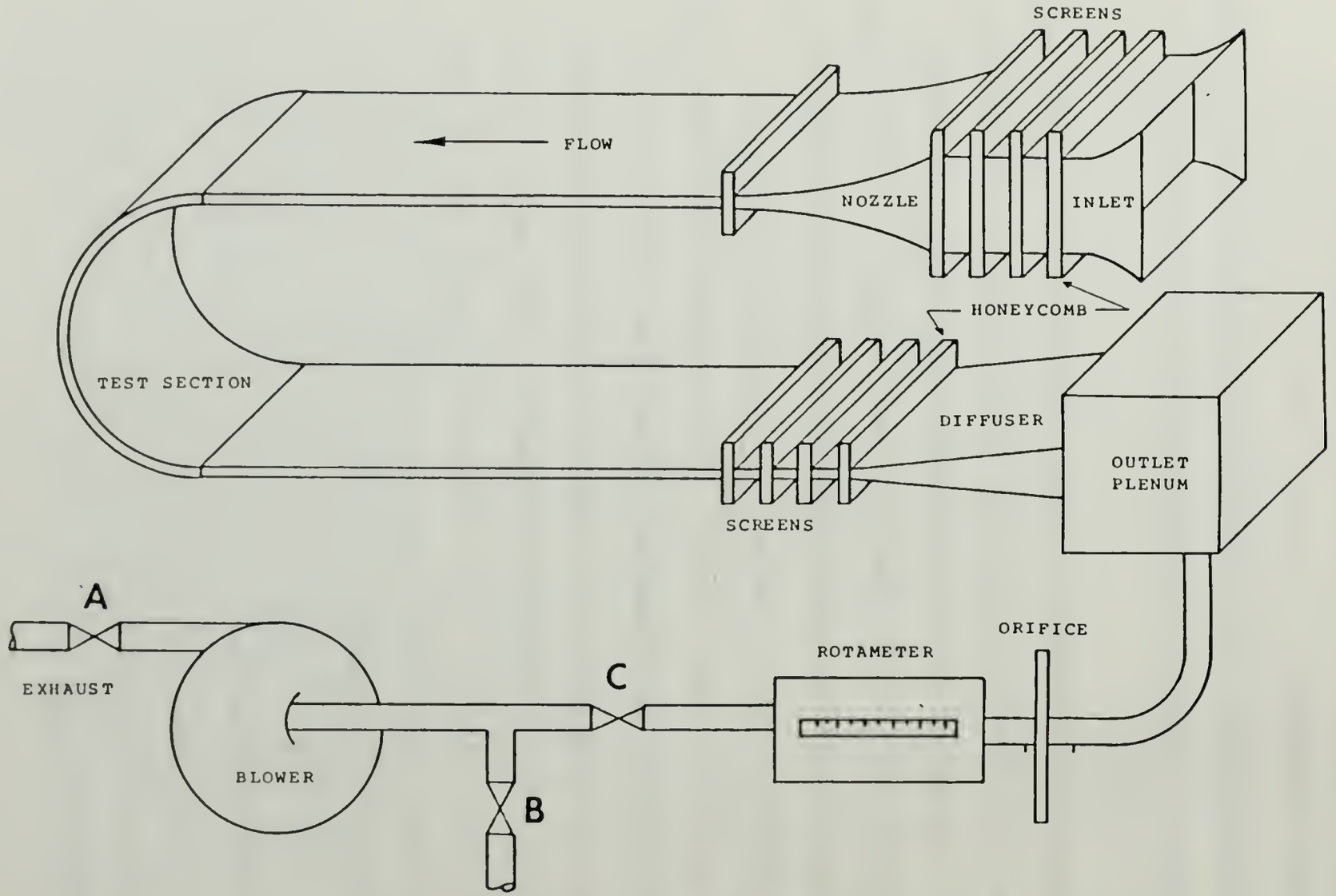

Figure 2. Schematic of test facility.

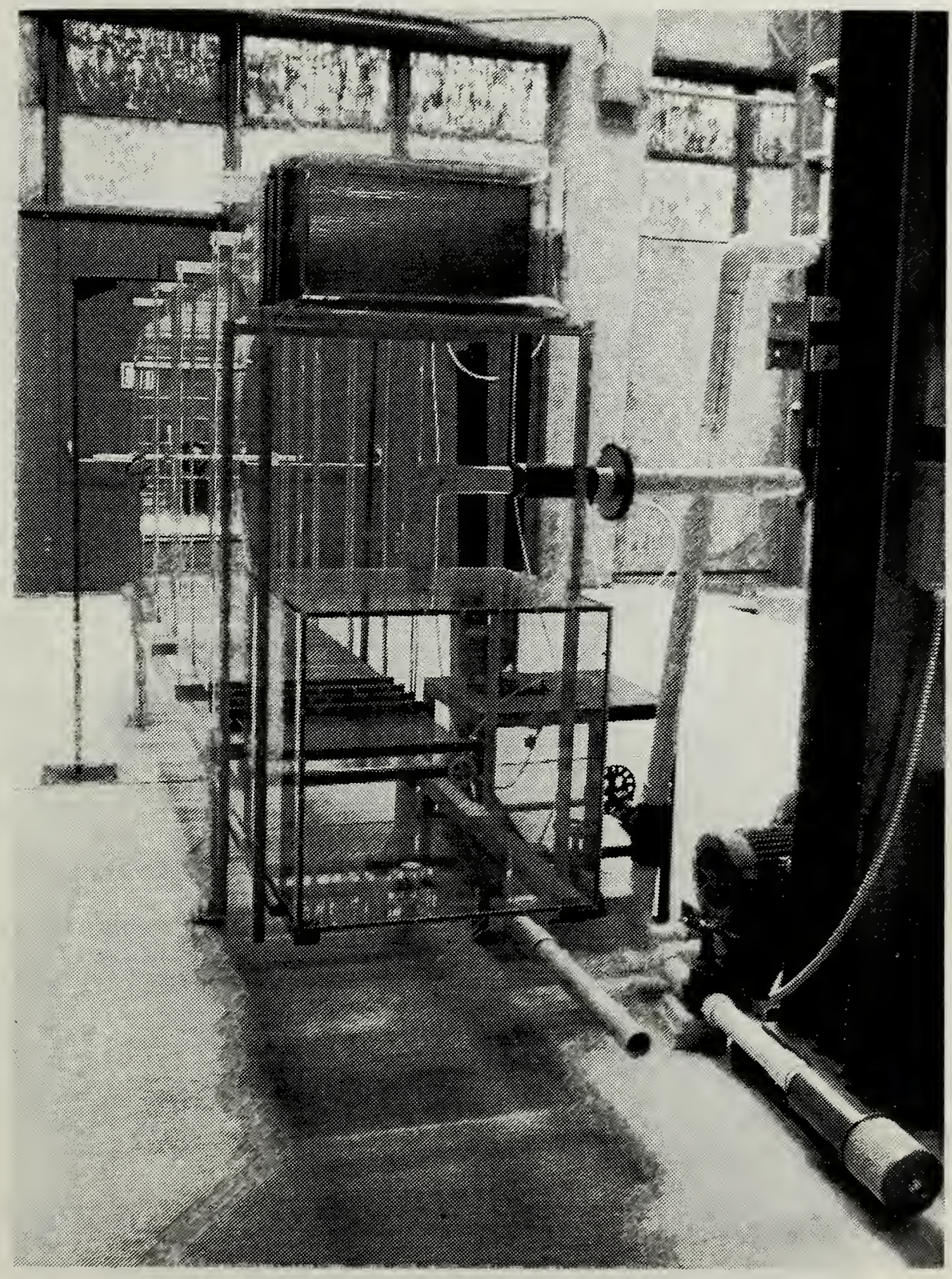

Figure 3. Test facility (front view).

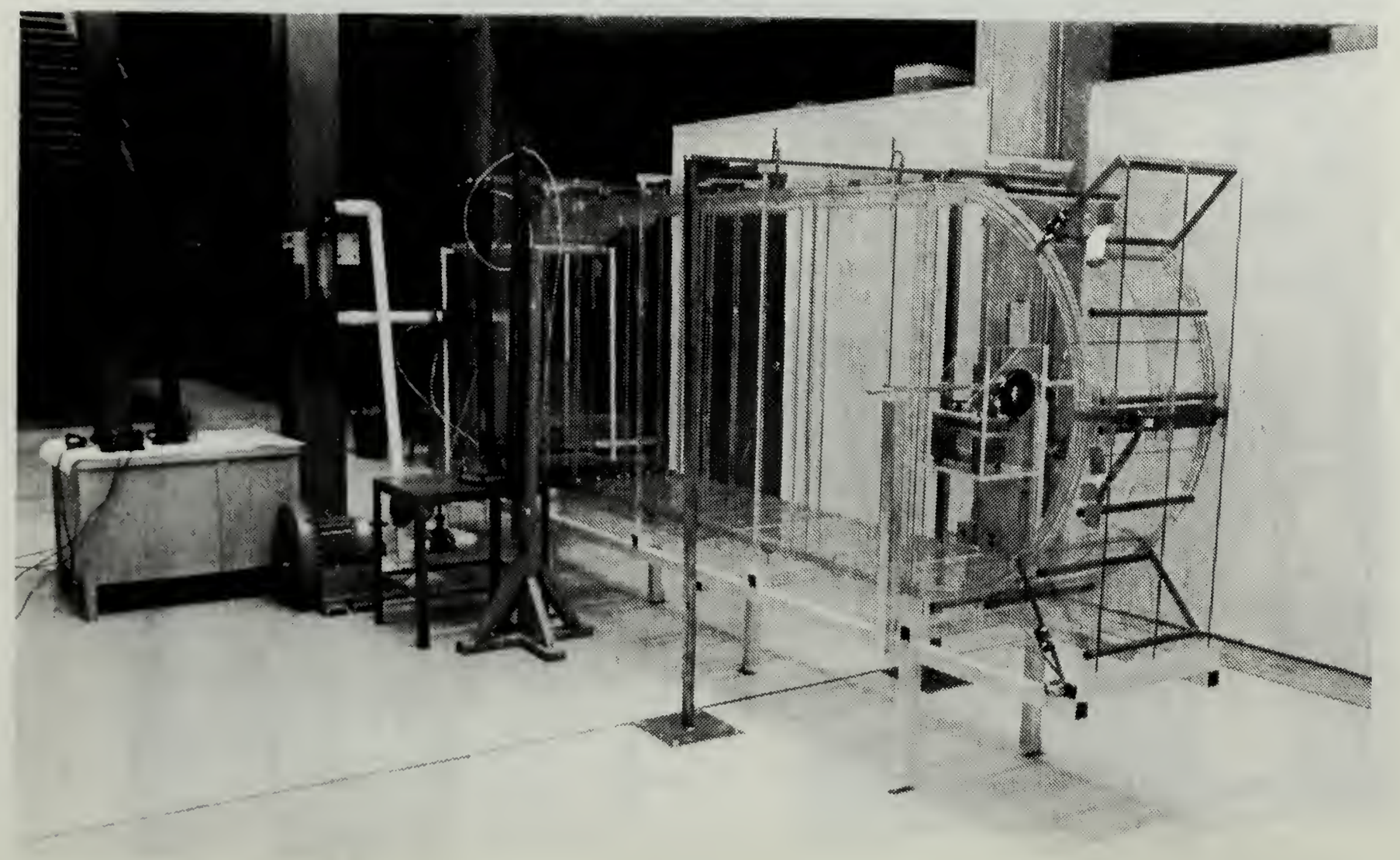

Figure 4. Test facility (side view).

The air next enters a two dimensional nozzle with a 20 to 1 contraction ratio. Designed using a fifth order polynomial to ensure continuous first through fourth order derivatives, nozzle dimensions were chosen to minimize the possibility of separation near the nozzle exit and to prevent laminar-to-turbulent transition. Figure 5 shows a graph of the design. This nozzle induces longitudinal strain on the flow, stretching it to further reduce spatial non-uniformities which may exist. To prevent tripping the flow at the critical point where it enters the duct, elaborate measures were taken to ensure that the seam between the nozzle and the duct straight section was smooth. Specifically, the mating surface between the nozzle and duct flanges was filled with automotive body putty (Bondo) and sanded smooth to the touch, ensuring that any discontinuity (step) inside the duct was less than 0.001 inches.

After the nozzle, the air passes through a 2.44 m (8 ft.) long straight duct. The duct inside dimensions are 1.27 cm by 50.8 cm (0.5 in. x 20 in.). This cross section is constant until the air reaches the diffuser in the outlet section. According to reference 14, fully developed laminar flow will exist for hydraulic Reynolds numbers up to 6,068 (Dean numbers up to 454) at the end of the straight duct (i.e. entry to the curved channel). The corresponding mean velocity is about 3.82 m/s. The flow is considered to be fully developed when normalized mean velocity profiles are self-similar. Appendix A

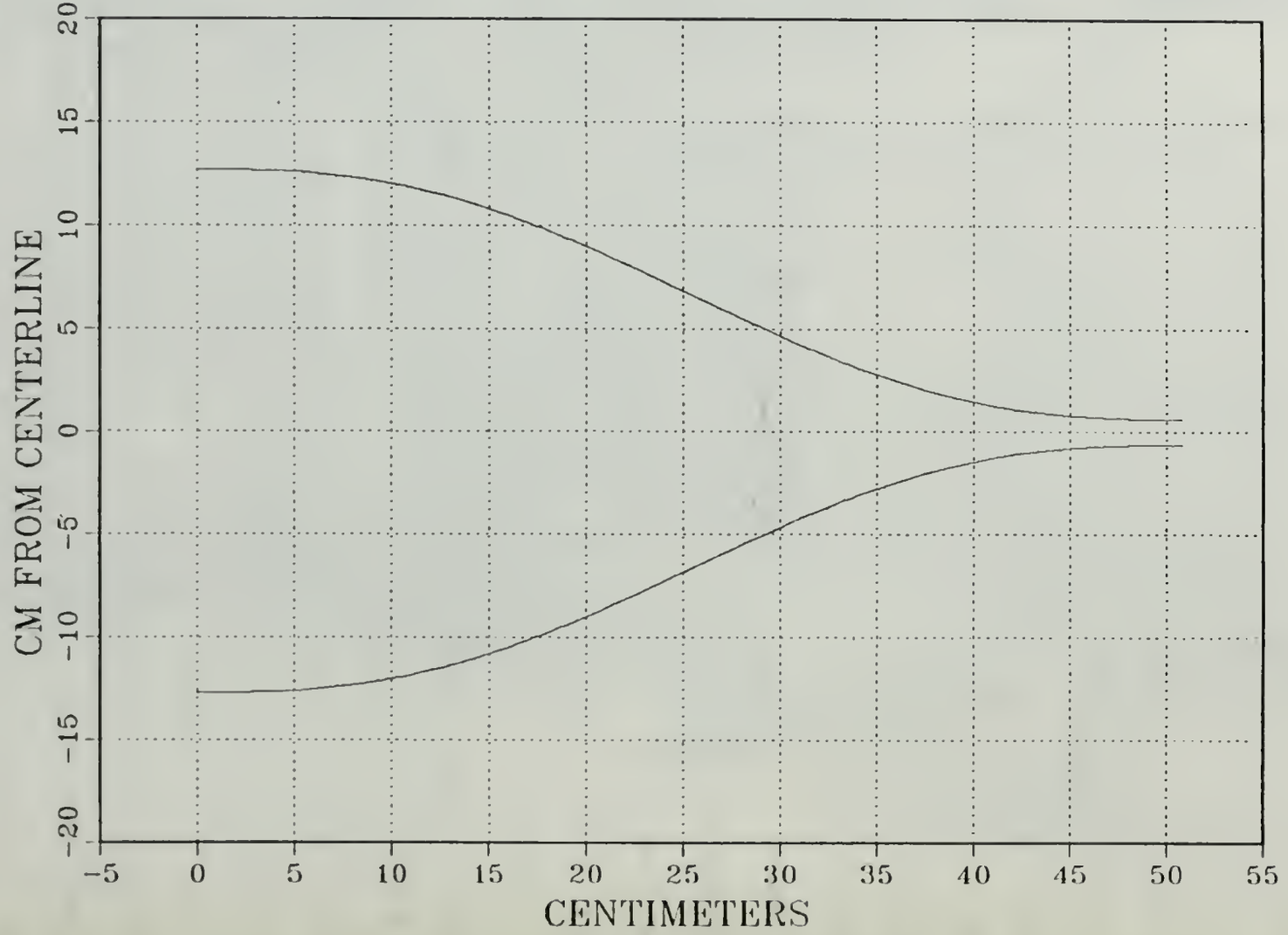

Figure 5. Graph of inlet nozzle design.

(section 1) shows the sample calculations using the Langhaar equation [Ref. 14] for development length in tubes and reference 15 for development length between flat plates. The Langhaar equation is shown to be the more conservative of the two.

The fully developed laminar flow next enters the curved test section. Here the duct has the same rectangular cross section as the straight section. The concave interior duct surface has a radius of curvature of 60.96 cm (2 ft.) and the convex surface has a radius of curvature of 59.69 cm (23.5 in.). To maintain these radii of curvature, the curved test section is pulled tightly into the circular support frame using band clamps (visible in Figure 4). Holes exist at various side wall locations for the installation of smoke wires. These wires are pulled taut in the spanwise direction in the channel.

The air exits the curved section, goes through another eight foot long straight duct, and reaches the outlet section. At the exit of the second straight section are four screens, a honeycomb, a diffuser, and an outlet plenum. The screens and honeycomb were designed to minimize the effects of any spatial non-uniformities in the outlet plenum. Because of the small channel height, honeycomb was made of plastic straws, 0.41 cm (0.16 in.) in diameter and 3.18 cm (1.25 in.) long, stacked firmly together. The 45.7 cm (1.5 ft.) long diffuser, having a total angle of three degrees, is used to provide some pressure recovery. The design, which uses the guidance provided in

reference 16, minimizes the possibility of stall in the diffuser. The cubic outlet plenum (61 cm on each side) is intended to create a volume of nearly stagnant air at uniform pressure.

The plenum is connected to the suction of a blower via a rotameter (125 cfm full scale) and a one inch standard ASME orifice plate shown in Figure 6. These are used for volumetric flow indication and calibration, respectively. Various valves are used to control the flow rate, and therefore the mean velocity and Dean number, in the curved channel. The blower exhaust valve is a two inch brass gate valve, while the other two valves shown in Figure 2 are two inch brass globe valves. Pipe used to connect the outlet plenum to the blower, valves, rotameter, and orifice is standard two inch PVC pipe.

Both the curved and straight sections of the duct are made of polycarbonate (Lexan). This material was chosen because it is transparent and flexible, as well as being easy to join and machine. To minimize the potential for flow tripping, both the upper and lower walls of the channel sections (straight/curved/straight) are made of three pieces of Lexan sheet bonded together in one continuous piece, so that no seams were present. Side wall, longitudinal, and cross-beam supports are employed, so that the inside dimensions of the entire channel at any streamwise location from the nozzle exit to the last straight section are approximately 0.5 $\pm$ 0.005 inches by 20.0 $\pm$ 0.020 inches. The top and bottom surfaces of the channel are secured to the side

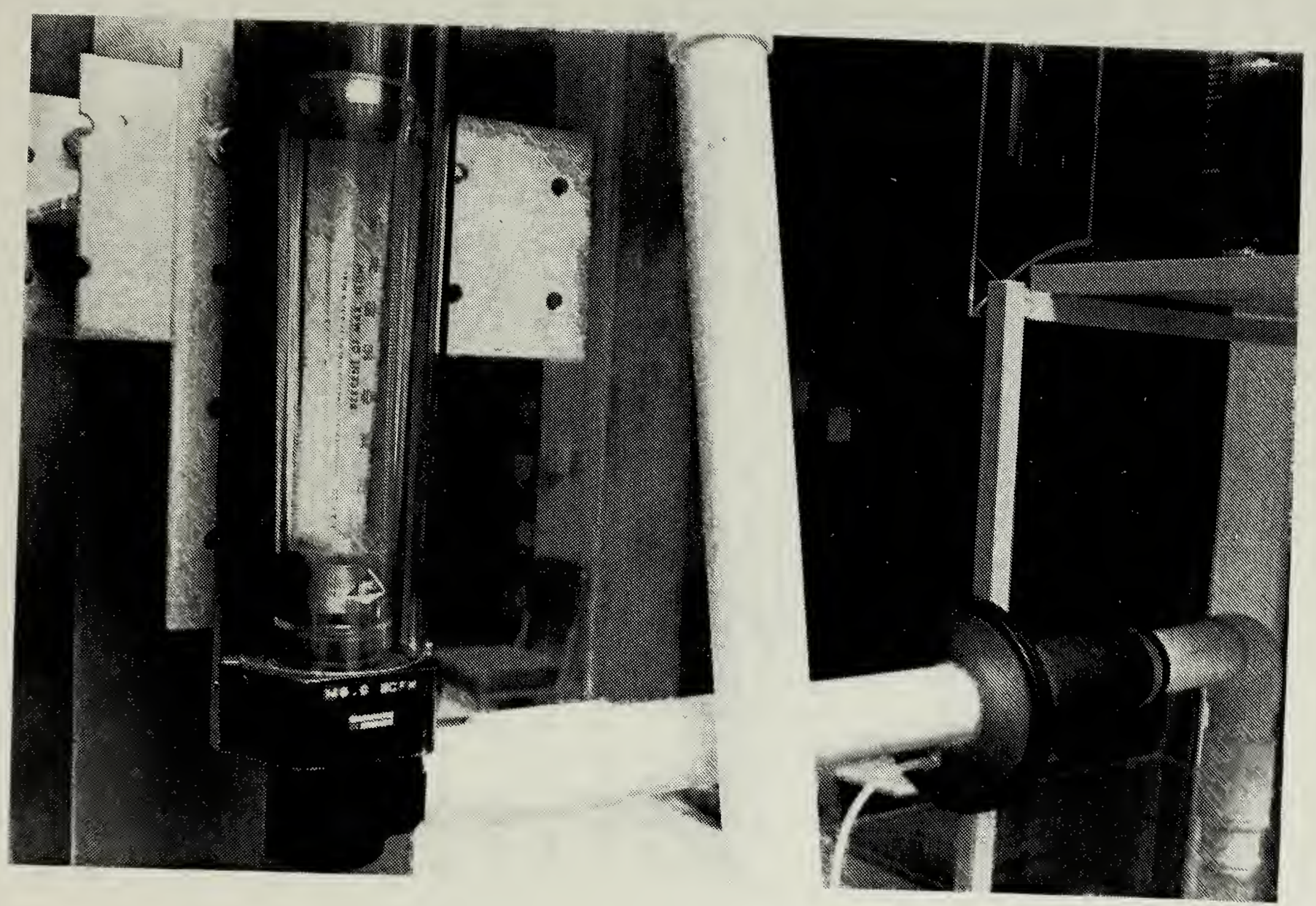

Figure 6. Photograph of rotameter and orifice plate.

walls as shown in Figure 7. Set screws in the wall segments are spaced about 10 cm (4 in.) apart. Wall segments are removable to facilitate cleaning of channel interior surfaces. Mating surfaces between wall segments and all flange mating surfaces (except for the nozzle flange) are sealed with 3-M foam tape. Construction of the steel support frame and all Lexan portions of the test facility was performed by McNeal Enterprises, Inc. of Santa Clara, California.

B. BLOWER

To provide a low pressure region at the outlet plenum, a Spencer VB-0370-E Vortex Blower is used. This blower is capable of producing about 60 inches of water vacuum at 140 cfm and was sized by scaling flow behavior from a channel with half the dimensions of the present one. Figure 8 shows the advertised blower performance curve and system curves. As can be seen in the figure, the blower exceeds the head requirements of the duct and must be throttled to achieve the desired flow rates. Appendix A (section 2) provides the sample calculations used in scaling system performance to determine required blower size.

C. SMOKE WIRE

Flow visualization is provided by smoke wires strung in the transverse direction at various locations in the curved section, as shown in Figure 9. (One wire is used at a time.)

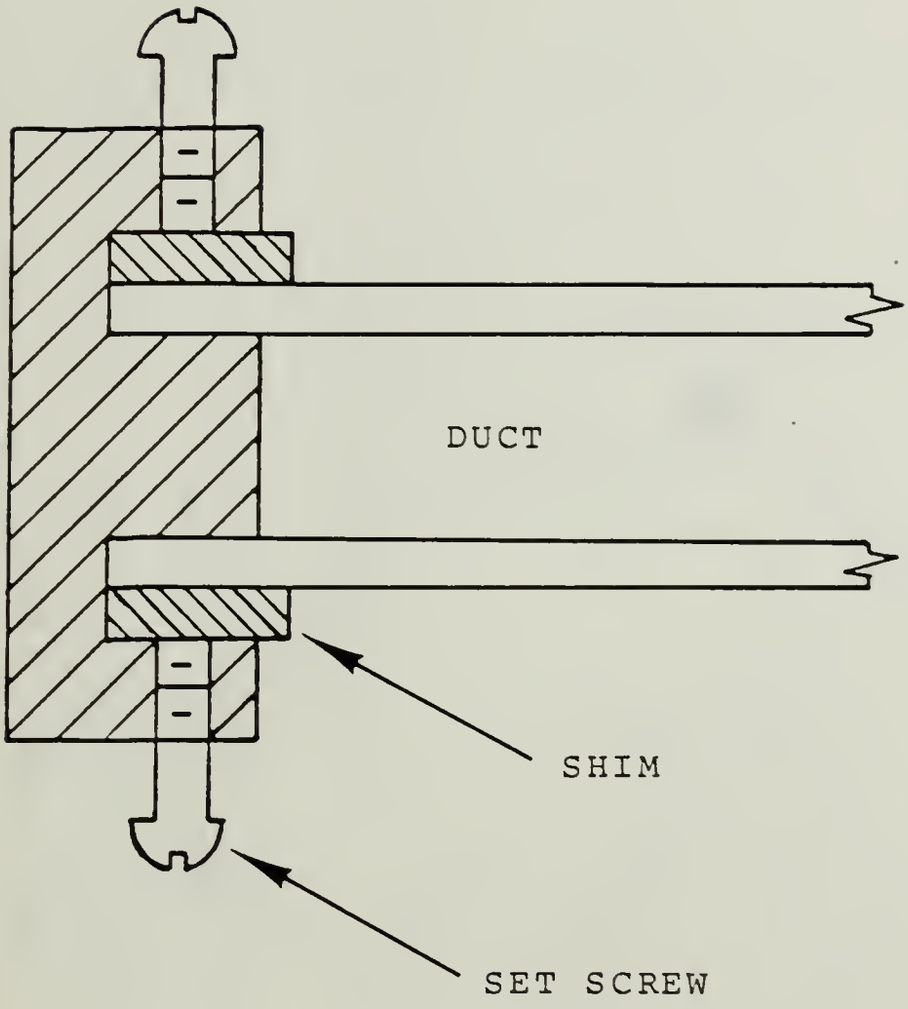

Figure 7. Duct side wall design.

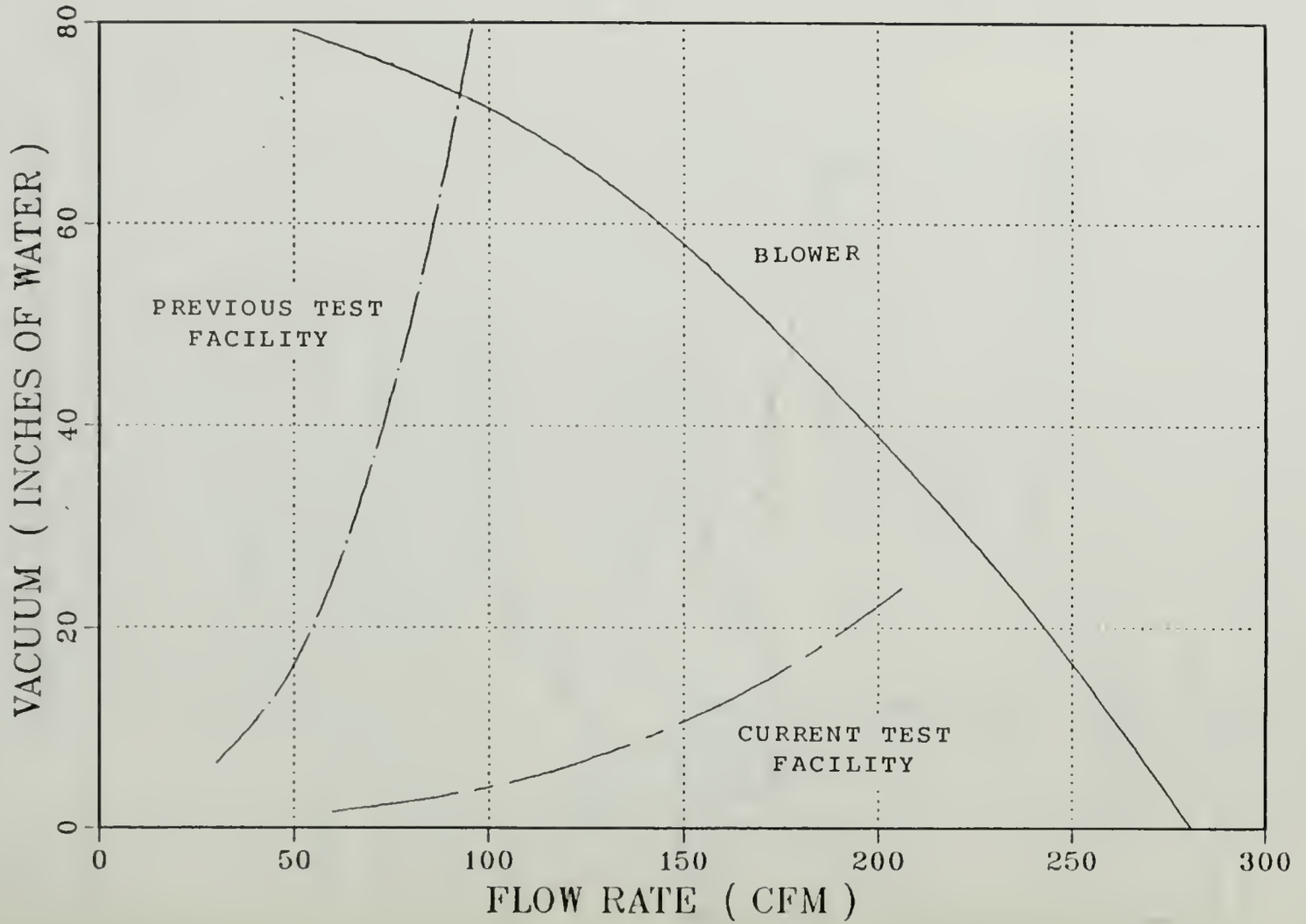

Figure 8. Blower performance and system curves.

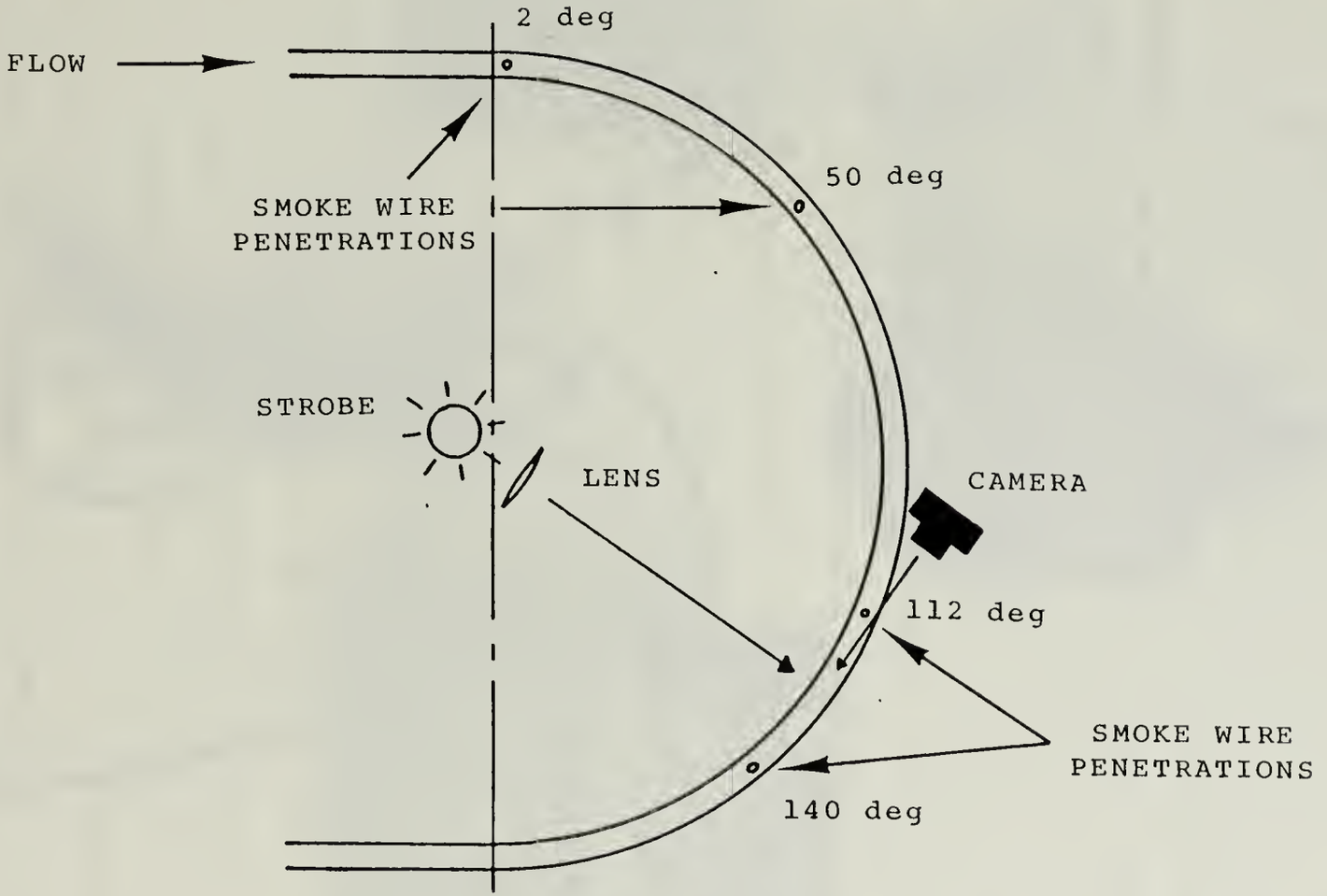

Figure 9. Schematic of smoke wire, strobe, and camera placement.

Because of the short delay between energizing the wire, smoke production, and arrival of that smoke a small distance downstream where it is photographed, a timing control system was used. The control device, manufactured by Flow Visualization Systems of Bolingbrook, Illinois, energizes the stainless steel smoke wire and, after a manually selected delay, triggers the strobe. Voltage applied to the wire is controlled by a Calrad 45-740 (0-130 VAC) variac. Figure 10 is a photograph of the control system. The delay time selected depends upon the mean velocity (i.e. Dean number) in the duct and was adjusted by trial and error. Of note is the fact that the two potentiometers on the control system which control wire "on time" and strobe delay time do not operate independently. As shown in Figure 11, the sequencing circuit timing diagram, the following events occur during one flow visualization run: the wire is energized, an adjustable time delay occurs, and simultaneously, the wire is turned off and the strobe is flashed. If the smoke wire "on time" selected is shorter than the strobe delay time chosen, the flash of the strobe will not occur.

Maximum wire diameter selected is based on a wire Reynolds number (Re_w) of 35 as discussed in reference 17. This Reynolds number is based on wire diameter. Higher Reynolds numbers may result in separation and an unstable wake behind the wire. Sample calculations are shown in Appendix A (section 3).

Wires penetrate the side wall segments of the test section through small (4.29 mm diameter) drilled holes. Pressed into

Figure 10. Photograph of smoke wire/strobe control system.

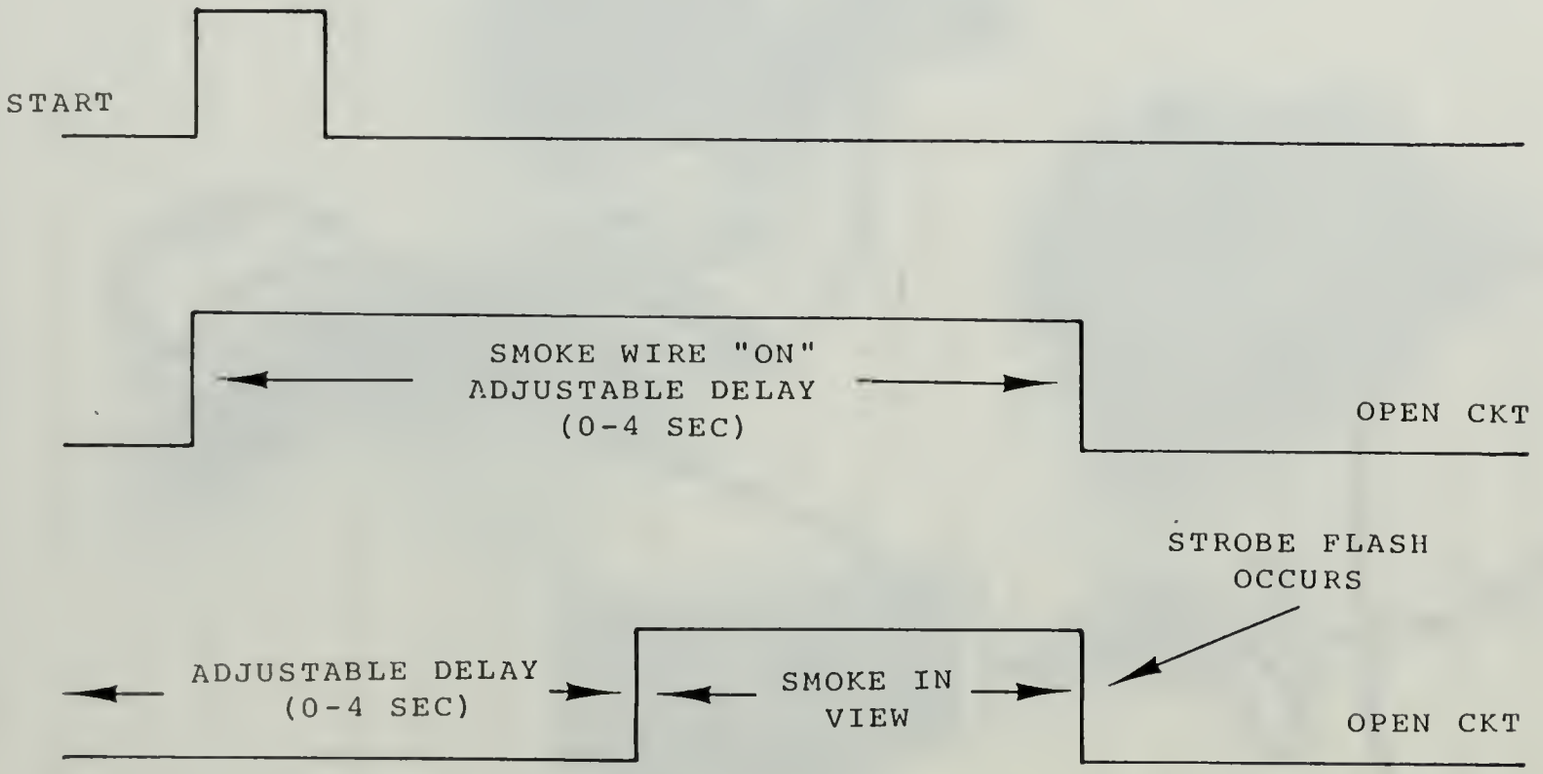

Figure 11. Smoke wire sequencing circuit timing diagram.

each hole is a small ceramic bead (bead hole diameter equal to 1.75 mm) which prevents the energized wire from burning into the Lexan side wall. To prevent air leakage through these holes, "CLAYOLA" non-hardening modeling clay is pressed flat, forming a patch, over each hole. Smoke wire holes are located at 2, 50, 112, and 140 degrees from the entry of the circular test section as shown in Figure 9.

D. LIGHTING

The strobe is a General Radio type 1531-A Strobotac, which is externally triggered. For the high intensity single flash operation used in this study, the peak light intensity is 7 million beam candle power. Flash duration is approximately 3 microseconds. The strobe, which is normally used to determine the speed of rotating equipment, can also provide more continuous illumination if flashed repeatedly at high frequency. The collumator lens is a 75mm (focal length), f1.1 Rodenstock-XR-Heligon mounted directly in front of the strobe as shown in Figure 12. The entire assembly can be pivoted and clamped in place to illuminate any point on the test section. Since the arc produced by the strobe lamp is almost a straight line, the lens produces a well collumated flat sheet of light through the channel.

To prevent undesired light reflections, the outer surface of the curved channel facing the strobe is lined with black construction paper (poster board). (Not shown in Figures 3 and

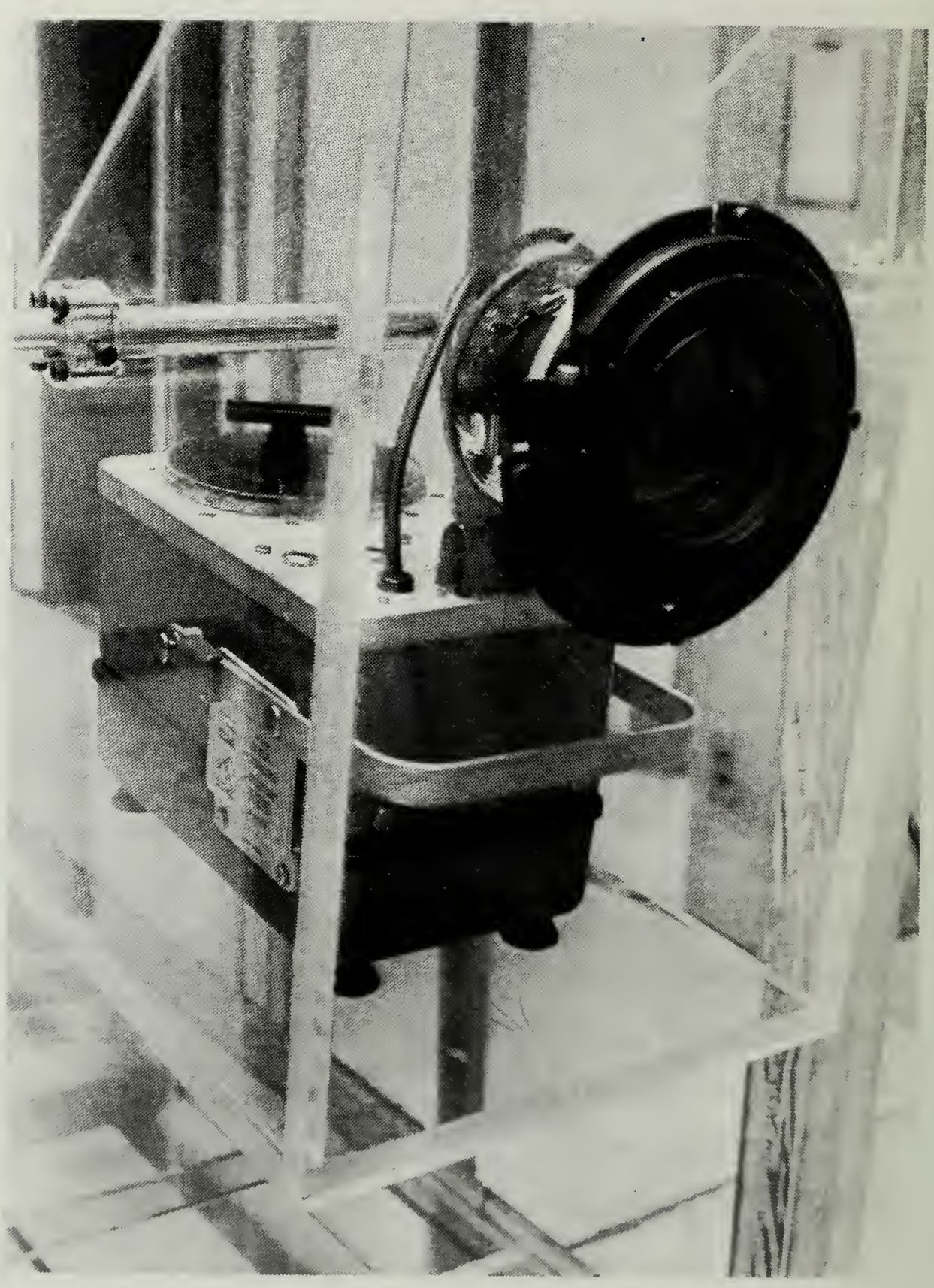

Figure 12. Photograph of strobe and collumator lens.

4.) Slits are cut two to ten inches downstream of each smoke wire to provide a path for the collimated light to illuminate a radial plane. To provide a basis for comparison, all slits are 2 mm by 4.6 cm (0.08 in x 1.8 in.) and are located so that the center of the slit is located 4.83 cm from the center of the channel.

E. CAMERA

A Nikon F-3 with a 55mm, f2.8 lens was used to record the flow pattern. Kodak Tri-X (ASA 400) or Kodak Recording Film 2475 (ASA 1000) was used. As shown in Figure 9, the camera views the illuminated plane of smoke particles at approximately a ninety degree angle to the beam of collumated light.

III. EXPERIMENTAL TECHNIQUE

A. CHANNEL OPERATION

In order to provide a variety of flow conditions for analysis in this study, duct flow rate (i.e. the Dean number) must be varied. Start-up of the channel and flow rate control are now described.

To initiate flow through the duct, the blower exhaust and inlet bypass valves ('A' and 'B' in Figure 2, respectively) are verified open and the duct outlet valve ('C') is checked shut. The blower is started and the duct outlet valve is opened. A reading of 29 percent on the rotameter can be achieved with all valves fully open. (Section III.B discusses rotameter calibration and indication.) It is necessary to throttle both the blower exhaust valve and the duct outlet valve to avoid unsteadiness (possibly due to slight blower stall) when operating at very low flow rates (i.e. less than 15% indicated flow). Failure to sufficiently throttle the blower exhaust valve results in severe oscillation of the rotameter float. Flow rates higher than 29 percent are achieved by throttling the blower inlet bypass valve, while valves 'A' and 'C' remain open. A maximum of 63 percent indicated flow through the duct can be achieved when the inlet bypass valve is completely shut. Higher flow rates (up to about 80%) can be achieved if the orifice plate is removed.

B. FLOW RATE MEASUREMENTS

Rotameter calibration was achieved by using a one inch diameter steel orifice, machined to ASME specifications, which was installed upstream of the rotameter. Orifice pressure taps were located at the 1-D upstream and 1/2-D downstream positions, where 'D' is the PVC pipe diameter (nominally 2 inches). Appendix A (Section 4) provides the data and sample calculations for rotameter calibration. References 18 and 19 were utilized in these calculations. Data was taken at an ambient pressure of 30.26 inches of mercury and an air temperature of 65°F (approx.).

As shown in Figure 13, rotameter indication is a linear function of volumetric flow rate. The equations to convert from rotameter indication (percent) to flow rate (cfm), to Dean number, and to Reynolds number are shown below. Appendix A (section 5) provides the sample calculations for these results.

$$Q\ [cfm] = 1.15\ X\ (ROTAMETER\ \%\ FLOW) + 10$$

$$De = 9.99\ X\ (ROTAMETER\ \%\ FLOW) + 86.87$$

$$Re_c = 68.49\ X\ (ROTAMETER\ \%\ FLOW) + 595.53$$

C. FLOW VISUALIZATION/PHOTOGRAPHY

The flow visualization method is similar to that described in reference 20. The method described here is for still photography of the smoke patterns.

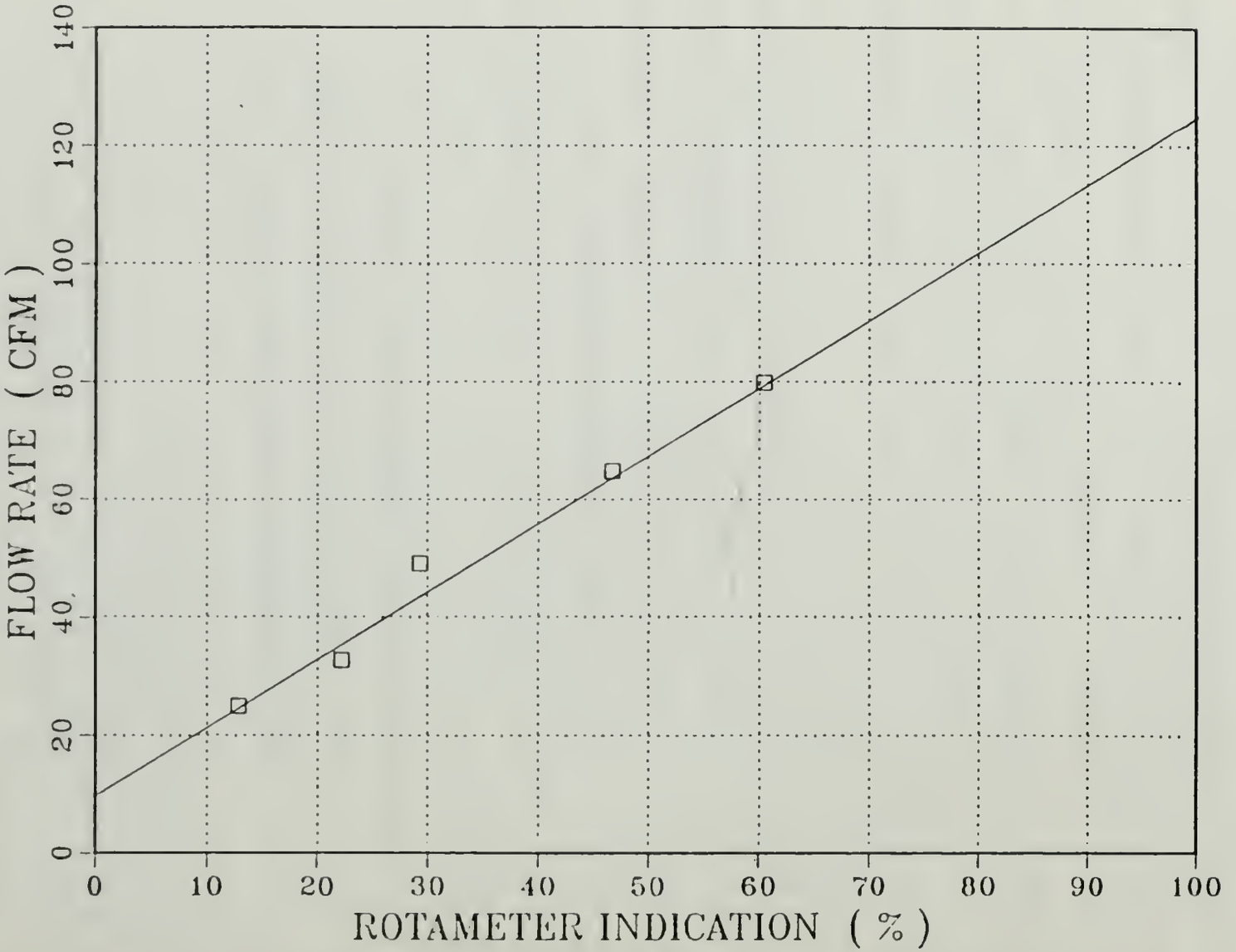

Figure 13. Rotameter calibration results.

To generate an adequate amount of smoke, the smoke wires must be frequently wetted with smoke oil. To accomplish this, the smoke wires are sufficiently long at 76.2 cm (30 in.) to enable them to be pulled back and forth through the duct, so they can be wetted with smoke oil as needed. Each time the wire is used, the clay sealing "patches" on either wall of the duct are removed and the wire is slid part way out of the duct and wetted with oil using the fingertips or a cotton swab. Finally, the wetted wire is reinserted into the duct and the clay patches are reapplied. Variac setting for a 0.005 inch diameter wire was found to vary between 30 and 40 volts, depending on the channel flow rate.

The strobe, already positioned for continuous illumination of the desired slit, is adjusted so that the image of the strobe arc is in focus on the black posterboard sheet which lines the test section. Focusing is accomplished by either using the adjusting ring on the lens or by simply moving the pivoted strobe reflector.

The trial-and-error timing adjustment is accomplished by watching the timing control system status lights on the control logic box (Fig. 10). Moments after the spring-loaded timing sequence start switch is depressed, the smoke pattern should be visible in the illuminated plane. As the strobe status light goes out, indicating that the strobe has flashed, the smoke should still be visible. Adjustments to the wire and strobe timer potentiometers are made to accomplish this and to ensure that smoke intensity is at its peak when the strobe status light

goes out. Camera set-up and focusing is also accomplished during this time.

Once the proper potentiometer adjustments are made, the strobe is switched to the "External Input - high intensity" position and photography may begin. The room is darkened as much as possible. (All photographs for this report were taken at night, since the laboratory windows could not be adequately shaded.) With the camera mounted securely on a tripod, shutter speed set to 'B', and f-stop at 2.8 (lens aperture fully open), the timing sequence start switch is depressed. Moments later, before the flash of the strobe, the camera shutter is opened. Immediately after the flash from the strobe, the shutter is closed. The focused image of the smoke trace appears on the film during the three microsecond strobe flash.

IV. RESULTS

A. SMOKE TRACE VARIATION WITH DEAN NUMBER

At a selected location in the curved channel, smoke trace appearance and characteristics change in a series of identifiable stages as the Dean number is increased. Results which follow are based on observations of smoke traces generated from the 0.005 inch diameter wire, and observed using continuous illumination over the time interval smoke was present. Observations are presented for different Dean numbers and percent rotameter flow, where rotameter full scale corresponds to 125 cfm at 18.3°C and atmospheric pressure.

A summary of results in the following discussion is also given in Figure 15a. This figure is discussed in section IV.B.

At the 6 degree slit location (smoke wire located 2 degrees from the start of the curved section), the smoke trace appeared as a reasonably flat line for all Dean numbers from 167 to 461 (8 to 37.5% flow by rotameter indication). For Dean numbers up to 407 (32% rotameter flow), smoke traces were particularly flat and stable. At De = 461 (approx.), the smoke appeared diffused across most of the illuminated plane, indicating that turbulence existed. Mean velocities at this location were the highest used, where the maximum corresponds to Re_w equal to 31.6 for a 0.005 inch diameter wire at 37.5% flow (De = 461, U = 3.89 m/sec). In

order to avoid unstable wakes from such a wire, Re_w should be less than a critical value of 35-40 [Ref. 17].

At the 55 degree slit location (smoke wire located 50 degrees from the start of the curved section), the smoke trace appeared as a flat line at Dean numbers between 167 and 247 (8 to 16% rotameter flow). As the Dean number was raised, the smoke line became blurred (De = 298 to 307). At a Dean number of 317, weak turbulence was observed along with a single wave peak (wave form) which was oscillating slightly in the transverse direction. At a Dean number of 327, turbulent appearance (i.e. diffused smoke) was observed. Due to apparent instabilities in this section of the duct, these effects were not completely reproducible each time the observations were performed: i.e., the same observations discussed above would occur at slightly different Dean numbers. During one series of observations, waves appeared on the smoke trace and oscillated at low frequency (3 to 8 Hz) in the transverse direction for Dean numbers between 257 and 307. These particular waves and wave oscillations were only seen during one series of observations, and were probably due to vibrations of the smoke wire, an effect minimized for all other observations.

At the 118 degree slit location (smoke wire located 112 degrees from the start of the curved section), observation of regularly spaced standing smoke pattern waves was made beginning with a Dean number of 167. Figure 14 shows a sequence of smoke pattern photographs at this location with increasing Dean

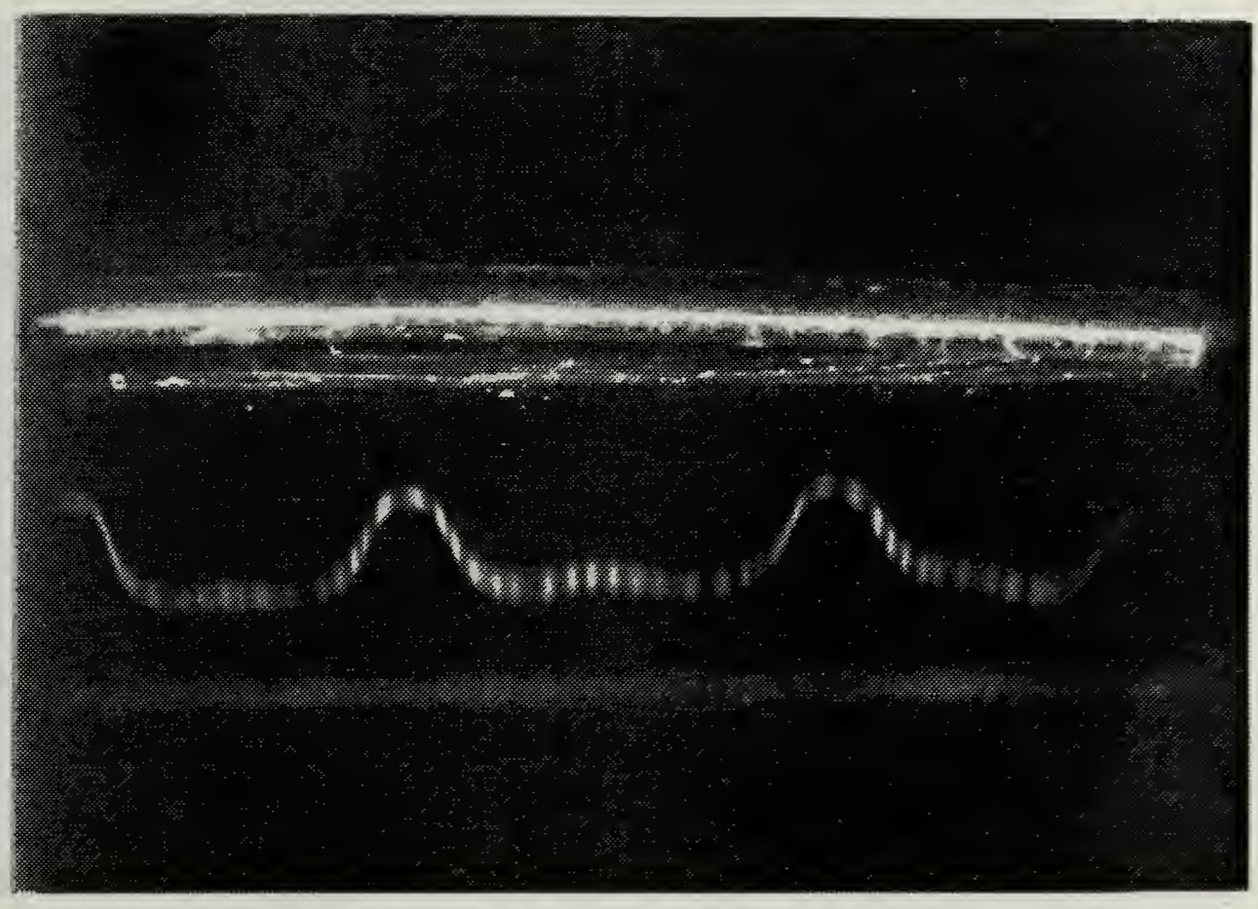

Figure 14a. Smoke trace photograph sequence (De = 182)

II-1 2100-2330 09 FEB 1987
9.5 % FLOW (rotameter)
MEAN AIR VELOCITY = 1.531 m/sec
VOLUMETRIC FLOW RATE = 0.00988 m^3/sec
MASS FLOW RATE = 0.01203 kg/sec
ATMOSPHERIC PRESS. & TEMP: 29.96 in. Hg, 65.0 deg F
SLIT LOC. = 118 deg.
WIRE LOC. = 112 deg.
WIRE DIA. = 0.0050 in. Re_w = 19
SLIT DISTANCE FROM START OF CURVE (X) = 1.242 m
Re_x = 121,895
De^x = 182
Re_c = 1246 Re_h = 2432
KODAK TRI-X FILM ASA 400 (f2.8, B)

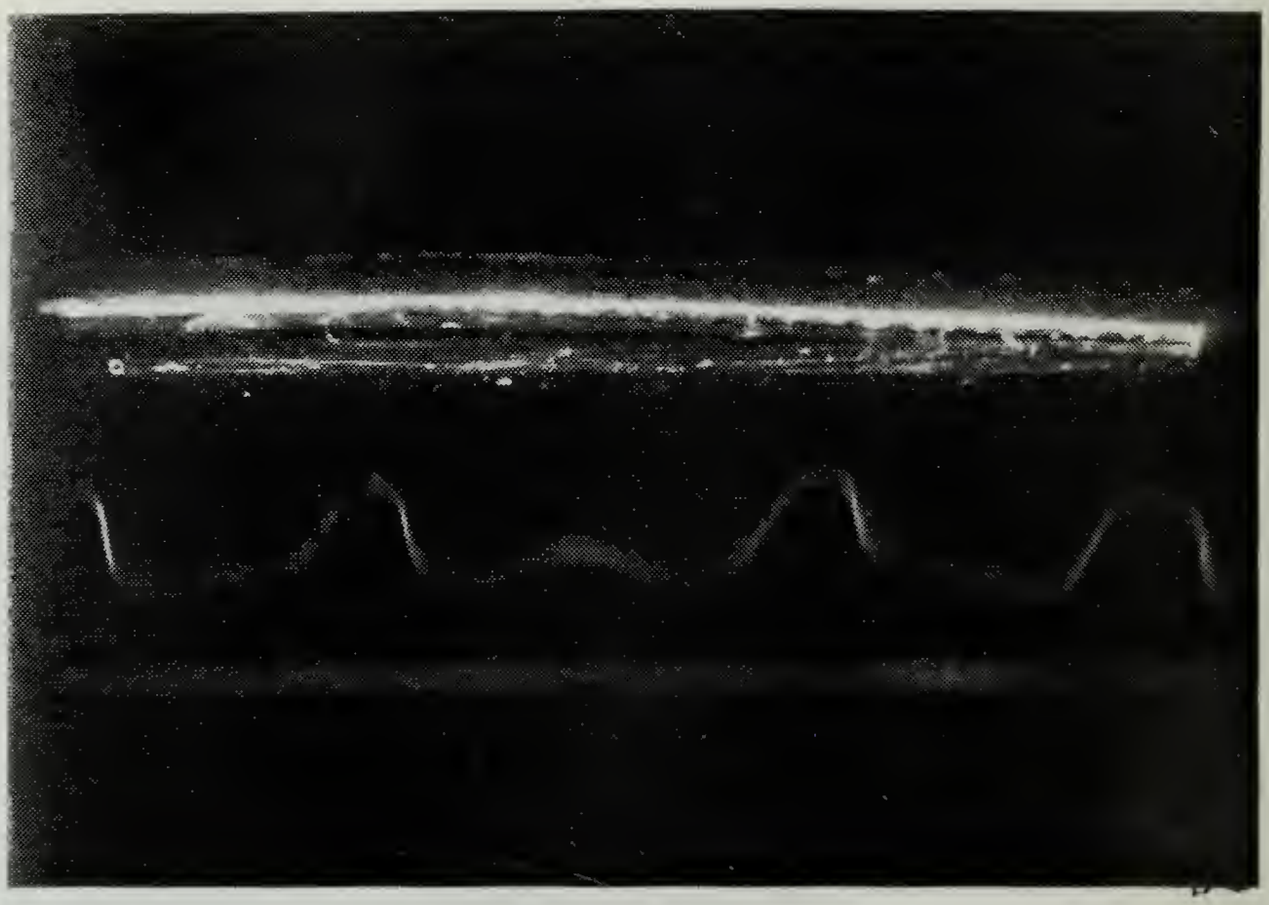

Figure 14b. Smoke trace photograph sequence (De = 207)

II-3 2100-2300 09 FEB 1987
12.0 % FLOW (rotameter)
MEAN AIR VELOCITY = 1.741 m/sec
VOLUMETRIC FLOW RATE = 0.01123 m^3/sec
MASS FLOW RATE = 0.01368 kg/sec
ATMOSPHERIC PRESS. & TEMP: 29.96 in. Hg, 65.0 deg F
SLIT LOC. = 118 deg.
WIRE LOC. = 112 deg.
WIRE DIA. = 0.0050 in. Re_w = 21
SLIT DISTANCE FROM START OF CURVE (X) = 1.242 m
Re_x = 138,643
De^x = 207
Re_c = 1417 Re_h = 2766
KODAK TRI-X FILM ASA 400 (f2.8, B)

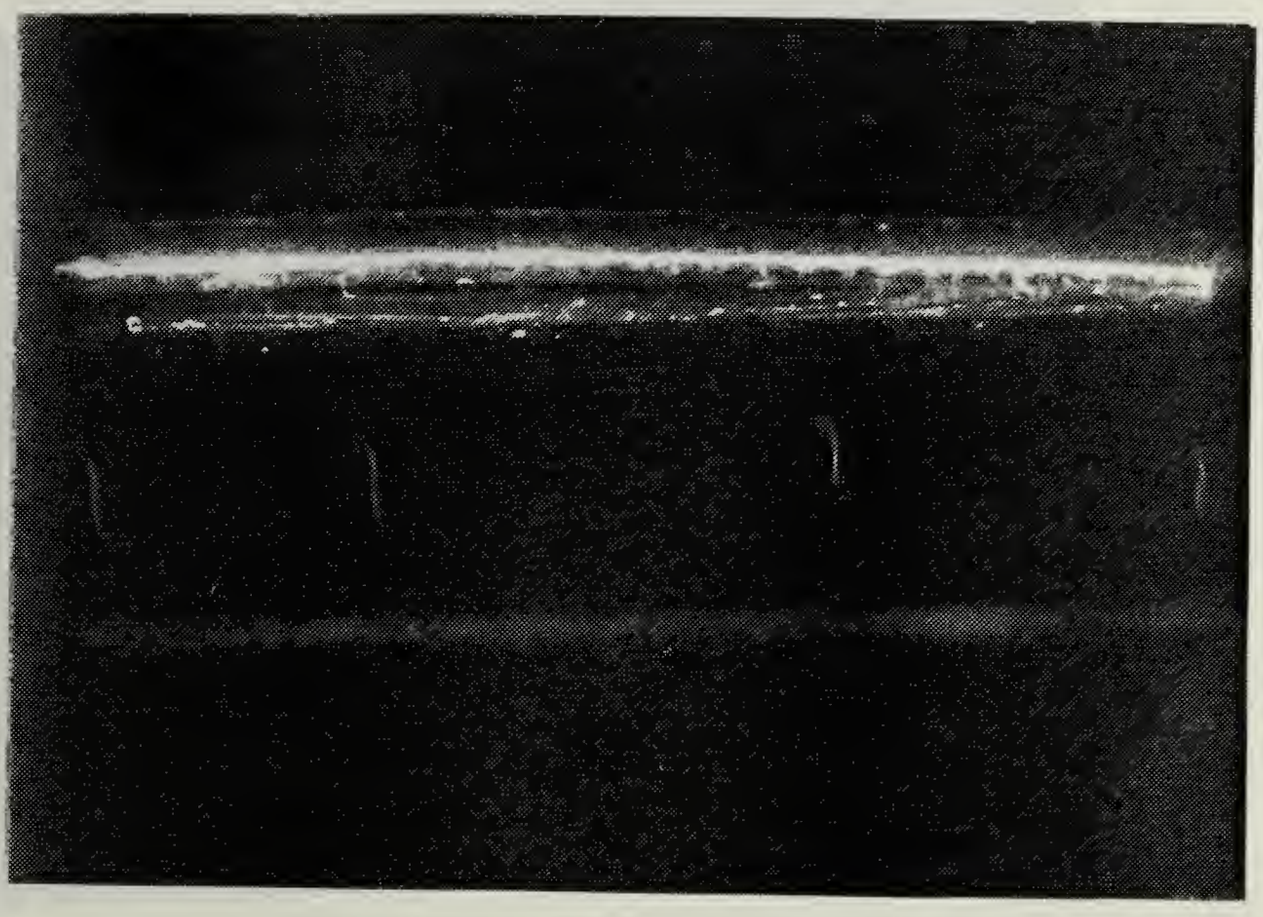

Figure 14c. Smoke trace photograph sequence (De = 227).

II-5 2100-2330 09 FEB 1987
14.0 % FLOW (rotameter)
MEAN AIR VELOCITY = 1.909 m/sec
VOLUMETRIC FLOW RATE = 0.01232 m^3/sec
MASS FLOW RATE = 0.01501 kg/sec
ATMOSPHERIC PRESS. & TEMP: 29.96 in. Hg, 65.0 deg F
SLIT LOC. = 118 deg.
WIRE LOC. = 112 deg.
WIRE DIA. = 0.0050 in. Re_w = 23
SLIT DISTANCE FROM START OF CURVE (X) = 1.242 m
Re_x = 152,041
De^x = 227
Re_c = 1554 Re_h = 3033
KODAK TRI-X FILM ASA 400 (F2.8, B)

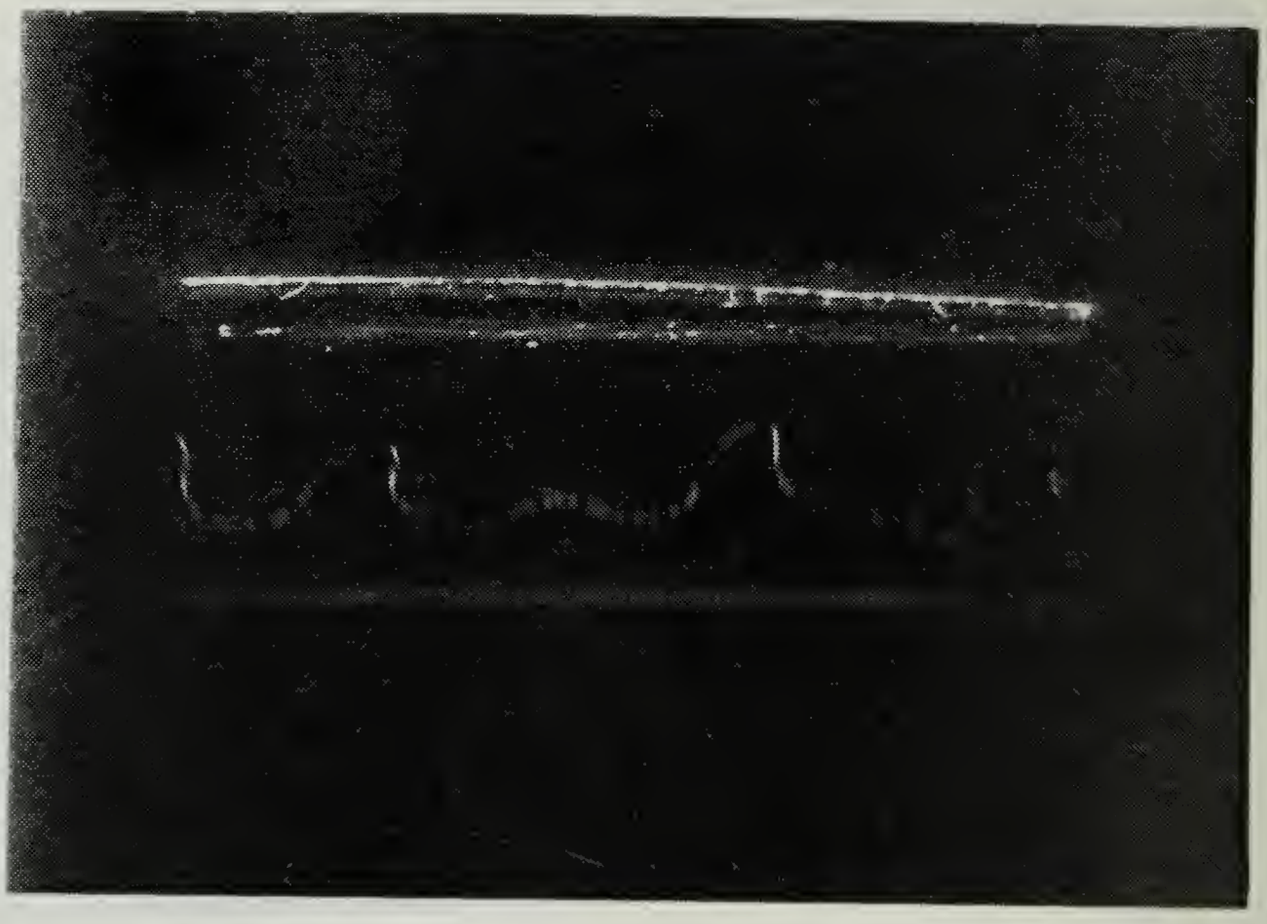

Figure 14d. Smoke trace photograph sequence (De = 237)

II-20 2100-2330 09 FEB 1987
15.0 % FLOW (rotameter)
MEAN AIR VELOCITY = 1.993 m/sec
VOLUMETRIC FLOW RATE = 0.01286 m^3/sec
MASS FLOW RATE = 0.01567 kg/sec
ATMOSPHERIC PRESS. & TEMP: 29.96 in. Hg, 65.0 deg F
SLIT LOC. = 118 deg.
WIRE LOC. = 112 deg.
WIRE DIA. = 0.0050 in. Re_w = 24
SLIT DISTANCE FROM START OF CURVE (X) = 1.242 m
Re_x = 158,740
De = 237
Re_c = 1623 Re_h = 3167
KODAK TRI-X FILM ASA 400 (f2.8, B)

number. (Photographs taken under other conditions and at other locations are provided in Appendix C.) The shape and spacing of the wave patterns at the 118 degree location became less regular as the Dean number was raised. During the three second time span (approx.) when the smoke trace was visible, the waves appeared to be motionless (De = 167 to 207). At a Dean number of 217, high frequency radial vibration (i.e. X_r direction in Figure 1) of the smoke trace wave peaks in the illuminated plane began to appear. Each wave was vibrating in place at its own transverse location in the channel. This vibration became progressively more violent (higher amplitude and frequency) as the Dean number was raised to 247. Only the portion of each wave peak closest to the convex surface was observed to oscillate. The approximately horizontal smoke line located between the convex and concave duct surfaces which connected successive wave peaks did not appear to be moving. (See Figure 14a.) At De = 252, oscillation became extremely violent and some low frequency transverse oscillations were evident. The turbulent appearance previously discussed was observed at this location at a Dean number of 257.

At the 146 degree slit location (smoke wire 140 degrees from the start of the curved section), the smoke trace appeared as a series of standing waves of very regular size and spacing (De = 167 to 187). An observation at a Dean number of 197 indicated that the waves had roughly the same size (amplitude), were spaced farther apart, and were "wobbling" in the

transverse (X_z) direction (i.e., the wave forms were staying in one transverse location, but their shape was changing in a wobbly fashion). This relatively low frequency wobble was still apparent when the smoke trace was observed at Dean numbers of 207 and 217, however, the wave forms were becoming progressively more irregularly spaced and shaped. At a Dean number of 227, the wobble became more violent, but the irregularly spaced and shaped waves continued to wobble in place. Weak turbulence (i.e., very blurred wave appearance) was observed at a Dean number of 237 and full turbulence appeared between values of 247 to 257.

The next section on stability mapping provides graphical analysis of the data just described.

B. STABILITY MAPS

Figure 15a is a graphical presentation of the results of this study. As shown in the figure, the standing wave smoke trace was observed at the 118 degree slit location and beyond for the lower Dean numbers (De < 210 approx.). Wave oscillations, either a low frequency wobble or high frequency vibration, was observed at the 55 degree slit location and beyond for moderate Dean values (210 < De < 310 approx.). It should be noted that for the 55 degree slit location, no waves were observed on the smoke trace until just prior to full turbulence. Here, the transition from weak turbulence, when wave oscillations were observed, to full turbulence occurred

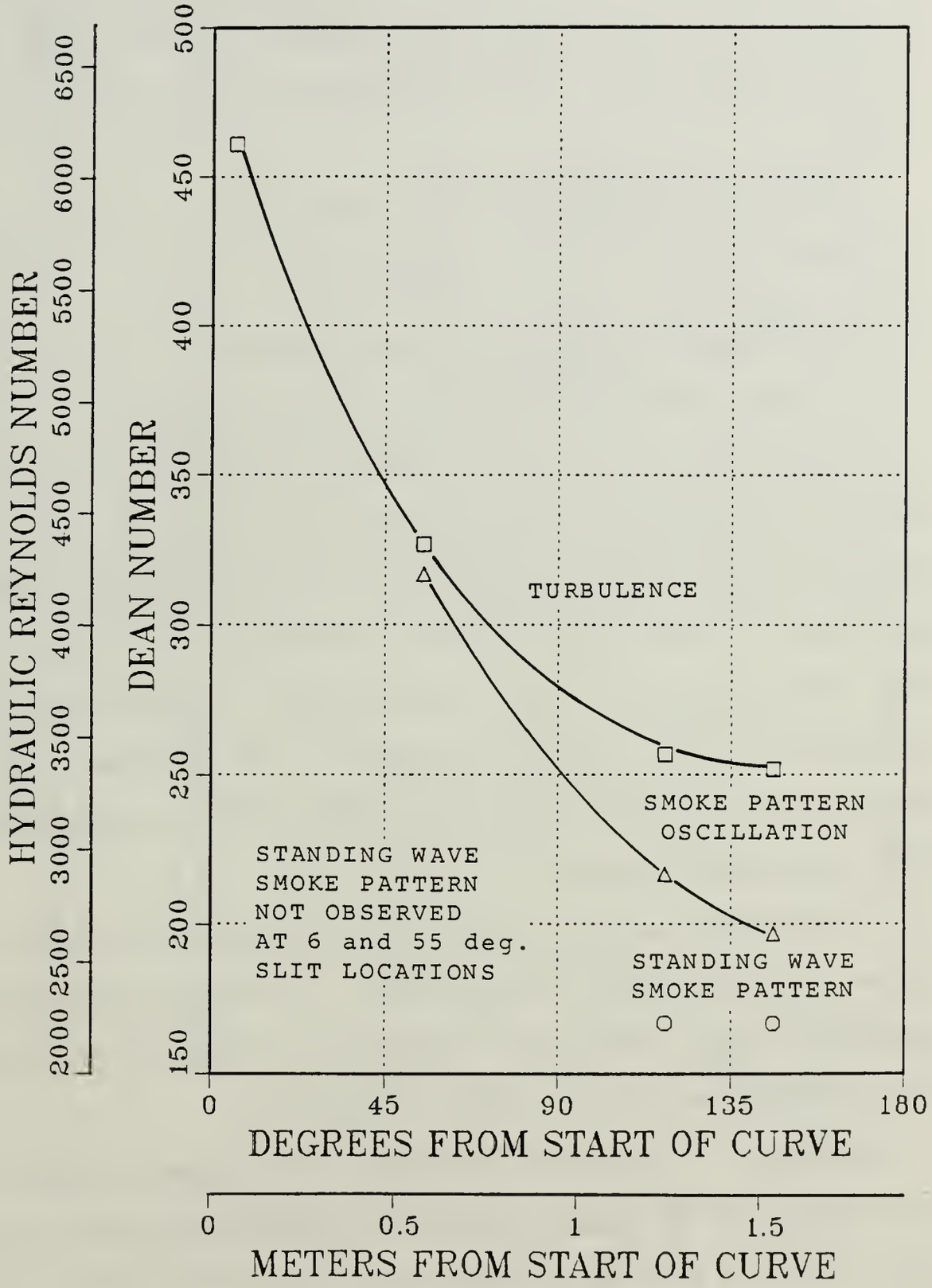

Figure 15a. Flow stability map.

over a flow rate change from 0.02096 kg/sec to 0.02162 kg/sec, corresponding to a one percent rotameter flow rate change relative to rotameter full scale. The Dean number variation for this change was about 10. Turbulent smoke trace appearance was observed at all locations above the upper-most line in the figure.

Figure 15b shows points on the stability map corresponding to several photographs in Appendix C.

C. FLOW VISUALIZATION, INTERPRETATION AND ANALYSIS

In some cases, the flow causes the smoke, which is initially generated along a straight line and convected downstream, to deform as shown in Figure 16. One possible arrangement of velocity vectors in the radial plane which could cause such a distortion is shown in Figure 17. Figure 18 shows that the smoke is further distorted into shapes expected if streamwise vortex pairs are present. The mushroom-like shape shown in Figure 18 becomes more like a row of omegas as the smoke convects further.

Transverse oscillations of the smoke pattern are probably caused by side-to-side vortex pair oscillation at a particular circumferential position. The causes of radial oscillations are less apparent.

Analysis of the smoke patterns can be used to make rough approximations of vortex strength (circulation) and spacing. Figure 16 is a photograph of a smoke trace for a Dean number of

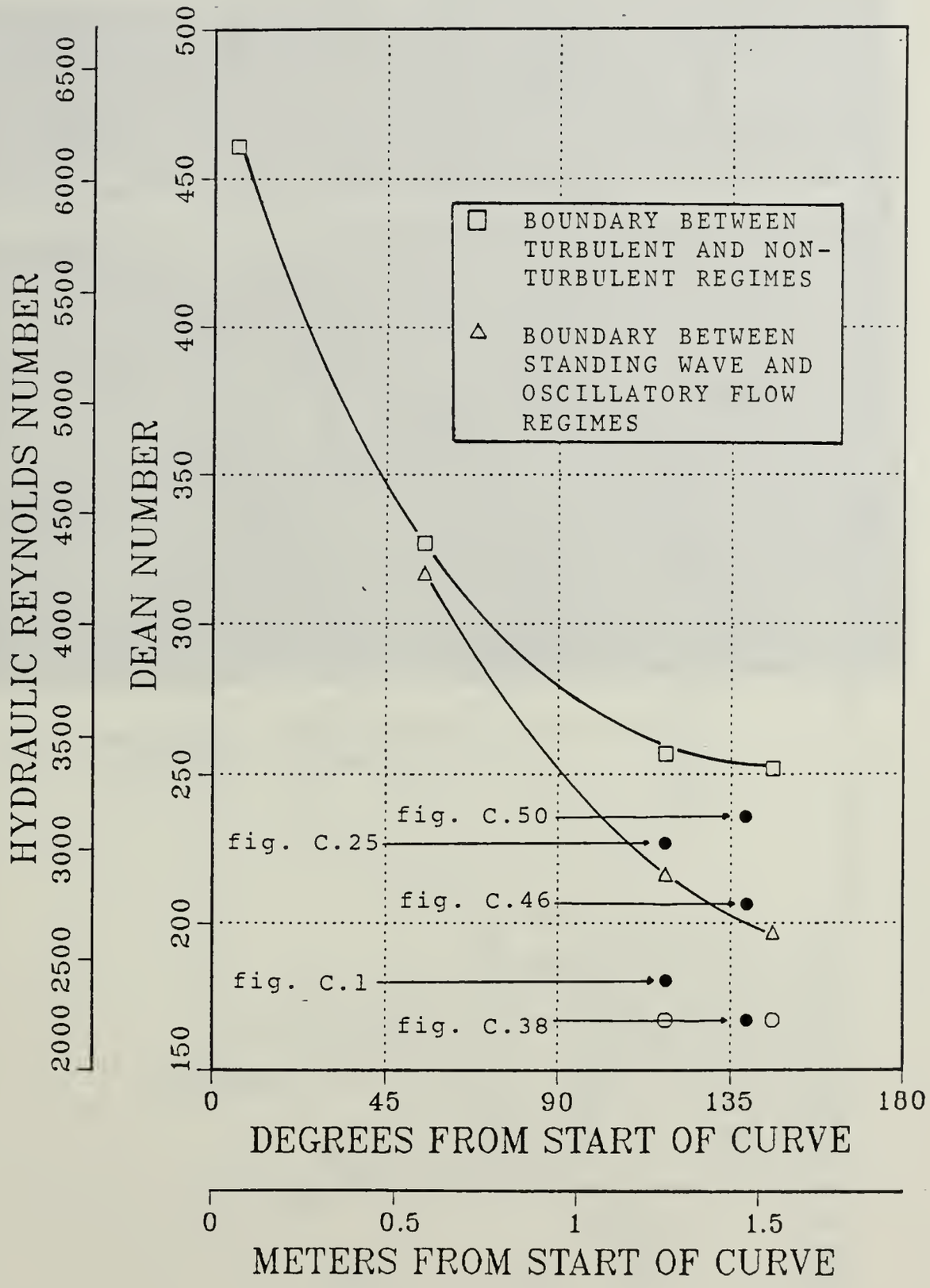

Figure 15b. Flow stability map indicating locations for several Appendix C photographs.

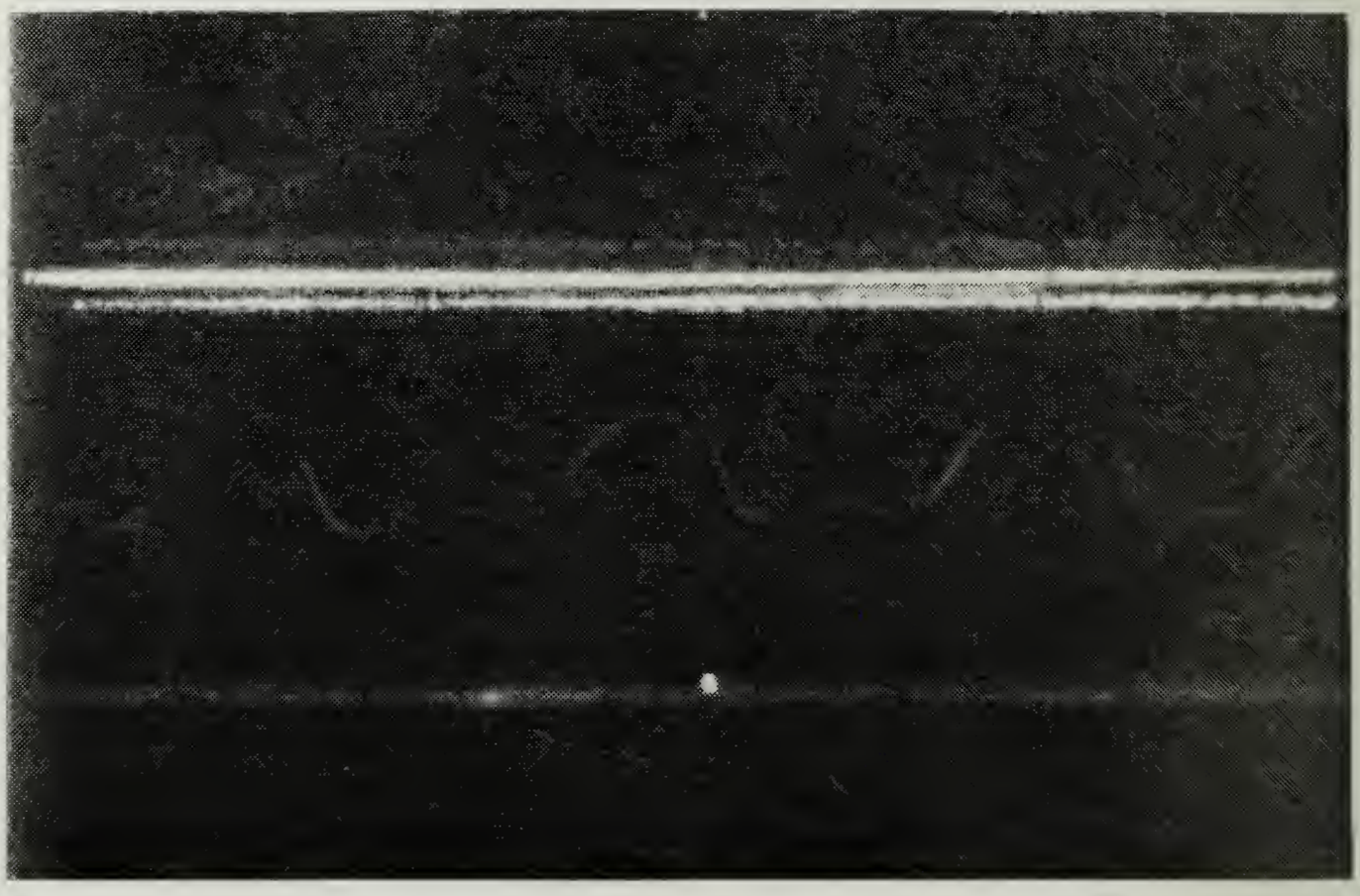

Figure 16. Smoke pattern photograph used in Figure 17 schematic.

O-1 FEB 1987
9.5 % FLOW (rotameter)
MEAN AIR VELOCITY = 1.531 m/sec
VOLUMETRIC FLOW RATE = 0.00988 m^3/sec
MASS FLOW RATE = 0.01203 kg/sec
ATMOSPHERIC PRESS. & TEMP: NOT RECORDED
SLIT LOC. = 119 deg.
WIRE LOC. = 112 deg.
WIRE DIA. = 0.0125 in. Re_w = 47
SLIT DISTANCE FROM START OF CURVE (X) = 1.256 m
Re_x = 123,238
De = 182
Re_c = 1246 Re_h = 2432
KODAK TRI-X ASA 1,000 (f2.8, B)

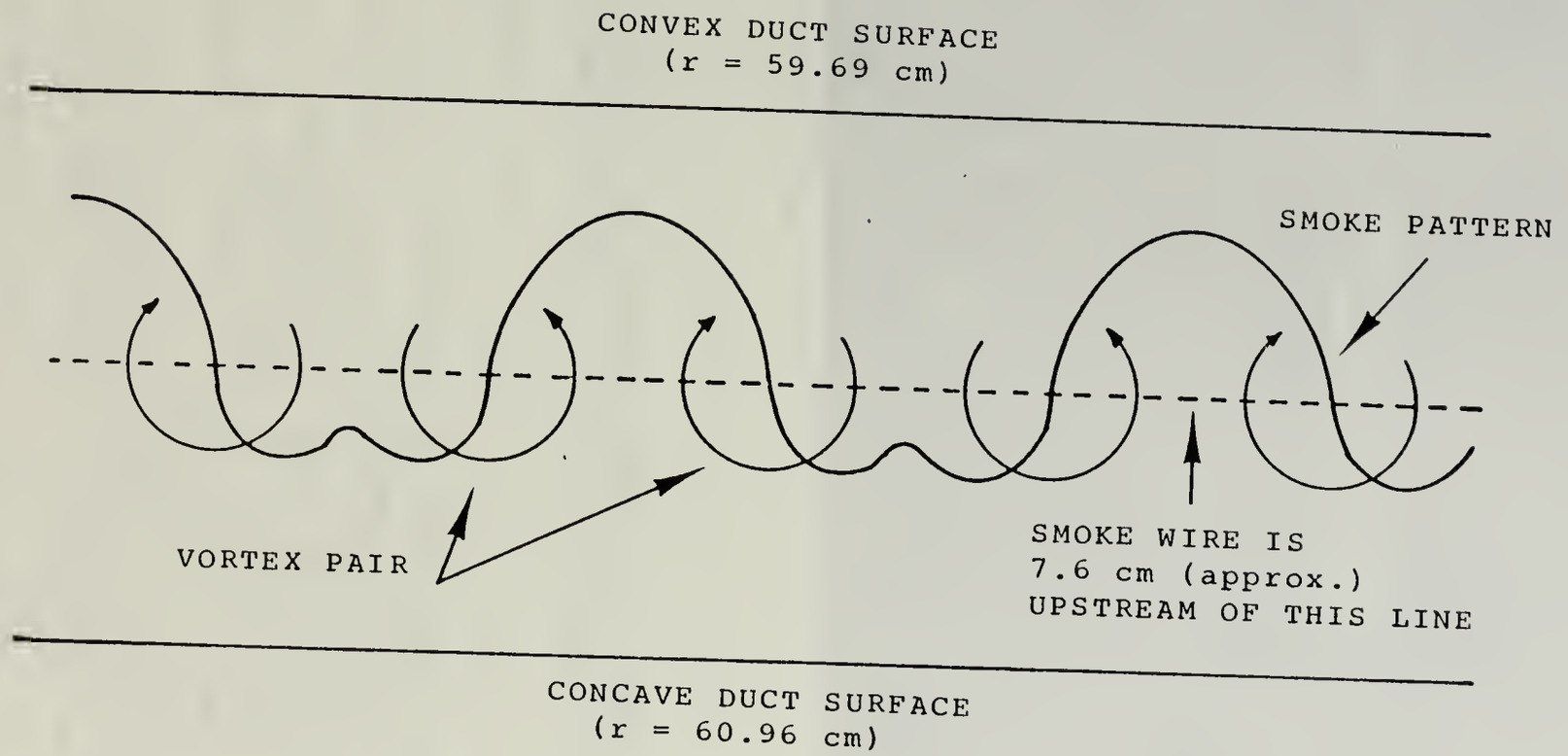

Figure 17. Theorized effect of streamwise vortices.

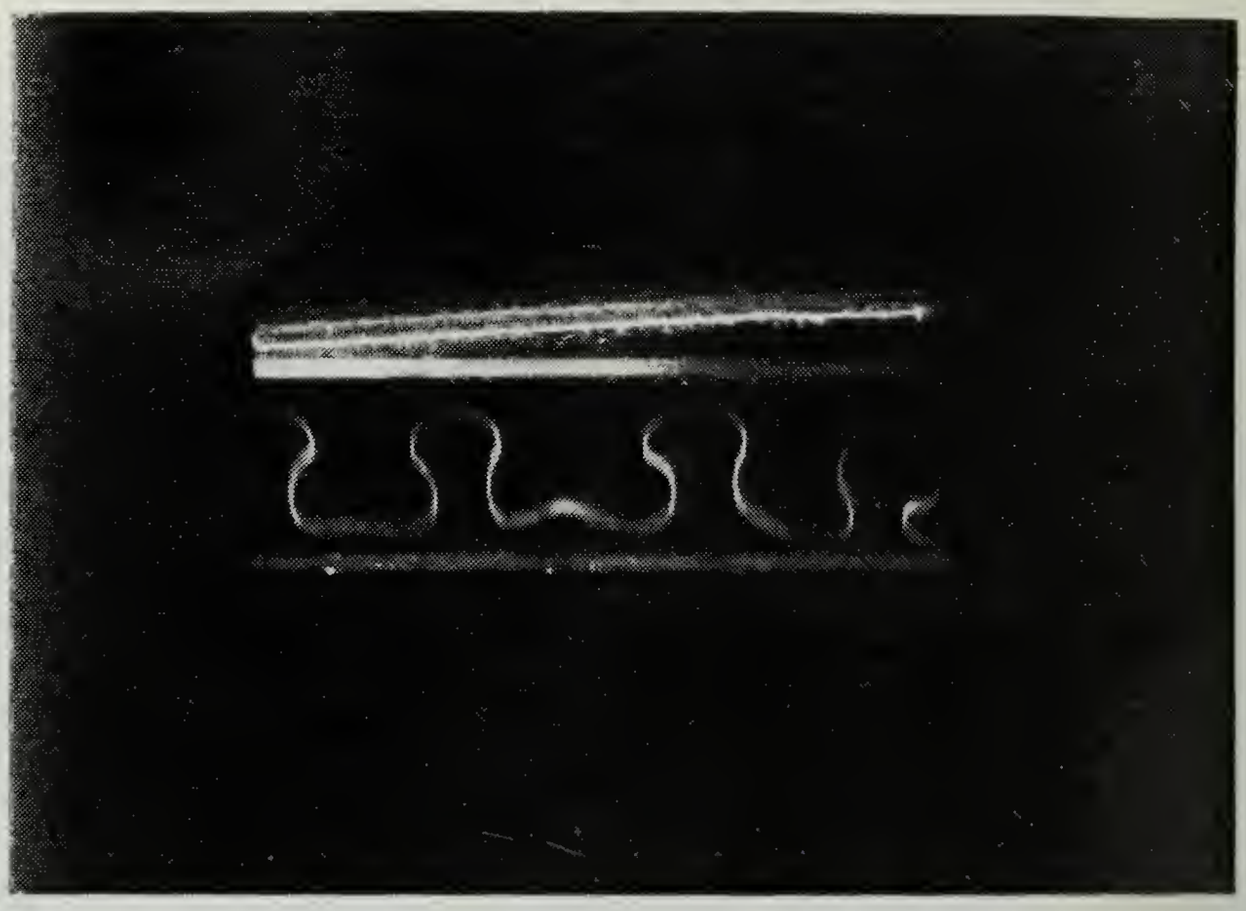

Figure 18. Smoke pattern photograph taken farther downstream of Figure 17 at the same Dean number.

II-14 2100-2330 09 FEB 1987
9.5 % FLOW (rotameter)
MEAN AIR VELOCITY = 1.531 m/sec
VOLUMETRIC FLOW RATE = 0.00988 m^3/sec
MASS FLOW RATE = 0.01203 kg/sec
ATMOSPHERIC PRESS. & TEMP: 29.96 in. Hg, 65.0 deg F
SLIT LOC. = 128 deg.
WIRE LOC. = 112 deg.
WIRE DIA. = 0.0050 in. Re_w = 19
SLIT DISTANCE FROM START OF CURVE (X) = 1.348 m
Re_x = 132,225
De = 182
Re_c = 1246 Re_h = 2432
KODAK TRI-X FILM ASA 400 (f2.8, B)

182 (9.5% rotameter flow). The 0.0125 inch diameter smoke wire was at the 112 degree location and the slit was approximately 0.0762 meters (3 in.) downstream, which corresponds to 119.3 degrees from the start of the curved section. Mean streamwise flow velocity for this Dean number is approximately 1.53 m/sec. (See section 5 of Appendix A for sample calculations.) Using this mean as an estimate of the convection velocity, the time between smoke generation at the wire to arrival at the illuminated plane is 0.0498 seconds.

Assuming that the streamwise vortices (if they exist and if they are causing the smoke distortion) are radially centered in the curved channel, the maximum vortex tangential velocity can be calculated from an estimate of the distance from the center of the illuminated plane to the wave peak (i.e., wave amplitude). It is also assumed that the vortex is like the inner part of a Rankine vortex, with velocity in the radial plane varying linearly from the vortex center over a small distance. Judging from the almost linear shape of the smoke pattern from channel center to wave peak, this seems to be a reasonable assumption. Knowing that the actual channel height is 1.27 cm (0.5 in.) and is 4.21 cm (1.66 in.) in the photograph, measurements of smoke pattern dimensions in the photograph may be scaled to the correct radial lengths. In this case, the wave peak average amplitude is roughly 2.16mm from the actual channel mid-plane. This means that maximum

vortex tangential flow velocity must be 0.0434 m/sec, or 2.8 percent of the mean streamwise velocity of 1.53 m/sec.

If the area, πr^2, includes all vorticity of a Rankine vortex, then its circulation is given by $\Gamma = 2\pi r V_r$, where V_r is the circumferential component of velocity relative to the vortex and r is the radial distance from the vortex center. Using V_r = 0.0434 m/sec and r = 2.09 mm for the smoke trace of Figure 16, circulation and vorticity are estimated to be 5.7×10^{-4} m^2/sec and 41.6 sec^{-1}, respectively.

V. CONCLUSIONS AND RECOMMENDATIONS

Laminar/turbulent flow transition was observed in a curved channel of rectangular cross section. The curved test section consisted of concentric surfaces with radii of curvature of 59.69 and 60.96 cm (23.5 and 24.0 in.). Channel width was 50.8 cm and the resulting aspect ratio was 40 to 1.

Using smoke wires at 6, 50, 112, and 140 degrees from the start of the curved test section, flow visualization studies were performed. The Dean number for these observations ranged from 167 to 461. Equivalent mean velocities in the duct were 1.40 to 3.89 m/sec.

Photographs and observations showed that under certain conditions and channel locations, smoke traces will appear as a series of standing waves at various radial planes. Smoke trace distortions are similar to what one would expect if pairs of counter-rotating vortices are present.

Smoke pattern behavior at varying channel location and Dean number shows that the standing wave smoke pattern is more likely to form closer to the exit of the curved section at lower Dean numbers. As the Dean number is raised, such wave patterns exist farther upstream (i.e. closer to the start of the curvature). Transition is also expected to occur farther upstream, closer to the start of the curvature, as the Dean number increases.

To prove that vortices do in fact exist and that their presence is shown by the smoke trace, more detailed studies are required. The smoke trace patterns, by strict interpretation, show only radial distortion. Transverse flow velocities must also be measured to adequately show that vorticity is present. Radially placed smoke wires may indicate transverse flow characteristics, but their placement must be known relative to a vortex center.

Other flow visualization and observation schemes might prove effective. Specifically, continuous smoke generation and injection of this smoke to enable following the behavior of an individual streamline might yield interesting results.

The more interesting photographs taken in the course of this study were taken at lower flow rates and well downstream of the smoke wire. Since the lowest indication on the rotameter was 8 percent (De = 167) and since the blower underwent significant throttling to achieve this flow rate, a lower capacity blower and smaller range rotameter would be helpful in further studies of transition in this test facility.

APPENDIX A

SAMPLE CALCULATIONS

1. DEVELOPMENT LENGTH FOR LAMINAR FLOW

a. Using the Langhaar equation for tubes [Ref. 14]

$$\frac{L'}{D} = 0.058\ Re_c$$

where

L' = Development length for laminar flow

D = Pipe diameter (or distance between flat plates (d) as discussed here).

Re_c = Reynolds number based on channel height,

it can be shown that the maximum Reynolds number ($Re_{c_{max}}$) based on an 8 foot development length is

$$Re_{c_{max}} = \frac{L'}{0.058\ d} = \frac{8\ ft\ (12\ in/ft)}{0.058\ (0.5\ in)}$$

$$Re_{c_{max}} = 3110 \quad .$$

The maximum Dean number is

$$De_{max} = Re_{c_{max}}\sqrt{d/r_i} = 3110\sqrt{0.5in/23.5\ in}$$

$$De_{max} = 454$$

The hydraulic diameter of the channel is

$d_h = \frac{4A}{P}$, where 'A' and 'P' are the channel area and perimeter, respectively.

$$D_h = \frac{4(0.5 \text{ in} \times 20 \text{ in})}{(2\times20) + (2\times0.5)} = 0.9756 \text{ inches}$$

$$D_h = 2.478 \text{ cm}$$

The maximum hydraulic Reynolds number is simply

$$Re_{h_{max}} = Re_{c_{max}} \frac{D_h}{d} = 3110 \frac{(0.9756 \text{ in.})}{0.5 \text{ in.}}$$

$$Re_{h_{max}} = 6068$$

b. For development length between parallel planes, it was shown in Reference 15 that

$L' = \phi D_h \, Re_h$,

where ϕ is a dimensionless parameter obtained from channel aspect ratio. For a channel with a 40:1 aspect ratio, ϕ is equal to 0.0115. The maximum hydraulic Reynolds number is then calculated as

$$Re_{h_{max}} = \frac{L'}{\phi D_h} = \frac{8 \text{ ft } (12 \text{ in./ft.})}{0.0115 \ (0.9756 \text{ in.})}$$

$$Re_{h_{max}} = 8557$$

Similarly, the maximum Dean number and Reynolds number (based on channel height) using Reference 15 results for parallel plates are

$$De_{max} = 640$$

$$Re_{c_{max}} = 4386$$

These results are about 30% higher than the more conservative results of the Langhaar equation for flow in tubes.

2. SCALING CALCULATIONS

To select a blower for the new test facility, which is twice the size of the previous facility, it is necessary to scale-up flow data from the smaller duct. The goal is having the same hydraulic Reynolds number in both channels. The hydraulic Reynolds number is

$Re_h = \frac{U D_h}{\nu}$. Since hydraulic diameter is

$\frac{4A}{P}$ and volumetric flow rate (Q) is $U A$,

$Re_h = \frac{4Q}{P\nu}$. Ultimately, since mass flow rate is ρQ and absolute viscosity (μ) is $\nu\rho$,

$Re_h = \frac{4\dot{m}}{P\mu}$. The perimeter (P) of the new channel is twice the old channel's perimeter and the cross sectional area (A) of the new channel is four times that of the older channel. Therefore, since hydraulic diameter is $\frac{4A}{P}$,

$D_{h_{new}} = 2D_{h_{old}}$. Since Reynolds numbers are equal, similitude is achieved when mean velocities are set forth as $U_{new} = \frac{1}{2} U_{old}$.

Volumetric flow rate (Q) is equal to UA. Since $U_{new} = \frac{1}{2} U_{old}$ and $A_{new} = 4 A_{old}$,

$Q_{new} = 2 Q_{old}$ achieves similitude. Since channel head loss (pressure change (ΔP) across the duct) is proportional to $U^2 \frac{L}{D}$, where 'L' is the length of the duct, and since the L-to-D ratio is the same for both ducts, similitude is also achieved when

ΔP_{new} equals $\frac{1}{4} \Delta P_{old}$.

The equations above enable the scaling-up of flow data from a channel half the size of the current one.

Figure 8 shows the old and scaled-up new curved channel systems curves as well as the new blower performance curve. Since the old channel did not have flow management devices (screens and honeycombs) or a rotameter, the effects of these items was considered small when compared to the suction capability of the blower and was neglected in generating the data for Figure 8.

3. REYNOLDS NUMBER BASED ON SMOKE WIRE DIAMETER

Wire diameter used most often was 0.005 inch diameter. Some 0.0125 inch diameter wire was also used at lower Dean numbers.

To avoid an unstable wake due to flow separation on the wire, maximum Reynolds number based on wire diameter should be less than 35 [Ref. 17].

$$(Re_w) = 35 = \frac{U_{max} d_w}{\nu} = \frac{U_{max}(0.000127\ m)}{1.56 \times 10^{-5}\ m^2/sec}$$

U_{max} = 4.30 m/sec. (Based on $Re_w \leq 35$ for 0.005 in. diameter wire.)

Since maximum fluid velocity for laminar flow between parallel flat plates is 1.5 times the mean velocity, mean velocity for Re_w = 35 is 2.87 m/sec.

Reynolds and Dean numbers based on the distance between flat plates are now required.

$$Re_c = \frac{Ud}{\nu}$$

($\nu = 1.56 \times 10^{-5}\ m^2/sec$)

Re_c = 2,336 (Using U = 2.87 m/sec.)

The Dean number is equal to $Re_c \sqrt{d/r_i}$,

where d = 0.5 inches

and r_i = 23.5 inches

De_{max} = 341 (Using U = 2.87 m/sec, the maximum velocity based on a wire diameter of 0.005 in.)

(This Dean number occurs at 25.4% indicated rotameter flow.) For a wire which is 0.0125 inches (0.3175mm) in diameter, it can be shown that

U_{MAX} = 1.72 m/sec

U = 1.15 m/sec

$Re_{c_{max}}$ = 934 and

De_{max} = 136

A table summarizing these values is shown below:

SUMMARY OF CRITICAL VALUES BASED ON A WIRE REYNOLDS NUMBER (Re_w) OF 35 (CHANNEL INSIDE DIMENSIONS ARE 0.5in.x20.0in.):

Wire Diameter	0.005 in.	0.0125 in.
U	2.87 m/sec	1.15 m/sec
U_{max}	4.30 m/s	1.72 m/sec
$Re_{c_{max}}$	2336	934
De_{max}	341	136

4. ROTAMETER CALIBRATION DATA AND SAMPLE CALCULATIONS.

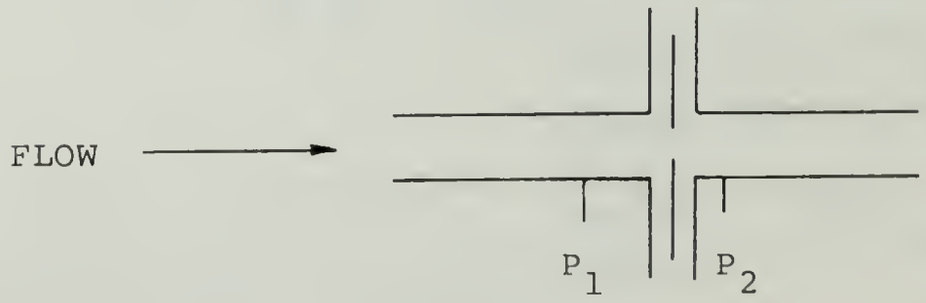

A one-inch ASME orifice is used, as shown above.

P_1 is the pressure upstream of the orifice and

P_2 is the downstream pressure.

Data:

	Barometric Pressure	Air Temperature
Conditions at start of calibration	30.26" Hg	63.1°F
Conditions at end of calibration	30.26" Hg	66.1°F

Data Point	P_1 Inches H_2O (Vacuum)	(P_1-P_2) Inches H_2O	Assumed Temp °F	Rotameter Flow (%)
1	8.15	41.40	63.1	60.5
2	4.45	24.25	63.85	46.8
3	2.20	13.60	64.60	29.3
4	0.92	5.90	65.35	22.2
5	0.35	1.90	66.10	12.9

Complete calculations for data point #1 are shown.

P_1 = -8.51 in. H_2O = -0.294 psi (below atmospheric pressure)

P_{atm} = 30.26 in. Hg = 14.86 psia

P_1 = 14.86 - 0.294 = 14.566 psia @ 63.1°F

$\Delta P_o = P_1 - P_2$ = 41.40" H_2O = 1.495 psi

$P_2 = P_1 - \Delta P_o$ = 13.071 psia

$$\rho_1 = \frac{P_1}{RT_1} = \frac{14.566 \text{ lbf/in}^2 \ (144 \text{ in}^2/\text{ft}^2)}{(53.34 \text{ ft lbf/lbm°R}(523.1°\text{R})}$$

ρ_1 = 0.07517 lbm/ft^3

$\frac{P_2}{P_1} = \frac{13.071}{14.566} = 0.8974$ Using this value in Reference 18 (Figure 7-15) with an orifice-to-pipe diameter ratio of 0.5 yields a 'Y' value of 0.939.

$$\dot{m} = KA_2Y\sqrt{2g_c\ \rho_1\ (P_1-P_2)}\ .$$

Assuming an initial Reynolds number of 5,000,

K = 0.6420 [Ref. 19].

$$\dot{m} = 0.6420\ \frac{\pi}{4}\ \frac{(1\ )^2}{(12)^2}\ ft^2(0.939)\sqrt{(2)32.174\ \frac{ftlbm}{lbfsec^2}\ 0.07517\ \frac{lbm}{ft^3}\ 215.28\ \frac{lbf}{ft^2}}$$

$\dot{m}$ = 0.1031 lbm/sec

Iterating ...

$$Re = \frac{4\dot{m}}{\mu\pi D} = \frac{4(0.1031\ lbm/sec)}{4.0x10^{-7}\ \frac{lbf\ sec}{ft^2}\ (\pi)\ \frac{1}{12}\ ft\ x\ 32.174\ \frac{ftlbm}{lbfsec^2}}$$

Re = 122,400

Using this Re value, find a new K value [Ref. 18] by interpolation.

K = 0.6229 Using this K, find a new $\dot{m}$.

$$\dot{m} = \frac{0.6229}{0.6420}\ (0.1031\ \frac{lbm}{sec}) = 0.1000\ lbm/sec$$

$$Re = \frac{4(0.1000)}{4x10^{-7}\ (\pi)\ \frac{1}{12}\ (32.174)} = 118,700$$

Iterating again ...

$K = 0.6229$ (same as before)

$\dot{m}_1 = 0.1000$ lbm/sec

$$Q_1 = \frac{\dot{m}_1}{\rho} = \frac{0.1000 \text{ lbm/sec}}{0.07517 \text{ lbm/ft}^3} = 133 \text{ ft}^3\text{sec}$$

$$= 79.8 \text{ cfm @ } 60.5\%$$

indicated flow.

5. CONVERTING ROTAMETER INDICATION TO FLOW RATE, DEAN NUMBER, AND REYNOLDS NUMBER

a. Flow Rate:

As shown in Figure 13, rotameter indication is a linear function of volumetric flow rate. The slope (m) of the line is equal to $\frac{115 \text{ cfm}}{100\%}$ or 1.15 and the y-intercept (b) occurs at 10 cfm. Since the equation of a straight line is $y = mx + b$, the equation converting rotameter indication to volumetric flow rate (Q) in cfm is

$$Q = 1.15 \times (\text{Rotameter \% Flow}) + 10$$

b. Reynolds Number (Re_c):

One hundred percent flow indication on the rotameter represents 125 cfm. Since mean velocity through the duct is Q/A, where 'A' is the duct cross sectional area (10 in^2), mean velocity at 100% flow is

$$125 \frac{ft^3}{min} \quad \frac{min}{60 \text{ sec}} \quad \frac{1}{10 \text{ in}^2} \quad \frac{144 \text{ in}^2}{ft^2} \quad \frac{12 \text{ in}}{1 ft} \quad \frac{0.0254 m}{in}$$

$U = 9.144$ m/sec (@ 100% flow).

Likewise, mean velocity at 0% indicated flow is

$$10 \ \frac{ft^3}{min} \ \frac{1}{60} \ \frac{1}{10} \ (12)^3 \ 0.0254 = 0.73152 \text{ m/sec.}$$

Reynolds number (based on channel height) is $\frac{Ud}{\nu}$.

$$Re_c = \frac{9.14 \text{ m/sec } (0.0127 \text{ m})}{(1.56 \times 10^{-5} \text{ m}^2/\text{sec})} = 7444.15 \quad @ \text{ 100\% flow indication}$$

$$Re_c = \frac{0.73152 \ (0.0127)}{(1.56 \times 10^{-5})} = 595.53 \quad @ \text{ 0\% flow indication}$$

As discussed in Part "A" above, $b = 595.53$ and

$$m = \frac{7444.15 - 595.53}{100} = 68.49$$

The equation converting rotameter indication to Reynolds number is

$$Re_c = 68.49 \times (\text{rotameter \% flow}) + 595.53$$

c. Dean Number:

Since the Dean number is defined as $De = Re\sqrt{d/r_i}$ (where $d = 0.5$ inches and $r_i = 23.5$ inches), the Dean number is actually $De = 0.146 \ Re_c$.

Expressing this in terms of rotameter indicated flow, the Dean number is

$$De = 9.99 \text{ (rotameter \% flow)} + 86.87$$

(Note that for this rotameter, the minimum indication is 8%.)

APPENDIX B

ACCURACY/UNCERTAINTY ANALYSIS

This section documents instrument accuracy/readability, as well as uncertainty in the calculation of channel flow rate and related quantities (i.e. De, Re_h, Re_c, etc.)

The following are estimates of the errors involved in reading the instruments used in the calibration of the rotameter. These values were conservatively chosen.

ΔP_1 (manometer)	± 0.4 inches of water (± 0.0144 psi)
ΔP_{atm} (barometer)	± 0.05 inches of mercury (0.025 psi)

$$\Delta P_1 = \sqrt{(0.0144)^2 + (0.025)^2} = 0.029 \text{ psi}$$

$\Delta(\Delta P)$ (U-tube manometer)	± 0.4 inches of water (±0.0144 psi)
ΔT_1 (mercury thermometer)	± 1.0 °F

From Appendix A (section 4), the mass flow rate through the orifice is:

$$\dot{m} = K A_2 Y \sqrt{2 g_c \rho_1 (\Delta P)}$$

Using the data in Appendix A (section 4) for data point #1, the uncertainty in the air density (ρ_1) is found.

$$\rho_1 = \frac{P_1}{RT_1}$$

$$\Delta\rho_1 = \left[\left(\frac{\partial\rho_1}{\partial P_1}\ \delta P_1\right)^2 + \left(\frac{\partial\rho_1}{\partial T_1}\ \delta T_1\right)^2\right]^{\frac{1}{2}}$$

$$= \left[\left(\frac{1}{RT_1}\ \delta P_1\right)^2 + \left(\frac{P_1}{RT_1^2}\ \delta T_1\right)^2\right]^{\frac{1}{2}}$$

$$\Delta\rho_1 = \left[\left(\frac{144(0.029)}{53.34(523.1)}\right)^2 + \left(\frac{144(14.566)\ (1)}{(53.34)(523.1)^2}\right)^2\right]^{\frac{1}{2}}$$

$$\Delta\rho_1 = \pm\ 0.0002\ \text{lbm/ft}^3$$

$$\rho_1 = 0.0752 \pm 0.002\ \text{lbm/ft}^3$$

The uncertainty in mass flow rate is found in a similar manner (assuming negligible uncertainty in K, A_2, Y, and g_c).

$$\Delta\dot{m} = \left[\left(\frac{\partial\dot{m}}{\partial\rho_1}\ \Delta\rho_1\right)^2 + \left(\frac{\partial\dot{m}}{\partial\Delta P}\ \Delta(\Delta P)\right)^2\right]^{\frac{1}{2}}$$

$$= \left[\left(\frac{KA_2Y}{2}\sqrt{\frac{2g_c\Delta P}{\rho_1}}\ \Delta\rho_1\right)^2 + \left(\frac{KA_2Y}{2}\sqrt{\frac{2g_c\rho_1}{\Delta P}}\ \Delta(\Delta P)\right)^2\right]^{\frac{1}{2}}$$

$$\Delta\dot{m} = 0.6229\ (0.005454)\ (0.939)\ (0.5)\sqrt{2(32.174)}\ \times$$

$$\left[\left(\frac{215.28}{0.07517}\ (0.0002)^2\right) + \left(\frac{0.07517}{215.28}\ (0.0144)^2(144)^2\right)\right]^{\frac{1}{2}}$$

$$\dot{m} = 0.1000 \pm 0.0005\ \text{lbm/sec.}$$

This uncertainty represents a 0.5 percent error in mass flow rate. An uncertainty of 0.5% is insignificant and not indicative of actual rotameter accuracy.

Typical oscillation in rotameter indication varies between ± 0.5 to 1.0% of rotameter full scale. An uncertainty of 0.5% in rotameter indicated flow, a conservative estimate, represents an uncertainty of 5 with respect to the Dean number and 30 with respect to the channel Reynolds number (Re_c). This represents an overall uncertainty in Dean and Reynolds numbers of about 3 percent. Considering the data scatter in the rotameter calibration curve (Fig. 13), these seem to be reasonable estimates for the uncertainties in channel flow rate, flow velocity, and Dean and Reynolds numbers.

APPENDIX C

SMOKE PATTERN PHOTOGRAPHS

This appendix contains the majority of the still pictures taken in the course of this study. Although the enlargements were not of uniform size, it is to be noted that all photos are of illuminated radial planes of identical size. Slit width, and therefore the width of the illuminated radial plane, is 4.57 cm (1.8 in.) across. The duct height, the distance between illuminated horizontal lines in each photograph, is 1.27 cm (0.5 in.). The brighter of the two horizontal lines (located at the top of each photograph) represents the convex internal surface of the duct. This bright line is the illuminated edge of the cardboard slit. In some photos, this line may not appear to be straight due to warpage of the cardboard.

While slit distance from the start of the curved test section varies between photos, all slits have the same transverse location in the duct. The distance from the slit centerline to the channel transverse centerline is 4.83 cm (1.9 in.). All slit locations and dimensions are ±2 mm and all angular measurements from the curved channel entrance are ± 0.5 degrees.

Photographs are arranged in the order that they were taken. The Roman and Arabic number in the upper left corner of each caption represent the roll number and the photograph on that roll, respectively.

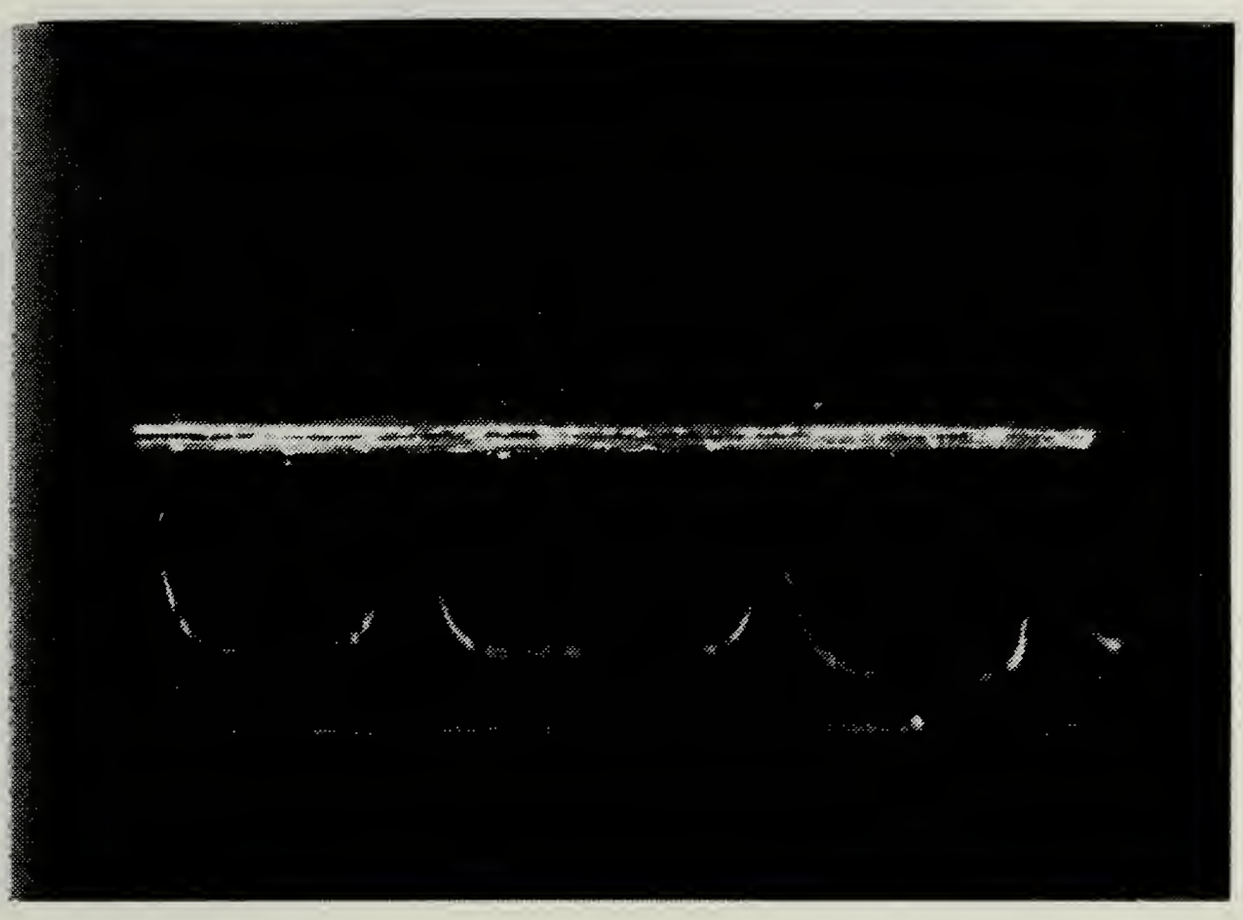

Figure C.1

I-5 2100-2315 08 FEB 1987
9.4 % FLOW (rotameter)
MEAN AIR VELOCITY = 1.522 m/sec
VOLUMETRIC FLOW RATE = 0.00982 m^3/sec
MASS FLOW RATE = 0.01196 kg/sec
ATMOSPHERIC PRESS. % TEMP: 29.92 in. Hg, 65.2 deg F
SLIT LOC. = 118 deg.
WIRE LOC. = 112 deg.
WIRE DIA. = 0.0125 in. Re_w = 46
SLIT DISTANCE FROM START OF CURVE (X) = 1.242 m
Re_x = 121,225
De = 181
Re_c = 1239 Re_h = 2418
KODAK TRI-X FILM ASA 400 (f2.8, B)

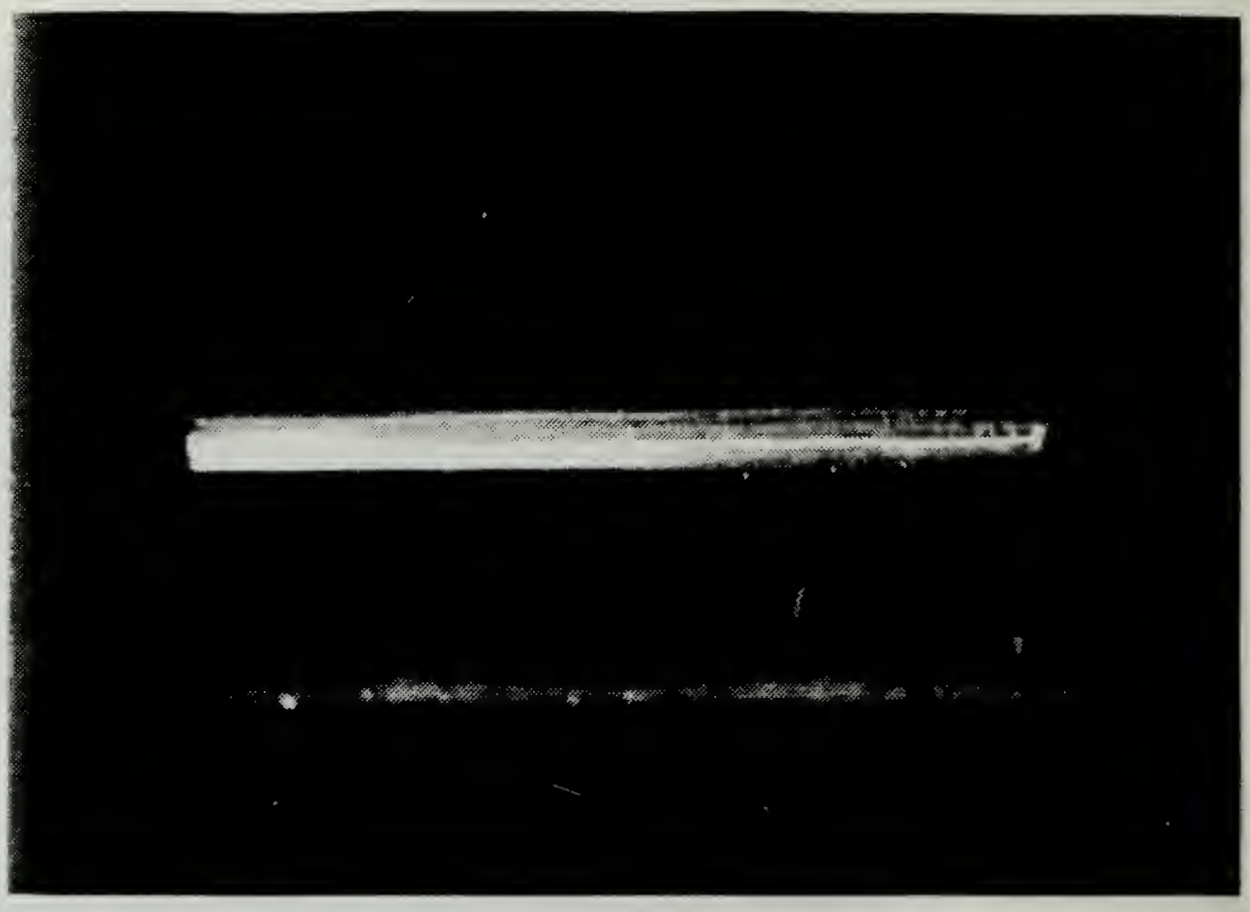

Figure C.2

I-18 2100-2315 08 FEB 1987
9.4 % FLOW (rotameter)
MEAN AIR VELOCITY = 1.522 m/sec
VOLUMETRIC FLOW RATE = 0.00982 m^3/sec
MASS FLOW RATE = 0.01196 kg/sec
ATMOSPHERIC PRESS. & TEMP: 29.92 in. Hg, 65.2 deg F
SLIT LOC. = 128 deg.
WIRE LOC. = 112 deg.
WIRE DIA. = 0.0125 IN. Re_w = 46
SLIT DISTANCE FROM START OF CURVE (X) = 1.348 m
Re_x = 131,499
De^x = 181
Re_c = 1239 Re_h = 2418
KODAK TRI-X FILM ASA 400 (f2.8, B)

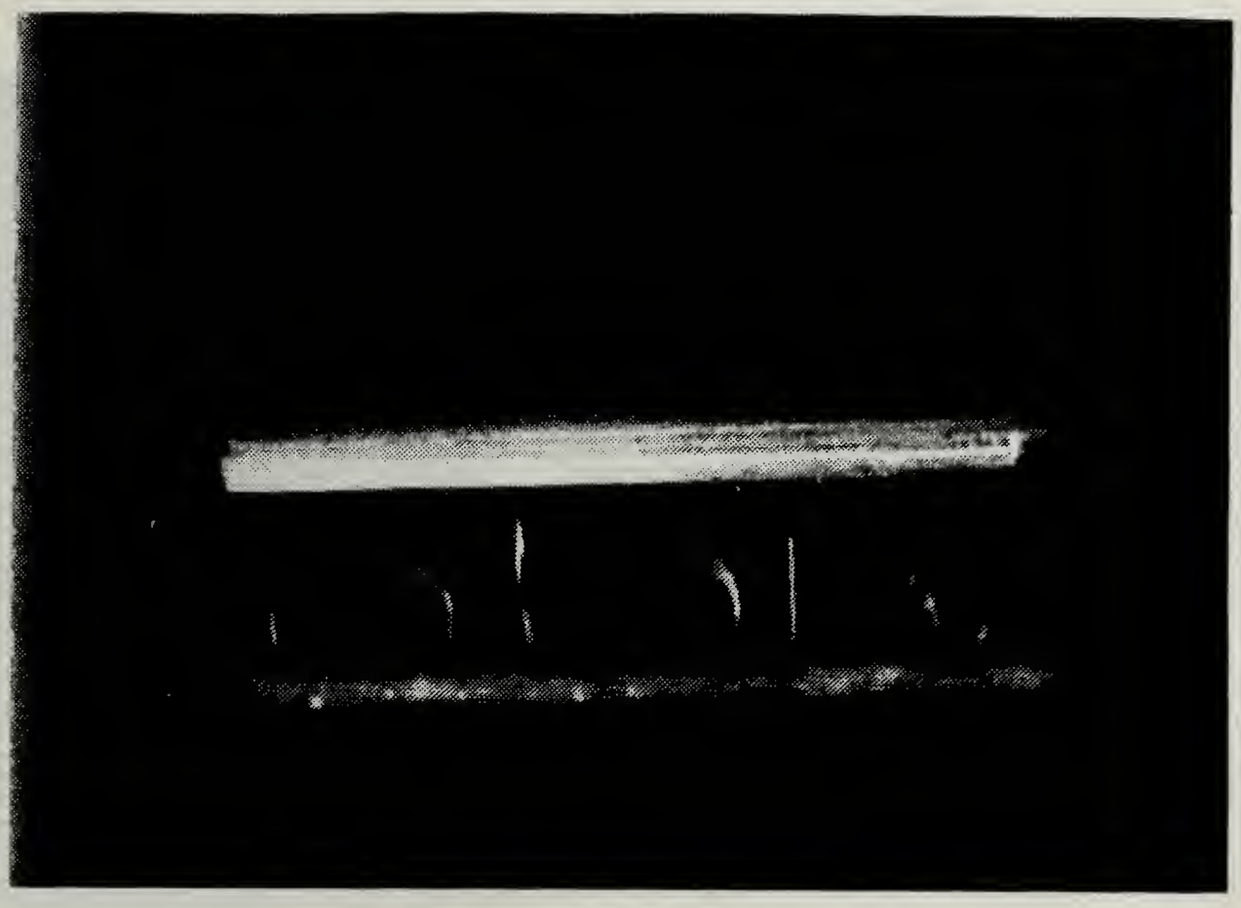

Figure C.3

I-23 2100-2315 08 FEB 1987
8.0 % FLOW (rotameter)
MEAN AIR VELOCITY = 1.405 m/sec
VOLUMETRIC FLOW RATE = 0.00906 m^3/sec
MASS FLOW RATE = 0.01104 kg/sec
ATMOSPHERIC PRESS. & TEMP: 29.92 in. Hg, 65.2 deg F
SLIT LOC. = 128 deg.
WIRE LOC. = 112 deg.
WIRE DIA = 0.0125 in. Re_w = 43
SLIT DISTANCE FROM START OF CURVE (X) = 1.348 m
Re_x = 121,325
De = 167
Re_c = 1143 Re_h = 2231
KODAK TRI-X FILM ASA 400 (f2.8, B)

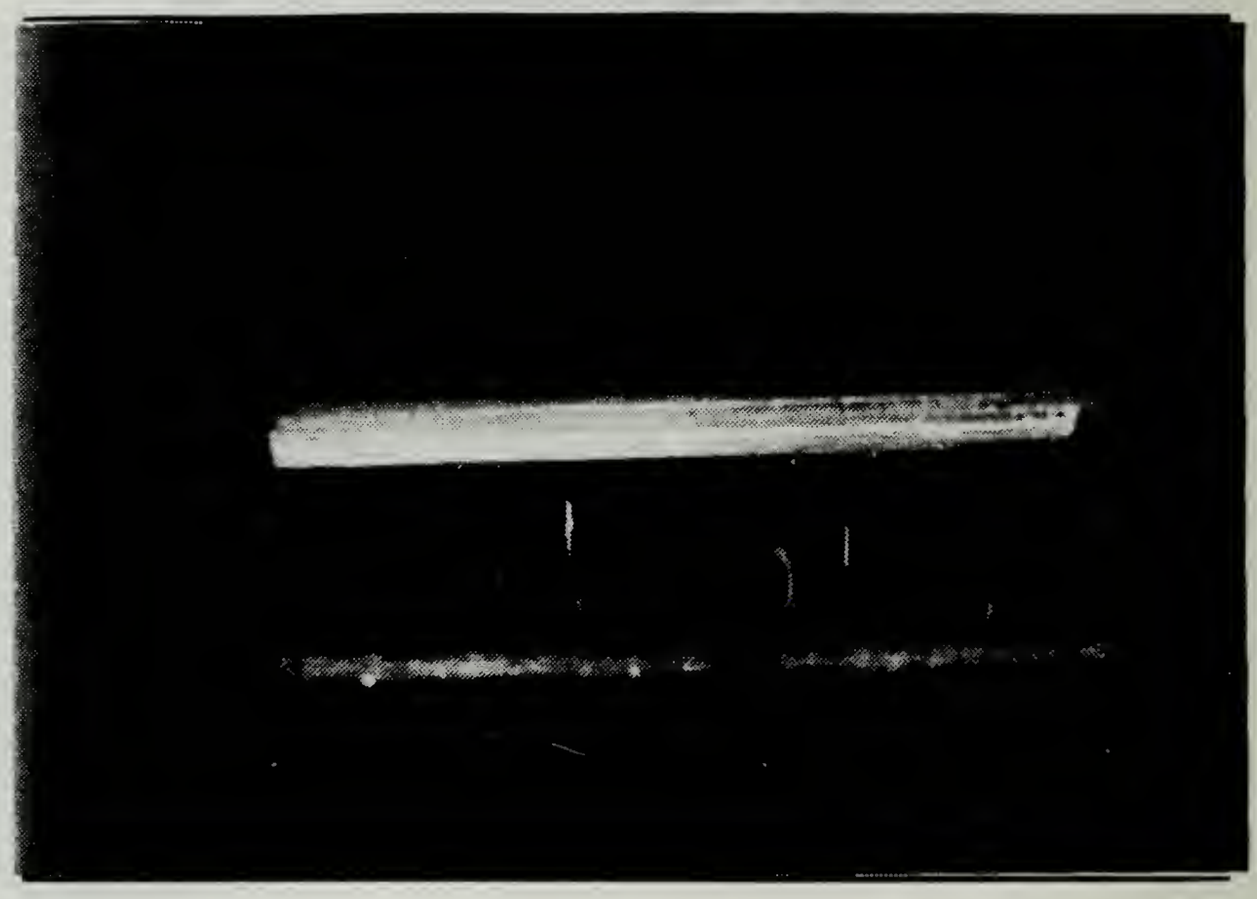

Figure C.4

I-24 2100-2315 08 FEB 1987
8.0 % FLOW (rotameter)
MEAN AIR VELOCITY = 1.405 m/sec
VOLUMETRIC FLOW RATE = 0.00906 m^3/sec
MASS FLOW RATE = 0.01104 kg/sec
ATMOSPHERIC PRESS. & TEMP: 29.92 in. Hg, 65.2 deg F
SLIT LOC. = 128 deg.
WIRE LOC. = 112 deg.
WIRE DIA. = 0.0125 IN. Re_w = 43
SLIT DISTANCE FROM START OF CURVE (X) = 1.348 m
Re_x = 121,325
De = 167
Re_c = 1143 Re_h = 2231
KODAK TRI-X FILM ASA 400 (F2.8, B)

Figure C.5

II-7 2100-2330 09 FEB 1987
9.5 % FLOW (rotameter)
MEAN AIR VELOCITY = 1.531 m/sec
VOLUMETRIC FLOW RATE = 0.00988 m^3/sec
MASS FLOW RATE = 0.01203 kg/sec
ATMOSPHERIC PRESS. & TEMP: 29.96 in. Hg, 65.0 deg F
SLIT LOC. = 123 deg.
WIRE LOC. = 112 deg.
WIRE DIA. = 0.0050 IN. Re_w = 19
SLIT DISTANCE FROM START OF CURVE (X) = 1.295 m
Re_x = 127,060
De = 182
Re_c = 1246 Re_h = 2432
KODAK TRI-X FILM ASA 400 (f2.8, B)

Figure C.6

II-10 2100-2330 09 FEB 1987
12.0 % FLOW (rotameter)
MEAN AIR VELOCITY = 1.741 m/sec
VOLUMETRIC FLOW RATE = 0.01123 m^3/sec
MASS FLOW RATE = 0.01368 kg/sec
ATMOSPHERIC PRESS. & TEMP: 29.96 in. Hg, 65.0 deg F
SLIT LOC. = 123 deg.
WIRE LOC. = 112 deg.
WIRE DIA. = 0.0050 in. Re_w = 21
SLIT DISTANCE FROM START OF CURVE (X) = 1.295 m
Re_x = 144,518
De^x = 207
Re_c = 1417 Re_h = 2766
KODAK TRI-X FILM ASA 400 (f2.8, B)

Figure C.7

II-12 2100-2330 09 FEB 1987
14.0 % FLOW (rotameter)
MEAN AIR VELOCITY = 1.909 m/sec
VOLUMETRIC FLOW RATE = 0.01232 m^3/sec
MASS FLOW RATE = 0.01501 kg/sec
ATMOSPHERIC PRESS. & TEMP: 29.96 in. Hg, 65.0 deg F
SLIT LOC. = 123 deg.
WIRE LOC. = 112 deg.
WIRE DIA. = 0.0050 in. Re_w = 23
SLIT DISTANCE FROM START OF CURVE (X) = 1.295 m
Re_x = 158,484
De^x = 227
Re_c = 1554 Re_h = 3033
KODAK TRI-X FILM ASA 400 (F2.8, B)

Figure C.8

II-16 2100-2330 09 FEB 1987
12.0 % FLOW (rotameter)
MEAN AIR VELOCITY = 1.741 m/sec
VOLUMETRIC FLOW RATE = 0.01123 m^3/sec
MASS FLOW RATE = 0.01368 kg/sec
ATMOSPHERIC PRESS. & TEMP: 29.96 in. Hg, 65.0 deg F
SLIT LOC. = 128 deg.
WIRE LOC. = 112 deg.
WIRE DIA. = 0.0050 in. Re_w = 21
SLIT DISTANCE FROM START OF CURVE (X) = 1.348 m
Re_x = 150,392
De = 207
Re_c = 1417 Re_h = 2766
KODAK TRI-X FILM ASA 400 (f2.8, B)

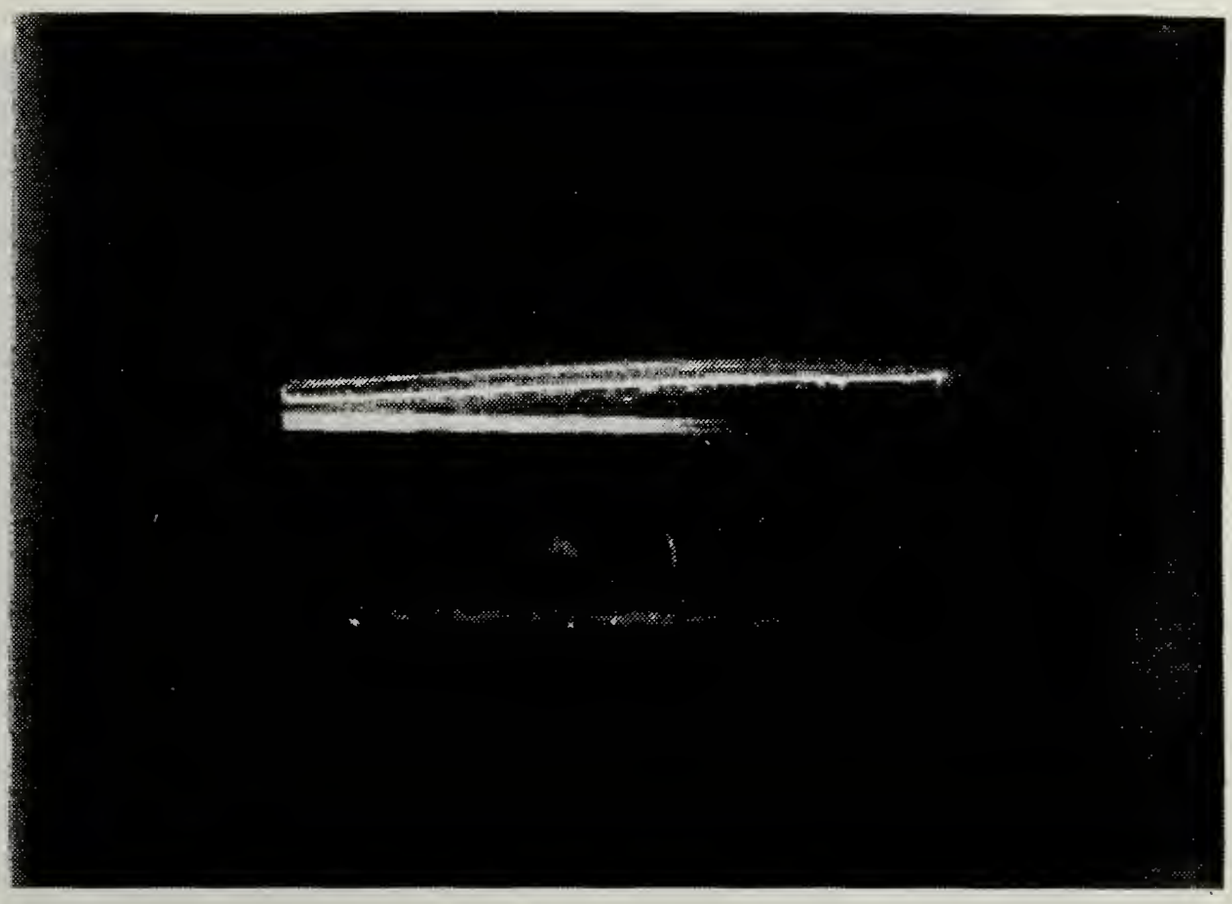

Figure C.9

II-18 2100-2300 09 FEB 1987
14.0 % FLOW (rotameter)
MEAN AIR VELOCITY = 1.909 m/sec
VOLUMETRIC FLOW RATE = 0.01232 m^3/sec
MASS FLOW RATE = 0.01501 kg/sec
ATMOSPHERIC PRESS. & TEMP: 29.96 in. Hg, 65.0 deg F
SLIT LOC. = 128 deg.
WIRE LOC. = 112 deg.
WIRE DIA. = 0.0050 in. Re_w = 23
SLIT DISTANCE FORM START OF CURVE (X) = 1.348
Re_x = 164,926
De = 227
Re_c = 1554 Re_h = 3033
KODAK TRI-X FILM ASA 400 (f2.8, B)

Figure C.10

II-22 2100-2330 09 FEB 1987
16.0 % FLOW (rotameter)
MEAN AIR VELOCITY = 2.078 m/sec
VOLUMETRIC FLOW RATE = 0.01340 m^3/sec
MASS FLOW RATE = 0.01633 kg/sec
ATMOSPHERIC PRESS. & TEMP: 29.96 in. Hg, 65.0 deg F
SLIT LOC. = 118 deg.
WIRE LOC. = 112 deg.
WIRE DIA. = 0.0050 in. Re_w = 25
SLIT DISTANCE FROM START OF CURVE (X) = 1.242 m
Re_x = 165,440
De = 247
Re_c = 1691 Re_h = 3300
KODAK TRI-X FILM ASA 400 (f2.8, B)

Figure C.11

III-1 2100-2300 14 FEB 1987
8.0 % FLOW (rotameter)
MEAN AIR VELOCITY = 1.405 m/sec
VOLUMETRIC FLOW RATE = 0.00906 m^3/sec
MASS FLOW RATE = 0.01104 kg/sec
ATMOSPHERIC PRESS. & TEMP: 29.96 in. Hg, 63.6 deg F
SLIT LOC. = 123 deg.
WIRE LOC. = 112 deg.
WIRE DIA. = 0.0050 in. Re_w = 17
SLIT DISTANCE FROM START OF CURVE (X) = 1.295 m
Re_x = 116,586
De = 167
Re_c = 1143 Re_h = 2231
KODAK RECORDING FILM ASA 1,000 (f2.8, B)

Figure C.12

III-5 2100-2300 14 FEB 1987
8.0 % FLOW (rotameter)
MEAN AIR VELOCITY = 1.405 m/sec
VOLUMETRIC FLOW RATE = 0.00906 m^3/sec
MASS FLOW RATE = 0.01104 kg/sec
ATMOSPHERIC PRESS. & TEMP: 29.97 in. Hg, 63.6 deg F
SLIT LOC. = 123 deg.
WIRE LOC. = 112 deg.
WIRE DIA. = 0.0050 IN. Re_w = 17
SLIT DISTANCE FROM START OF CURVE (X) = 1.295 m
Re_x = 116,586
De = 167
Re_c = 1143 Re_h = 2231
KODAK RECORDING FILM ASA 1,000 (f2.8, B)

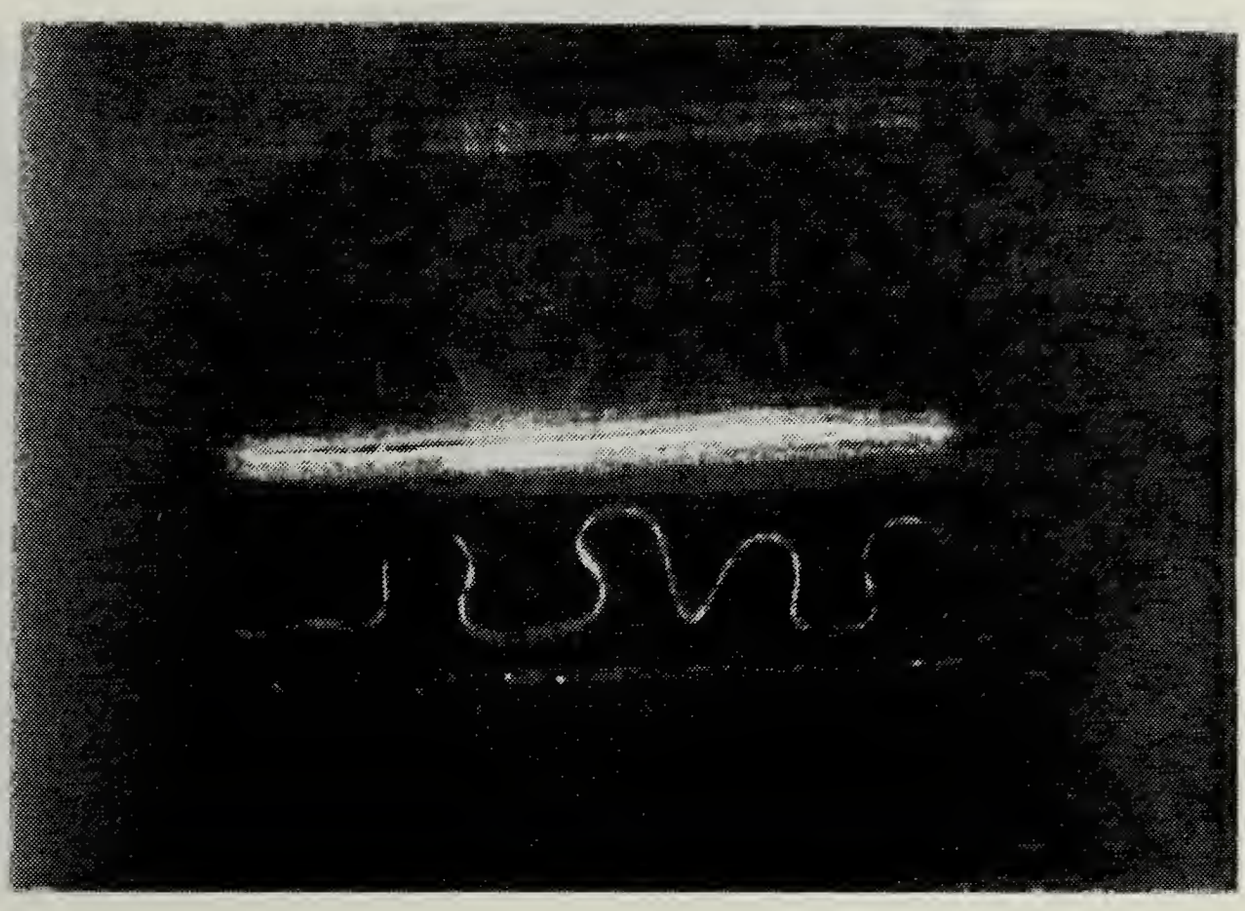

Figure C.13

III-9 2100-2300 14 FEB 1987
9.0 % FLOW (rotameter)
MEAN AIR VELOCITY = 1.489 m/sec
VOLUMETRIC FLOW RATE = 0.00960 m^3/sec
MASS FLOW RATE = 0.01170 kg/sec
ATMOSPHERIC PRESS. & TEMP: 29.97 in. Hg, 63.6 deg F
SLIT LOC. = 123 deg.
WIRE LOC. = 112 deg.
WIRE DIA. = 0.0050 in. Re_w = 18
SLIT DISTANCE FROM START OF CURVE (X) = 1.295 m
Re_x = 123,569
De = 177
Re_c = 1212 Re_h = 2365
KODAK RECORDING FILM ASA 1,000 (f2.8, B)

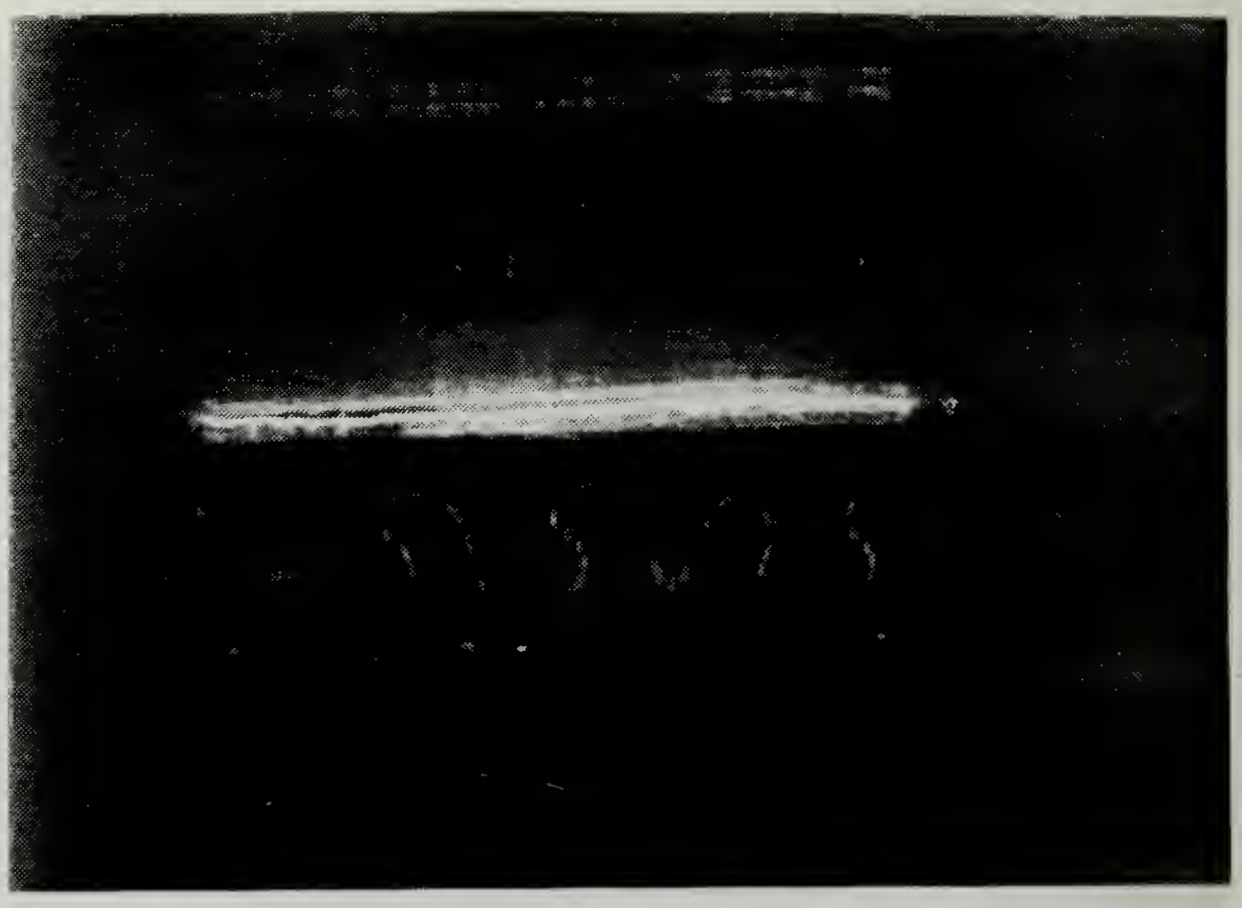

Figure C.14

III-11 2100-2300 14 FEB 1987
10.0 % FLOW (rotameter)
MEAN AIR VELOCITY = 1.573 m/sec
VOLUMETRIC FLOW RATE = 0.01015 m^3/sec
MASS FLOW RATE = 0.01236 kg/sec
ATMOSPHERIC PRESS. & TEMP: 29.97 in. Hg, 63.6 deg F
SLIT LOC. = 123 deg.
WIRE LOC. = 112 deg.
WIRE DIA. = 0.0050 in. Re_w = 19
SLIT DISTANCE FROM START OF CURVE (X) = 1.295 m
Re_x = 130,522
De = 187
Re_c = 1280 Re_h = 2498
KODAK RECORDING FILM ASA 1,000 (f2.8, B)

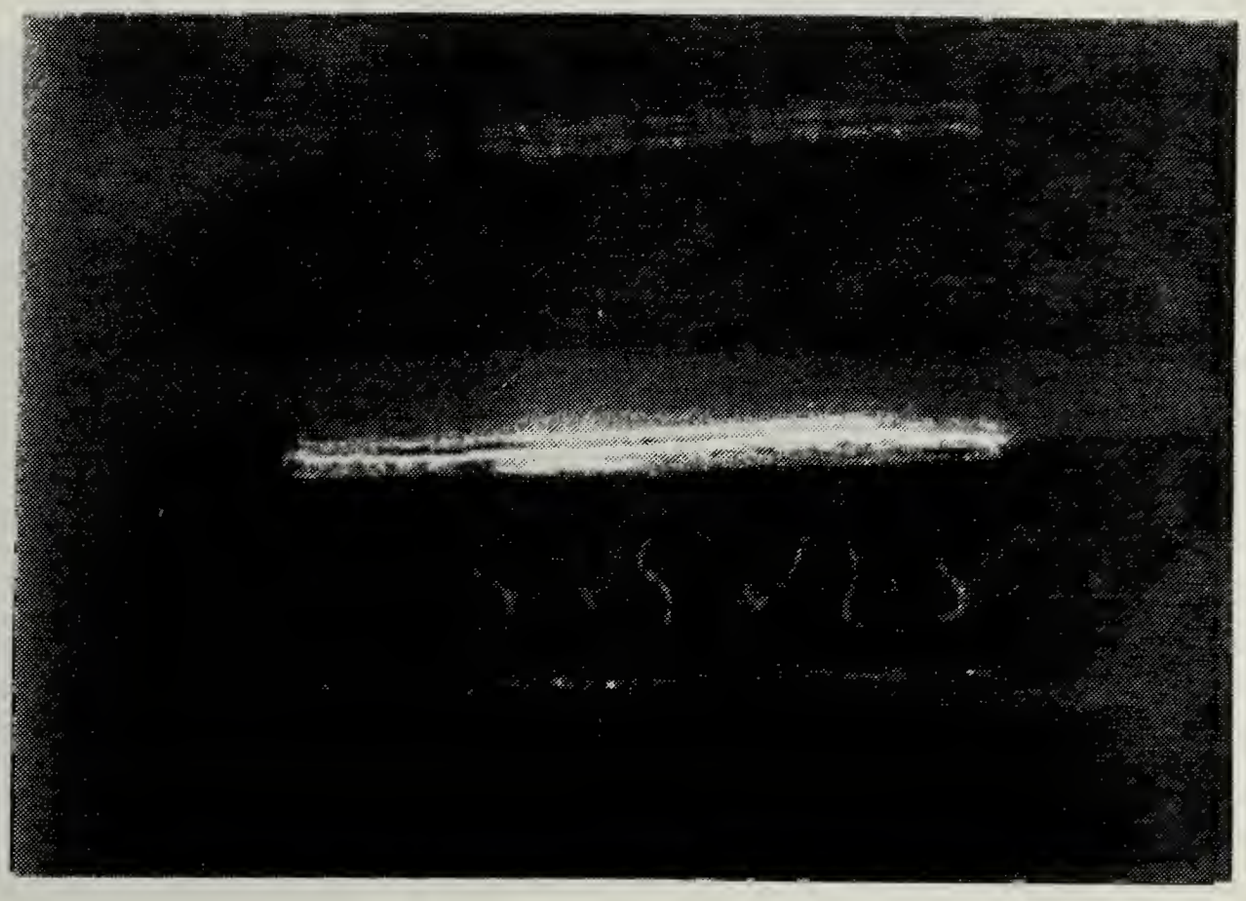

Figure C.15

III-13 2100-2300 14 FEB 1987
11.0 % FLOW (rotameter)
MEAN AIR VELOCITY = 1.657 m/sec
VOLUMETRIC FLOW RATE = 0.01069 m^3/sec
MASS FLOW RATE = 0.01302 kg/sec
ATMOSPHERIC PRESS. & TEMP: 29.97 in. Hg, 63.6 deg F
SLIT LOC. = 123 deg.
WIRE LOC. = 112 deg.
WIRE DIA. = 0.0050 in. Re_w = 20
SLIT DISTANCE FROM START OF CURVE (X) = 1.295 m
Re_x = 137,535
De = 197
Re_c = 1349 Reh = 2632
KODAK RECORDING FILM ASA 1,000 (f2.8, B)

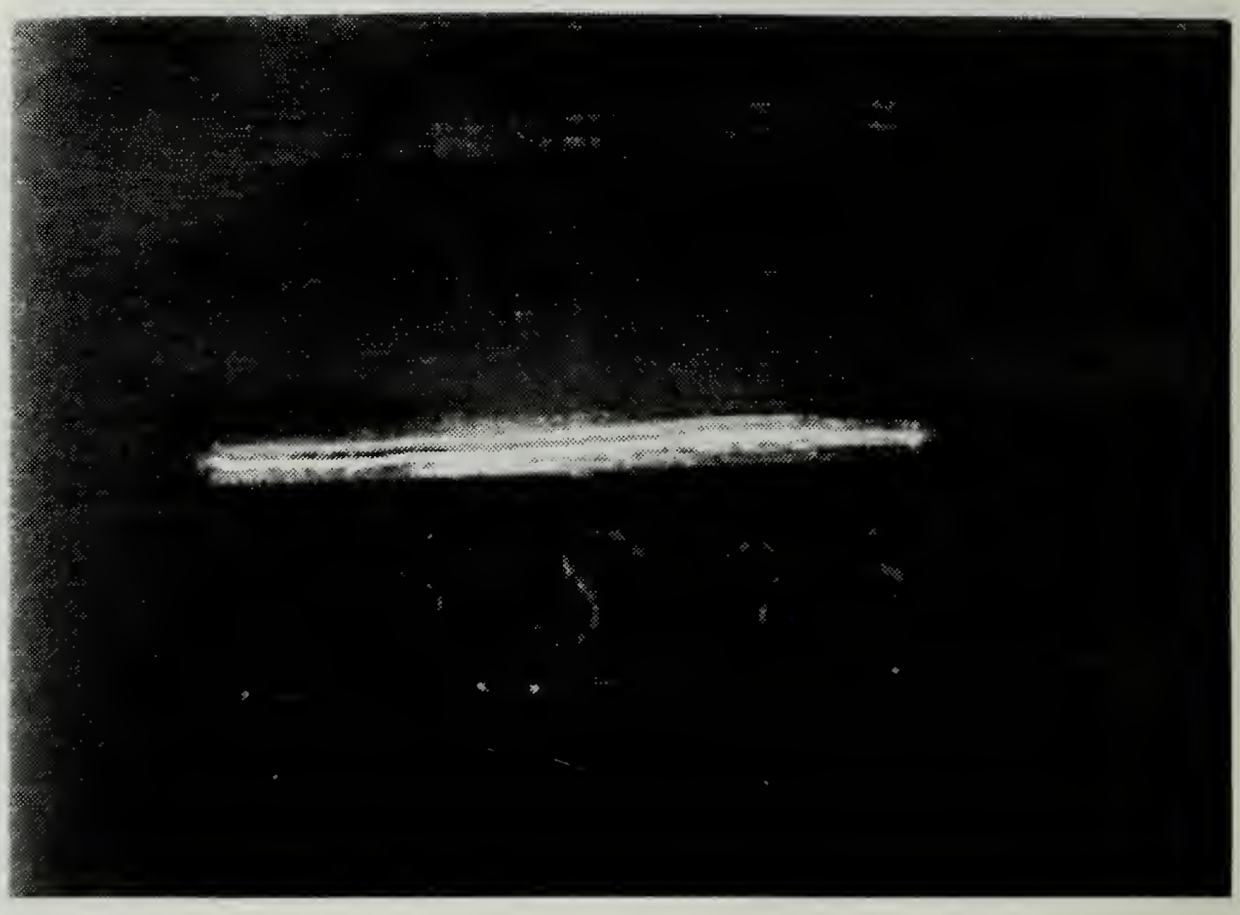

Figure C.16

III-15 2100-2300 14 FEB 1987
12.0 % FLOW (rotameter)
MEAN AIR VELOCITY = 1.741 m/sec
VOLUMETRIC FLOW RATE = 0.01123 m^3/sec
MASS FLOW RATE = 0.01368 kg/sec
ATMOSPHERIC PRESS. & TEMP: 29.97 in. Hg, 63.6 deg F
SLIT LOC. = 123 deg.
WIRE LOC. = 112 deg.
WIRE DIA. = 0.0050 in. Re_w = 21
SLIT DISTANCE FROM START OF CURVE (X) = 1.295 m
Re_x = 144,518
De^x = 207
Re_c = 1417 Re_h = 2766
KODAK RECORDING FILM ASA 1,000 (f2.8, B)

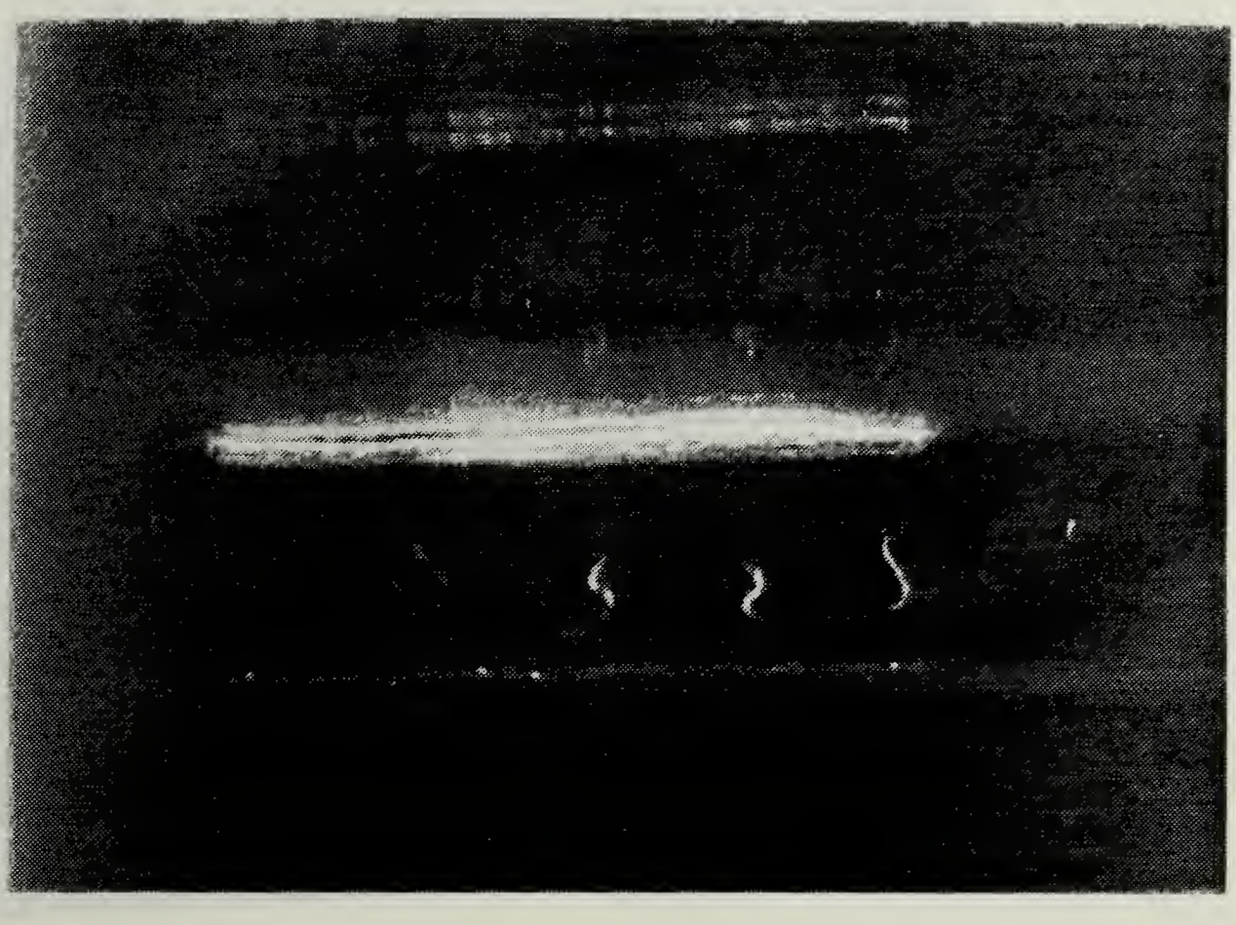

Figure C.17

III-17 2100-2300 14 FEB 1987
13.0 % FLOW (rotameter)
MEAN AIR VELOCITY = 1.825 m/sec
VOLUMETRIC FLOW RATE = 0.01178 m^3/sec
MASS FLOW RATE = 0.01434 kg/sec
ATMOSPHERIC PRESS. & TEMP: 29.97 in. Hg, 63.6 deg F
SLIT LOC. = 123 deg.
WIRE LOC. = 112 deg.
WIRE DIA. = 0.0050 in. Re_w = 22
SLIT DISTANCE FROM START OF CURVE (X) = 1.295 m
Re_x = 151,501
De = 217
Re_c = 1486 Re_h = 2899
KODAK RECORDING FILM ASA 1,000 (f2.8, B)

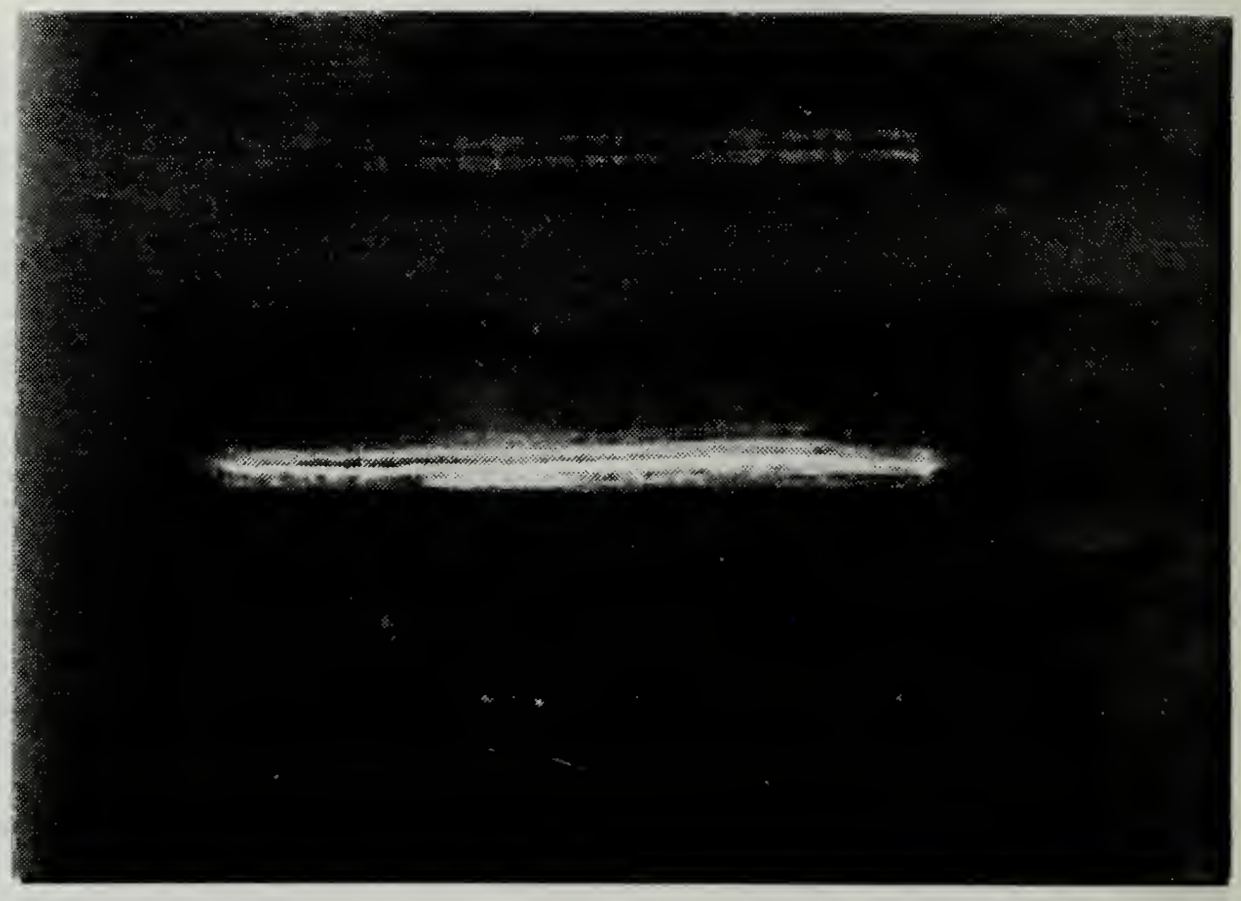

Figure C.18

III-19 2100-2300 14 FEB 1987
14.0 % FLOW (rotameter)
MEAN AIR VELOCITY = 1.909 m/sec
VOLUMETRIC FLOW RATE = 0.01232 m^3/sec
MASS FLOW RATE = 0.01501 kg/sec
ATMOSPHERIC PRESS. & TEMP: 29.97 in. Hg, 63.6 deg F
SLIT LOC. = 123 deg.
WIRE LOC. = 112 deg.
WIRE DIA. = 0.0050 in. Re_w = 23
SLIT DISTANCE FROM START OF CURVE (X) = 1.295 m
Re_x = 158,484
De = 227
Re_c = 1554 Re_h = 3033
KODAK RECORDING FILM ASA 1,000 (f2.8, B)

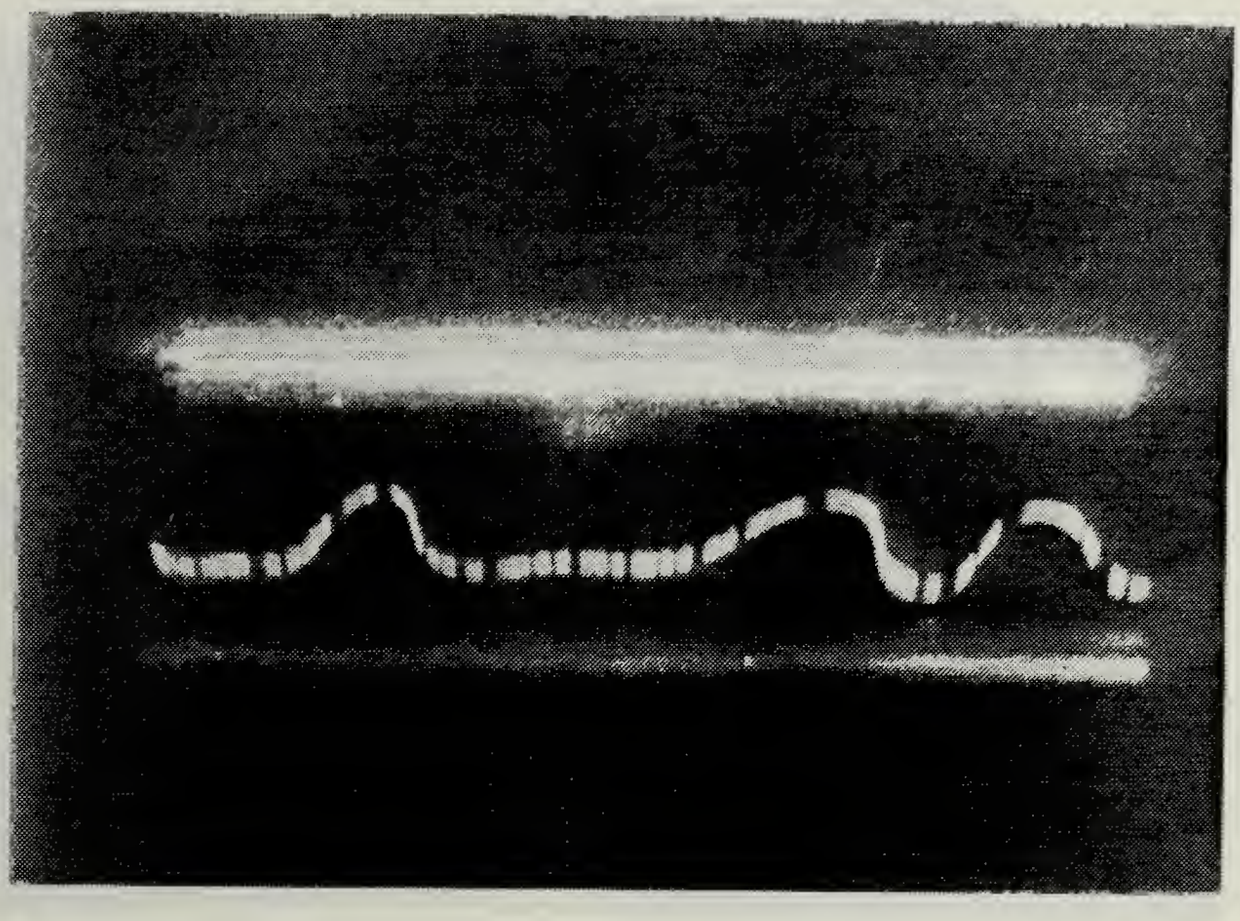

Figure C.19

III-21 2100-2300 14 FEB 1987
8.0 % FLOW (rotameter)
MEAN AIR VELOCITY = 1.405 m/sec
VOLUMETRIC FLOW RATE = 0.00906 m^3/sec
MASS FLOW RATE = 0.01104 kg/sec
ATMOSPHERIC PRESS. & TEMP: 29.97 in. Hg, 63.6 deg F
SLIT LOC. = 118 deg.
WIRE LOC. = 112 deg.
WIRE DIA. = 0.0050 in. Re_w = 17
SLIT DISTANCE FROM START OF CURVE (X) = 1.242 m
Re_x = 111,846
De^x = 167
Re_c = 1143 Re_h = 2231
KODAK RECORDING FILM ASA 1,000 (f2.8, B)

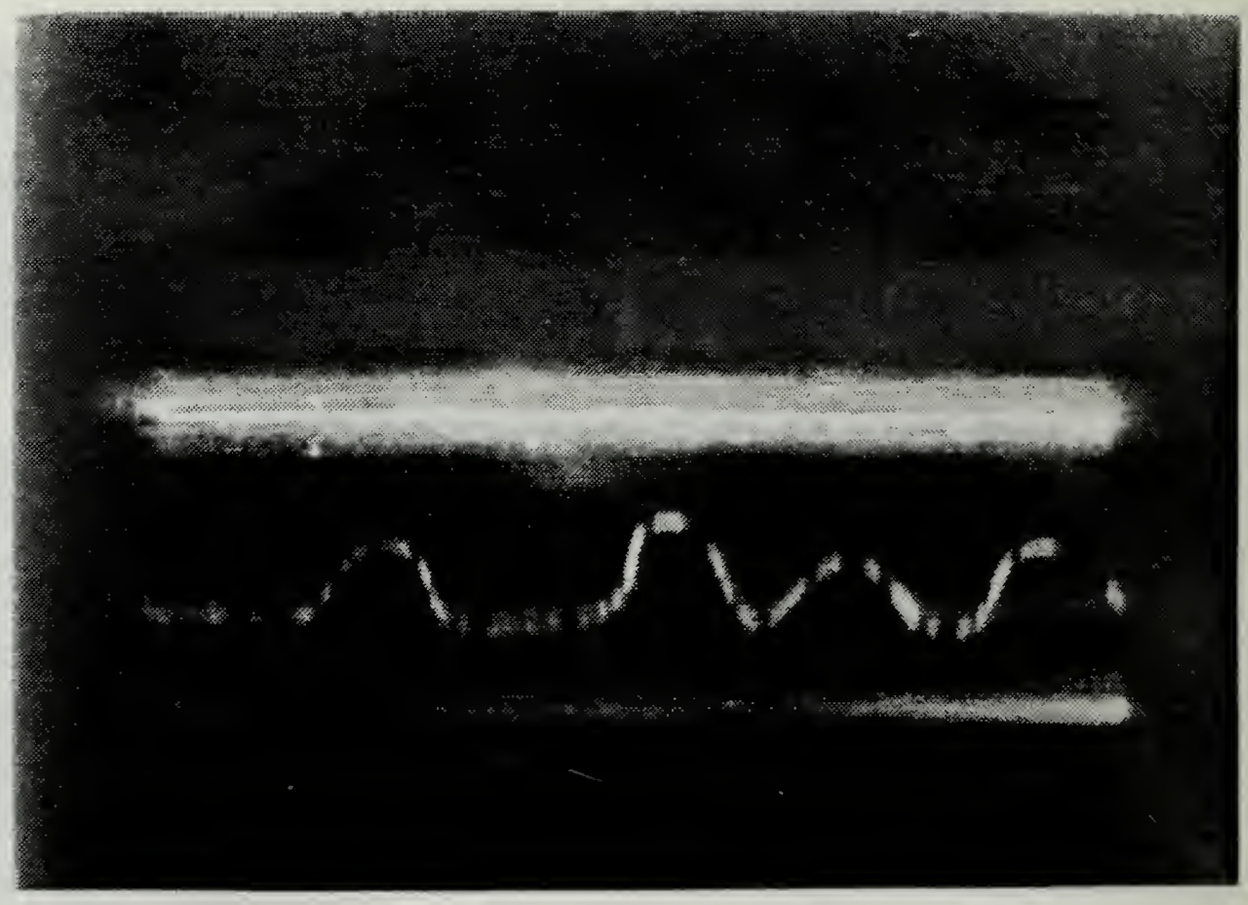

Figure C.20

III-22 2100-2300 14 FEB 1987
9.0 % FLOW (rotameter)
MEAN AIR VELOCITY = 1.489 m/sec
VOLUMETRIC FLOW RATE = 0.00960 m^3/sec
MASS FLOW RATE = 0.01170 kg/sec
ATMOSPHERIC PRESS. & TEMP: 29.97 in. Hg, 63.6 deg F
SLIT LOC. = 118 deg.
WIRE LOC. = 112 deg.
WIRE DIA. = 0.0050 in. Re_w = 18
SLIT DISTANCE FROM START OF CURVE (X) = 1.242 m
Re_x = 118,546
De = 177
Re_c = 1212 Re_h = 2365
KODAK RECORDING FILM ASA 1,000 (f2.8, B)

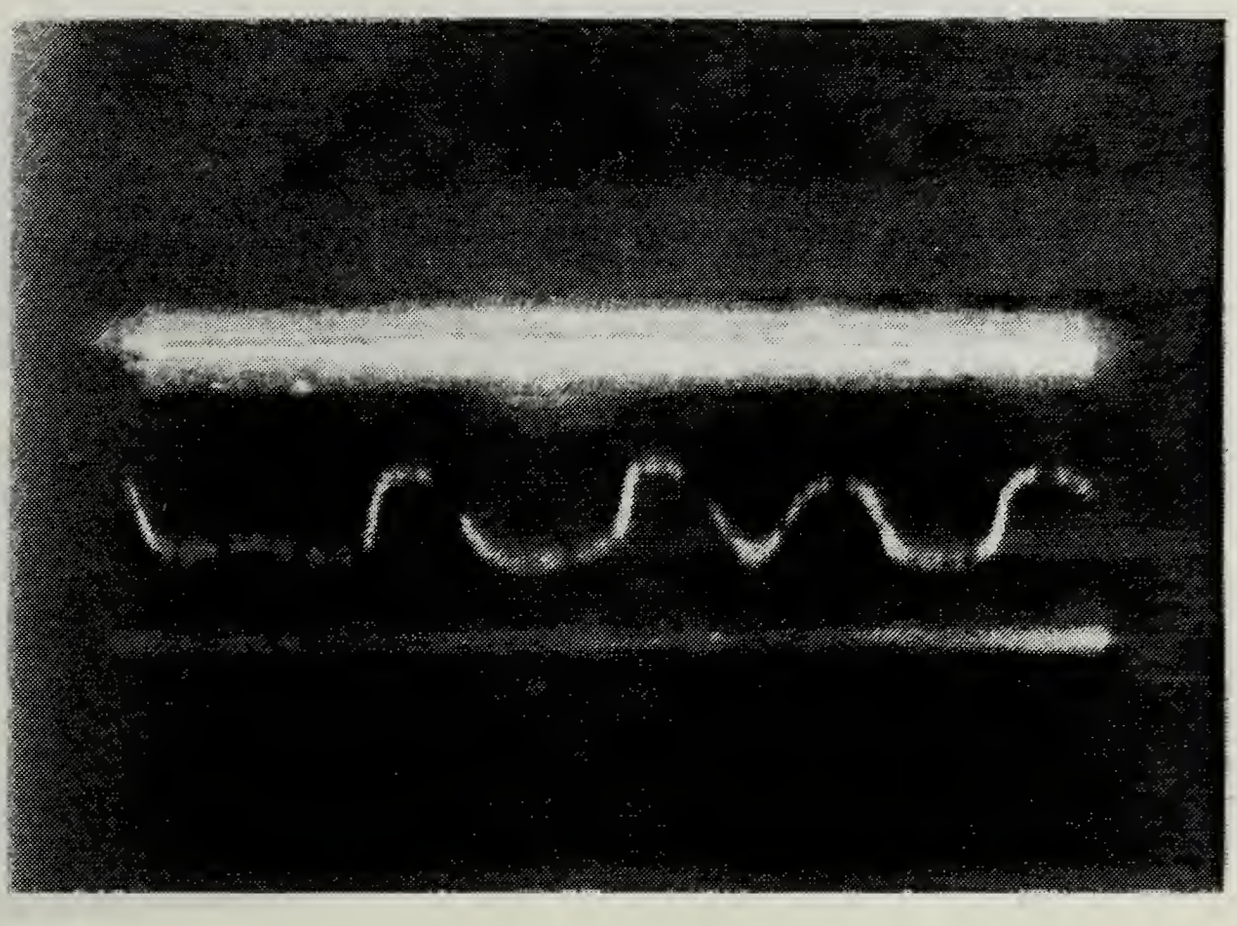

Figure C.21

III-23 2100-2300 14 FEB 1987
10.0 % FLOW (rotameter)
MEAN AIR VELOCITY = 1.573 m/sec
VOLUMETRIC FLOW RATE = 0.01015 m^3/sec
MASS FLOW RATE = 0.01236 kg/sec
ATMOSPHERIC PRESS. & TEMP: 29.97 in. Hg, 63.6 deg F
SLIT LOC. = 118 deg.
WIRE LOC. = 112 deg.
WIRE DIA. = 0.0050 in. Re_w = 19
SLIT DISTANCE FROM START OF CURVE (X) = 1.242 m
Re_x = 125,245
De = 187
Re_c = 1280 Re_h = 2498
KODAK RECORDING FILM ASA 1,000 (f2.8, B)

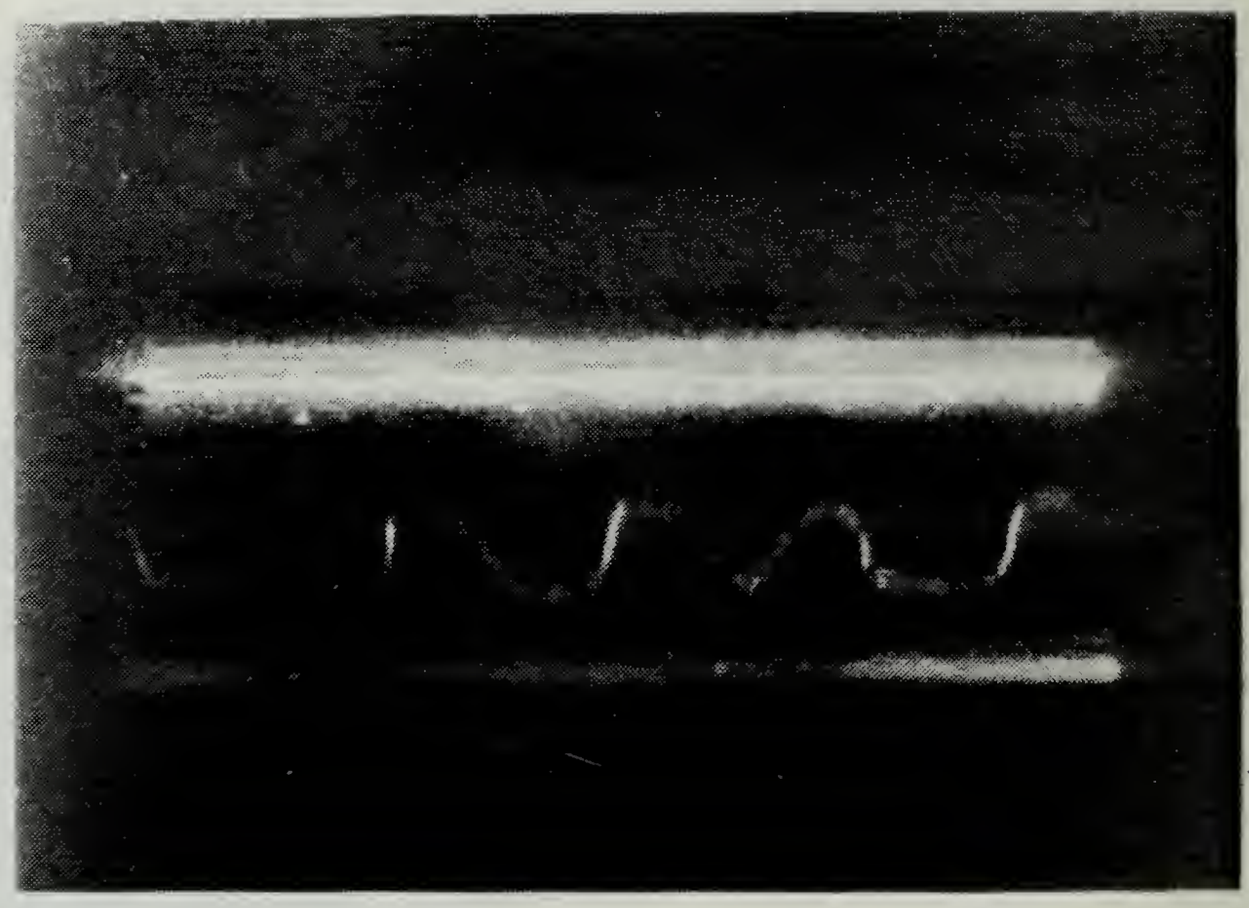

Figure C.22

III-24 2100-2300 14 FEB 1987
11.0 % FLOW (rotameter)
MEAN AIR VELOCITY = 1.657 m/sec
VOLUMETRIC FLOW RATE = 0.01069 m^3/sec
MASS FLOW RATE = 0.01302 kg/sec
ATMOSPHERIC PRESS. & TEMP: 29.97 in. Hg, 63.6 deg F
SLIT LOC. = 118 deg.
WIRE LOC. = 112 deg.
WIRE DIA. = 0.0050 in. Re_w = 20
SLIT DISTANCE FROM START OF CURVE (X) = 1.242 m
Re_x = 131,944
De^x = 197
Re_c = 1349 Re_h = 2632
KODAK RECORDING FILM ASA 1,000 (f2.8, B)

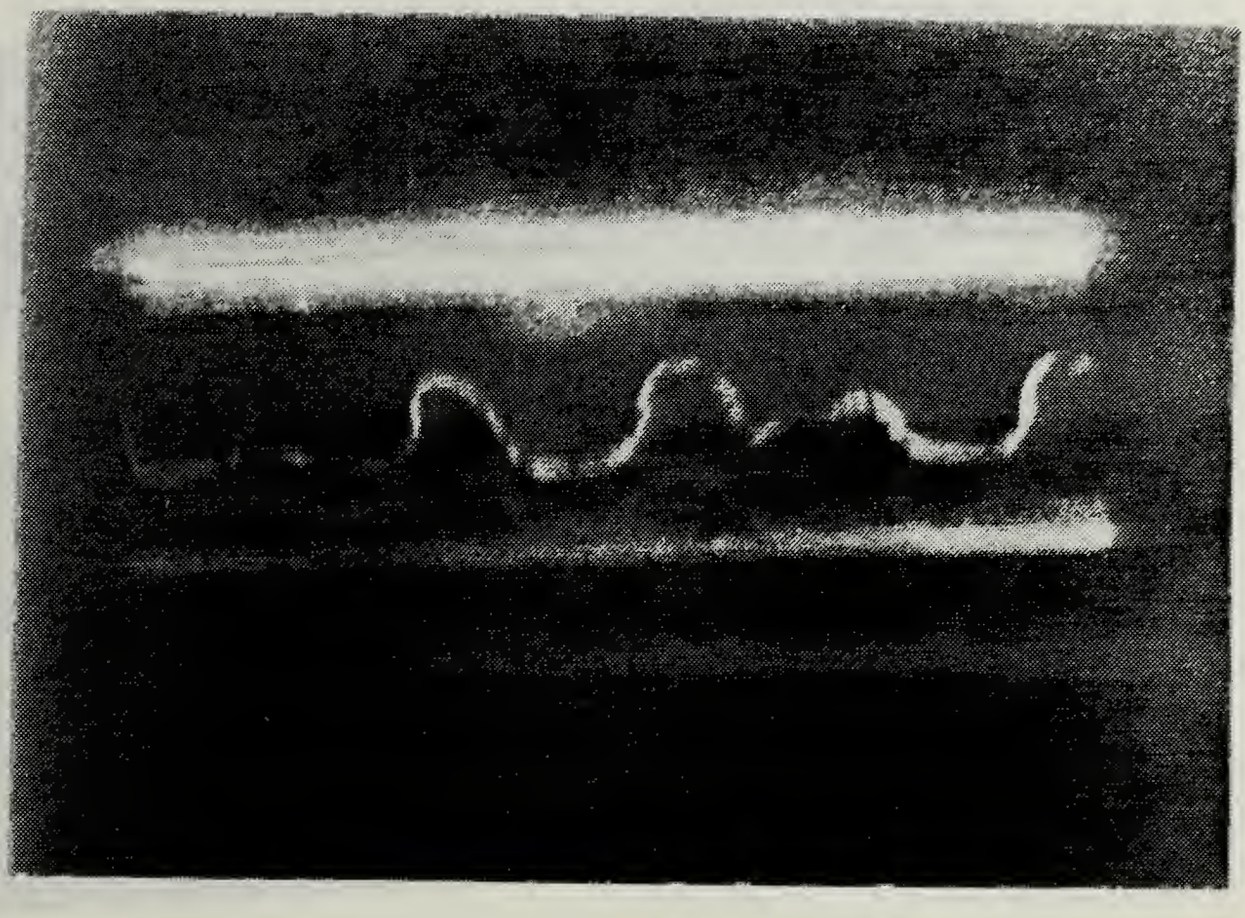

Figure C.23

III-25 2100-2300 14 FEB 1987
12.0 % FLOW (rotameter)
MEAN AIR VELOCITY = 1.741 m/sec
VOLUMETRIC FLOW RATE = 0.01123 m^3/sec
MASS FLOW RATE = 0.01368 kg/sec
ATMOSPHERIC PRESS. & TEMP: 29.97 in. Hg, 63.6 deg F
SLIT LOC. = 118 deg.
WIRE LOC. = 112 deg.
WIRE DIA. = 0.0050 in. Re_w = 21
SLIT DISTANCE FROM START OF CURVE (X) = 1.242 m
Re_x = 138,643
De = 207
Re_c = 1417 Re_h = 2766
KODAK RECORDING FILM ASA 1,000 (f2.8, B)

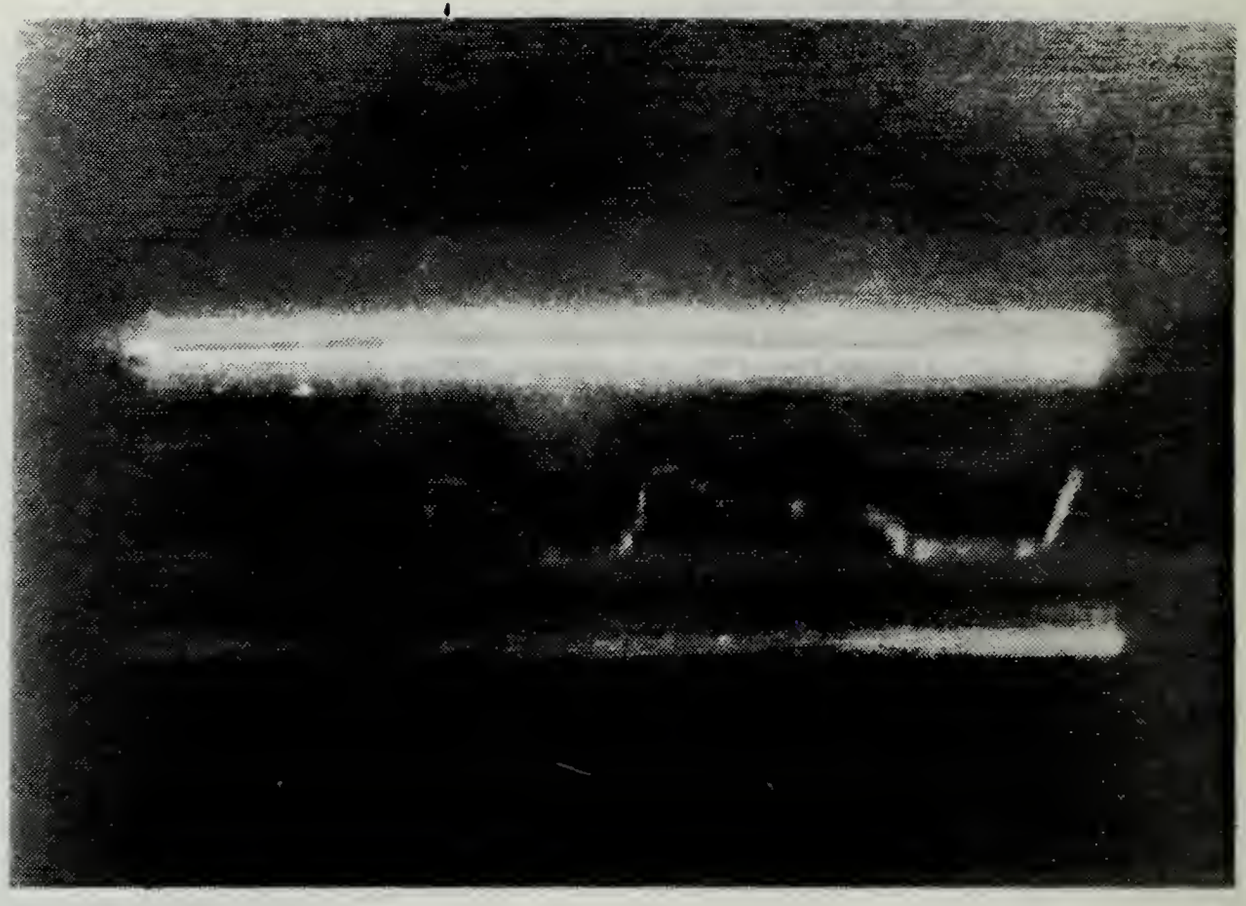

Figure C. 24

III-26 2100-2300 14 FEB 1987
13.0 % FLOW (rotameter)
MEAN AIR VELOCITY = 1.825 m/sec
VOLUMETRIC FLOW RATE = 0.01178 m^3/sec
MASS FLOW RATE = 0.01434 kg/sec
ATMOSPHERIC PRESS. & TEMP: 29.97 in. Hg, 63.6 deg F
SLIT LOC. = 118 deg.
WIRE LOC. = 112 deg.
WIRE DIA. = 0.0050 in. Re_w = 22
SLIT DISTANCE FROM START OF CURVE (X) = 1.242 m
Re_x = 145,342
De = 217
Re_c = 1486 Re_h = 2899
KODAK RECORDING FILM ASA 1,000 (f2.8, B)

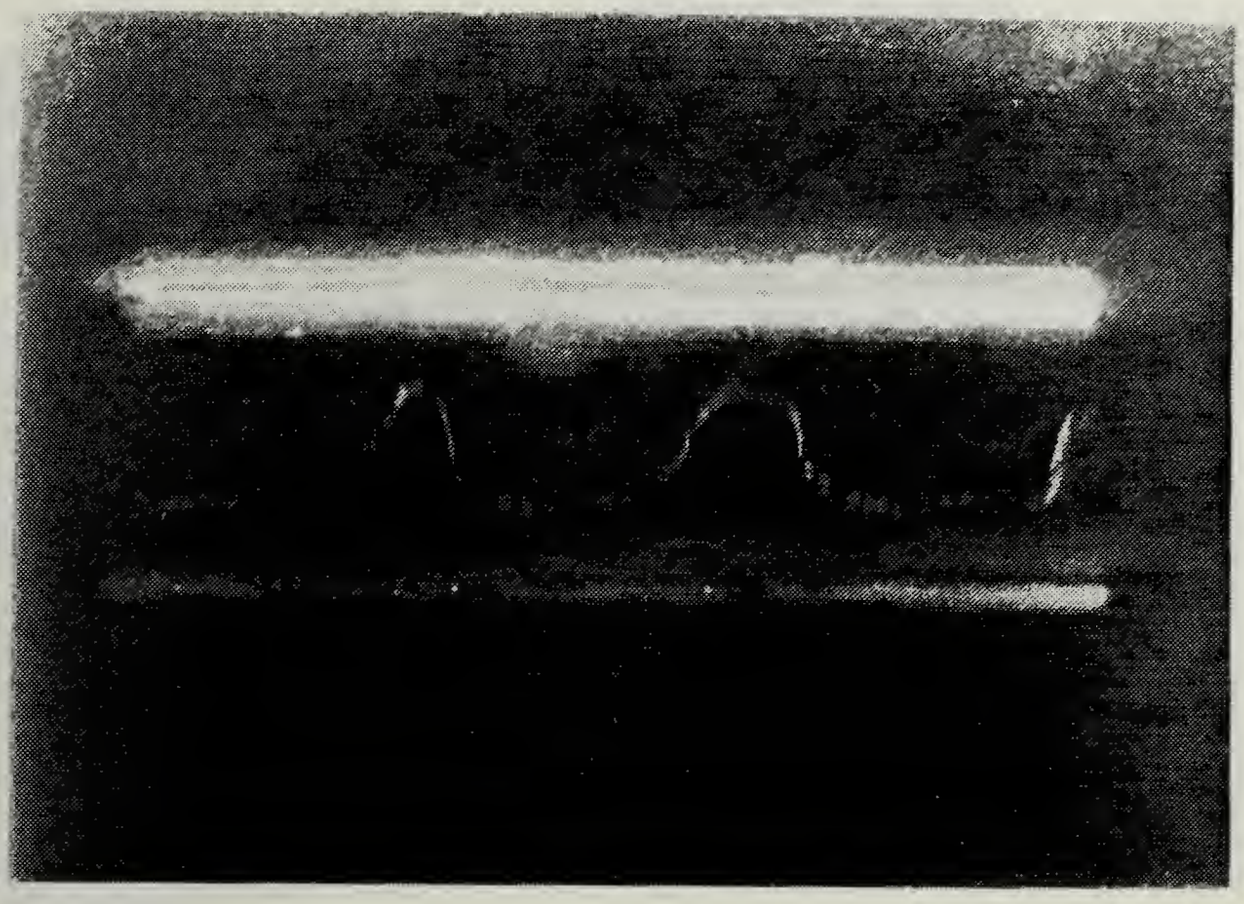

Figure C.25

III-27 2100-2300 14 FEB 1987
14.0 % FLOW (rotameter)
MEAN AIR VELOCITY = 1.909 m/sec
VOLUMETRIC FLOW RATE = 0.01232 m^3/sec
MASS FLOW RATE = 0.01501 kg/sec
ATMOSPHERIC PRESS. & TEMP: 29.97 in. Hg, 63.6 deg F
SLIT LOC. = 118 deg.
WIRE LOC. = 112 deg.
WIRE DIA. = 0.0050 in. Re_w = 23
SLIT DISTANCE FROM START OF CURVE (X) = 1.242 m
Re_x = 152,041
De^x = 227
Re_c = 1554 Re_h = 3033
KODAK RECORDING FILM ASA 1,000 (f2.8, B)

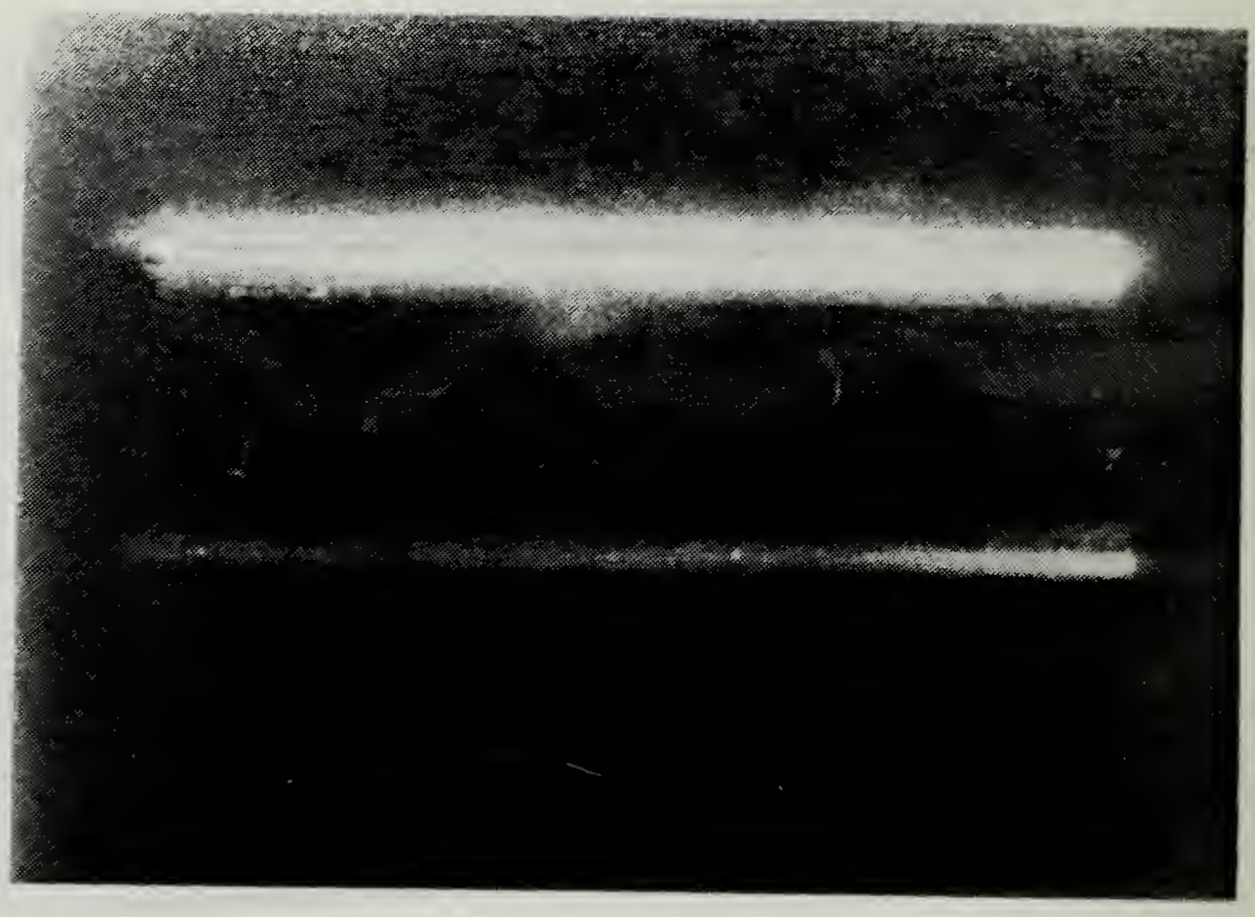

Figure C.26

III-28 2100-2300 14 FEB 1987
15.0 % FLOW (rotameter)
MEAN AIR VELOCITY = 1.993 m/sec
VOLUMETRIC FLOW RATE = 0.01286 m^3/sec
MASS FLOW RATE = 0.01567 kg/sec
ATMOSPHERIC PRESS. & TEMP: 29.97 in Hg, 63.6 deg F
SLIT LOC. = 118 deg.
WIRE LOC. = 112 deg.
WIRE DIA. = 0.0050 in. Re_w = 24
SLIT DISTANCE FROM START OF CURVE (X) = 1.242 m
Re_x = 158,740
De = 237
Re_c = 1623 Re_h = 3167
KODAK RECORDING FILM ASA 1,000 (f2.8, B)

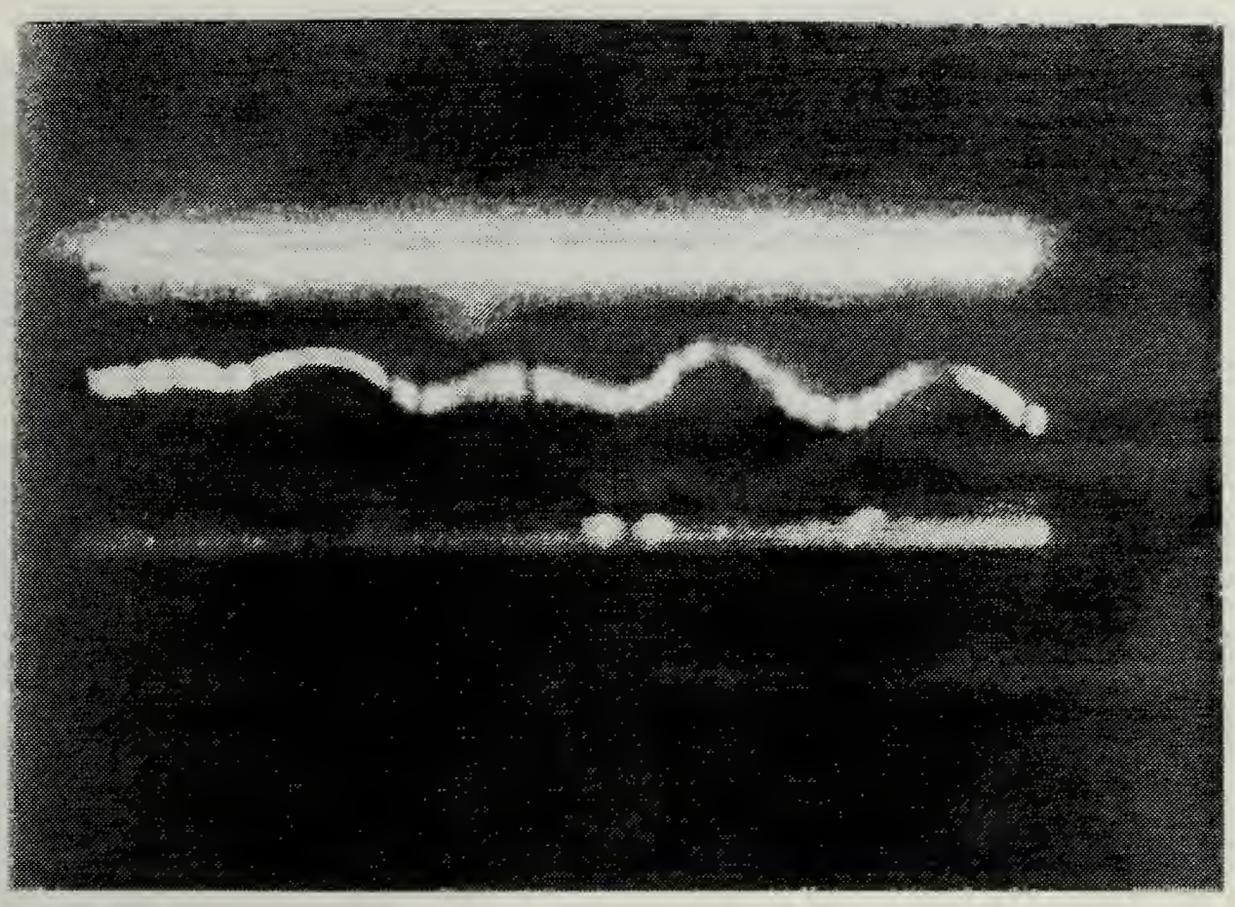

Figure C.27

III-33 2100-2300 14 FEB 1987
8.0 % FLOW (rotameter)
MEAN AIR VELOCITY = 1.405 m/sec
VOLUMETRIC FLOW RATE = 0.00906 m^3/sec
MASS FLOW RATE = 0.01104 kg/sec
ATMOSPHERIC PRESS. & TEMP: 29.97 in. Hg, 63.6 deg F
SLIT LOC. = 118 deg.
WIRE LOC. = 112 deg.
WIRE DIA. = 0.0125 in. Re_w = 43
SLIT DISTANCE FROM START OF CURVE (X) = 1.242 m
Re_x = 111,846
De = 167
Re_c = 1143 Re_h = 2231
KODAK RECORDING FILM ASA 1,000 (f2.8, B)

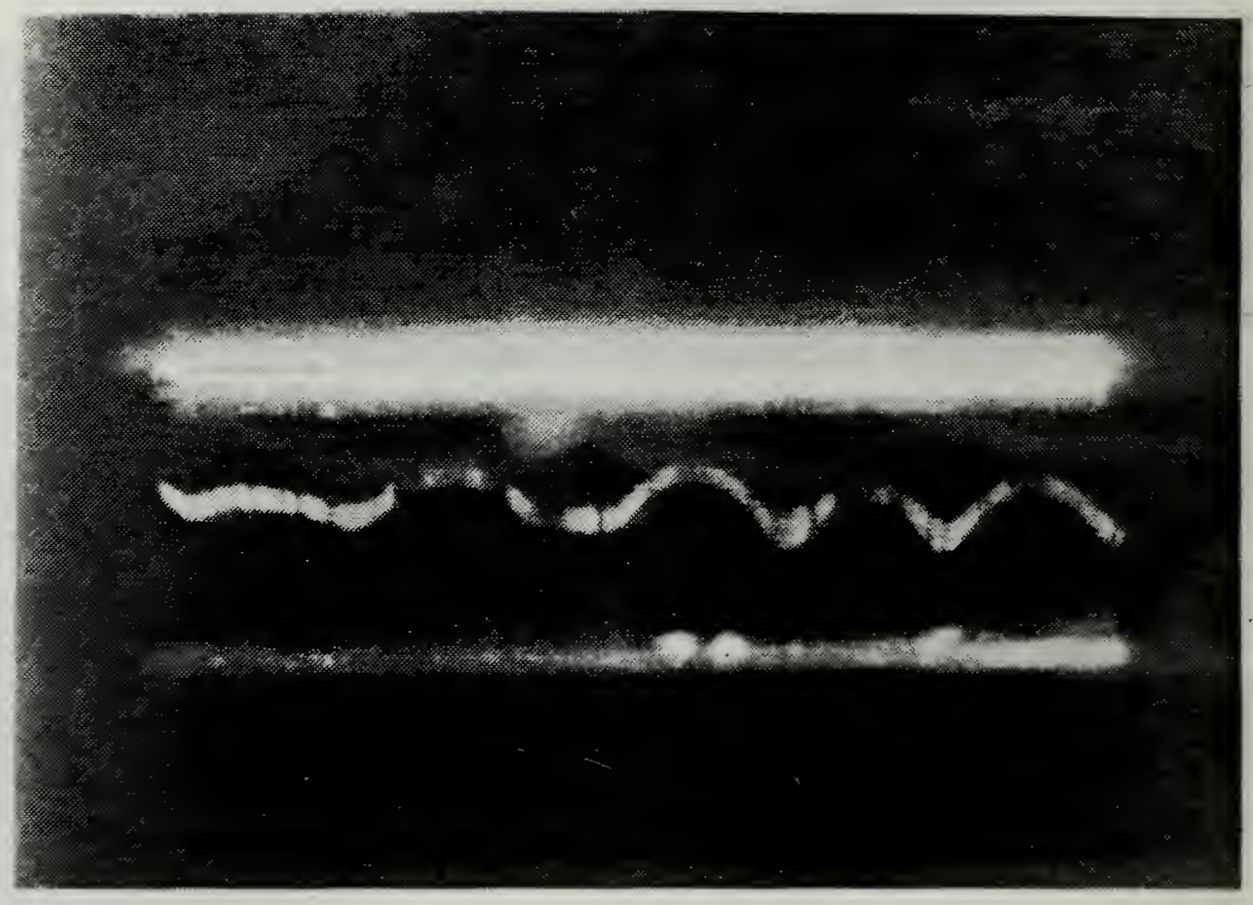

Figure C.28

III-34 2100-2300 14 FEB 1987
10.0 % FLOW (rotameter)
MEAN AIR VELOCITY = 1.573 m/sec
VOLUMETRIC FLOW RATE = 0.01015 m^3/sec
MASS FLOW RATE = 0.01236 kg/sec
ATMOSPHERIC PRESS. & TEMP: 29.97 in. Hg, 63.6 deg F
SLIT LOC. = 118 deg.
WIRE LOC. = 112 deg.
WIRE DIA. = 0.0125 in. Re_w = 48
SLIT DISTANCE FROM START OF CURVE (X) = 1.242 m
Re_x = 125,245
De = 187
Re_c = 1280 Re_h = 2498
KODAK RECORDING FILM ASA 1,000 (f2.8, B)

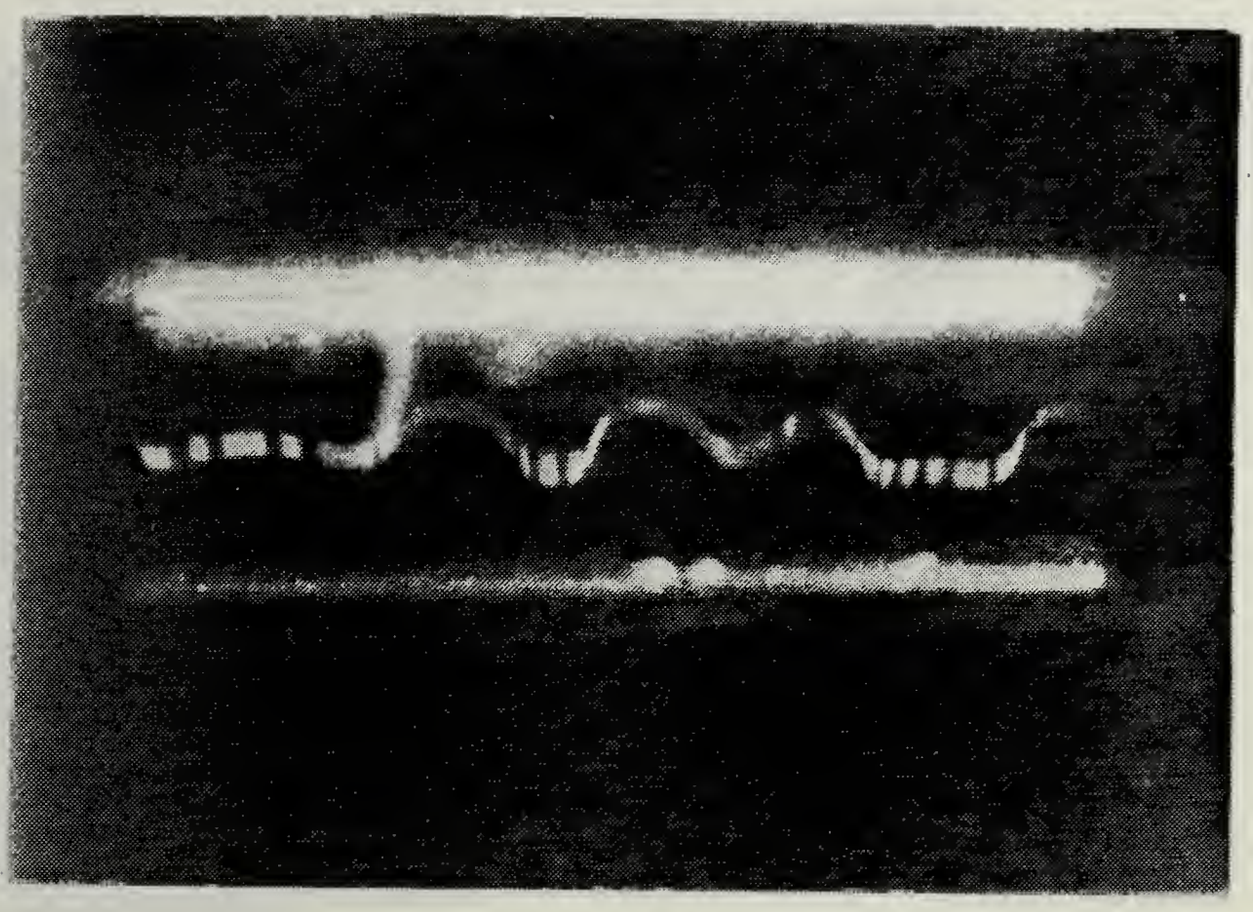

Figure C.29

III-35 2100-2300 14 FEB 1987
12.0 % FLOW (rotameter)
MEAN AIR VELOCITY = 1.74 m/sec
VOLUMETRIC FLOW RATE = 0.01123 m^3/sec
MASS FLOW RATE = 0.01368 kg/sec
ATMOSPHERIC PRESS. & TEMP: 29.97 in. Hg, 63.6 deg F
SLIT LOC. = 118 deg.
WIRE LOC. = 112 deg.
WIRE DIA. = 0.0125 in. Re_w = 53
SLIT DISTANCE FROM START OF CURVE (X) = 1.242 m
Re_x = 138,643
De = 207
Re_c = 1417 Re_h = 2766
KODAK RECORDING FILM ASA 1,000 (f2.8, B)

Figure C.30

III-36 2100-2300 14 FEB 1987
41.0 % FLOW (rotameter)
MEAN AIR VELOCITY = 1.909 m/sec
VOLUMETRIC FLOW RATE = 0.01232 m^3/sec
MASS FLOW RATE = 0.01501 kg/sec
ATMOSPHERIC PRESS. & TEMP: 29.97 in. Hg, 63.6 deg F
SLIT LOC. = 118 deg.
WIRE LOC. = 112 deg.
WIRE DIA. = 0.0125 in. Re_w = 58
SLIT DISTANCE FROM START OF CURVE (X) = 1.242 m
Re_x = 152,041
De = 227
Re_c = 1554 Re_h = 3033
KODAK RECORDING FILM ASA 1,000 (f2.8, B)

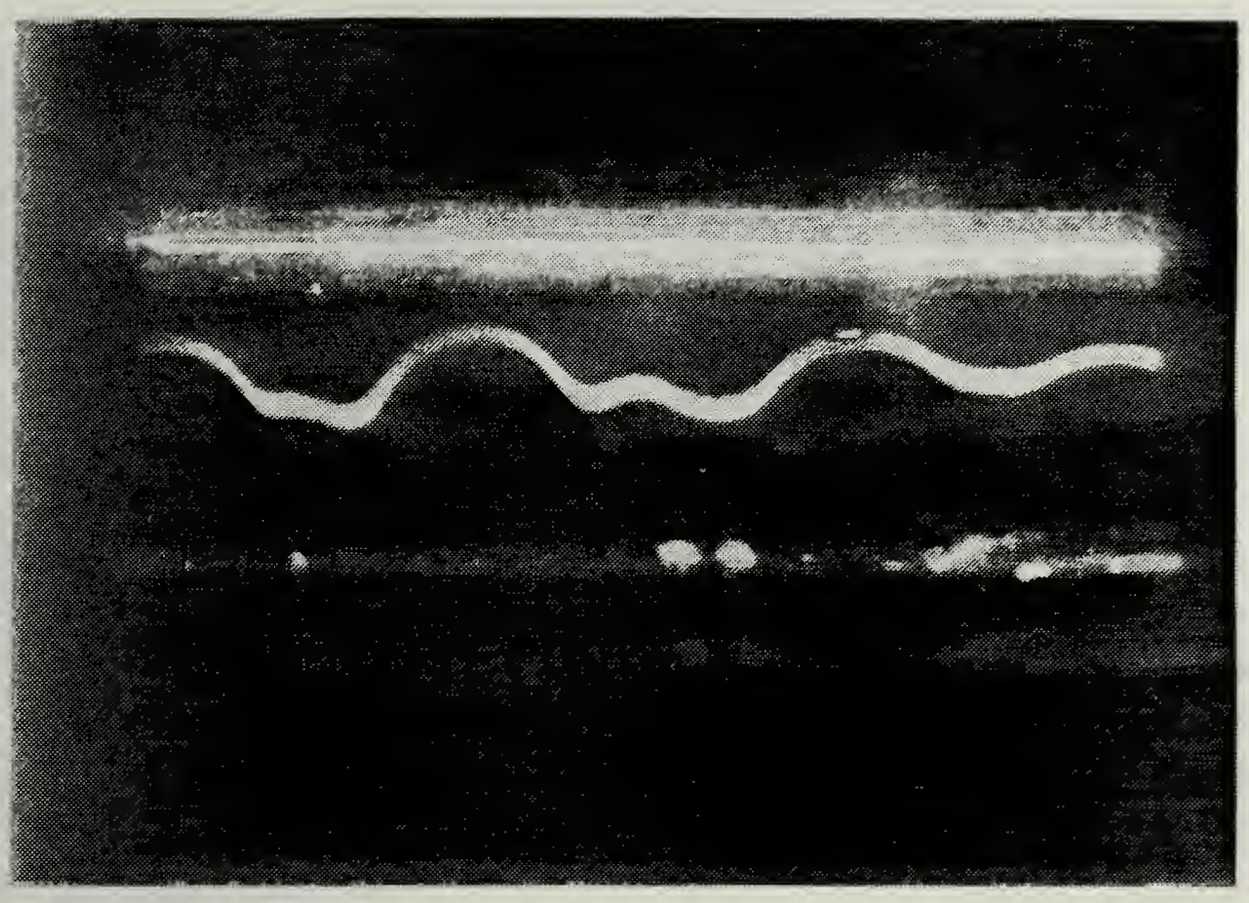

Figure C.31

IV-1 2100-2330 15 FEB 1987
8.0 % FLOW (rotameter)
MEAN AIR VELOCITY = 1.405 m/sec
VOLUMETRIC FLOW RATE = 0.00906 m^3/sec
MASS FLOW RATE = 0.01104 kg/sec
ATMOSPHERIC PRESS. & TEMP: 30.24 in. Hg, 64.0 deg F
SLIT LOC. = 118 deg
WIRE LOC. = 112 deg.
WIRE DIA. = 0.0125 in. Re_w = 43
SLIT DISTANCE FROM START OF CURVE (X) = 1.242 m
Re_x = 111,846
De = 167
Re_c = 1143 Re_h = 2231
KODAK RECORDING FILM ASA 1,000 (f2.8, B)

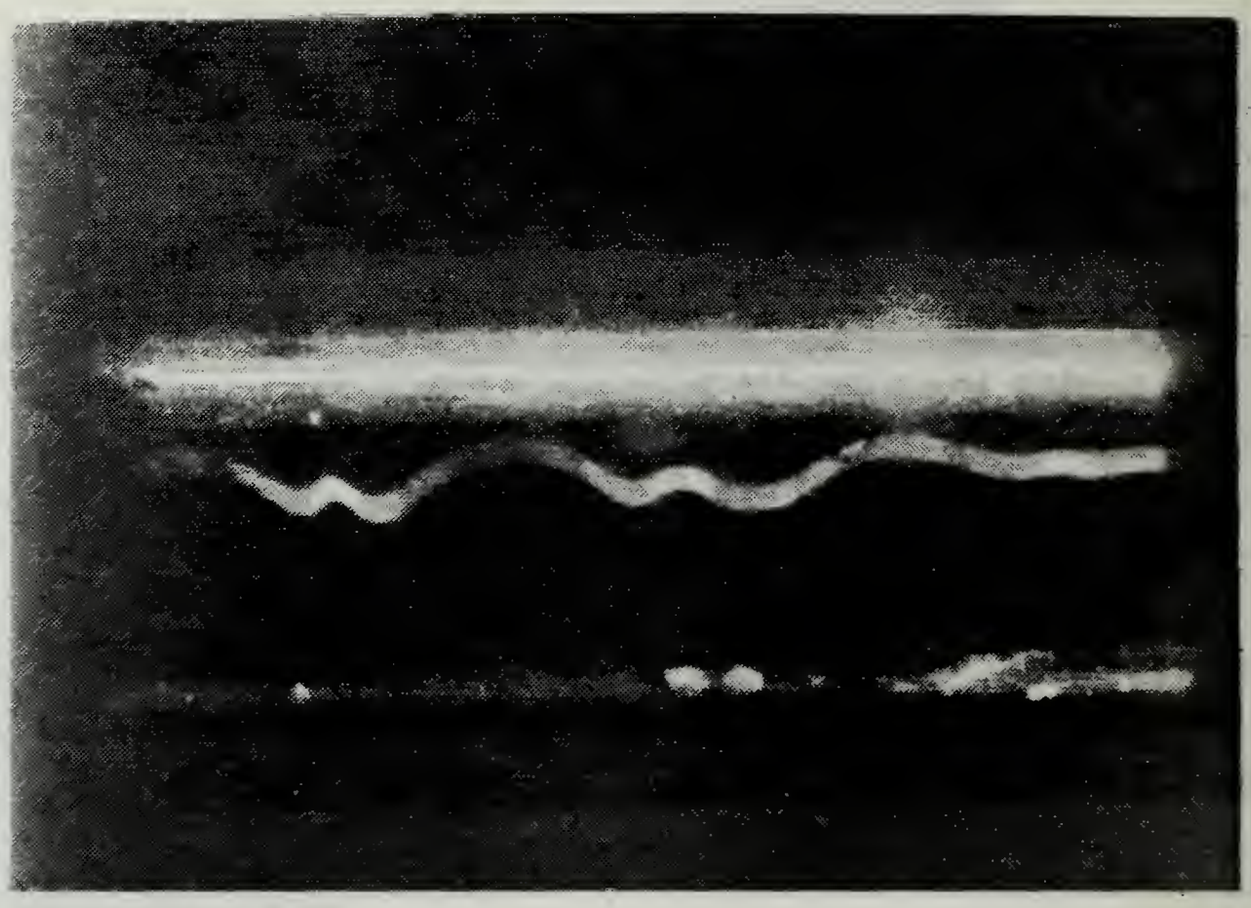

Figure C.32

IV-3 2100-2330 15 FEB 1987
8.0 % FLOW (rotameter)
MEAN AIR VELOCITY = 1.405 m/sec
VOLUMETRIC FLOW RATE = 0.00906 m^3/sec
MASS FLOW RATE = 0.01104 kg/sec
ATMOSPHERIC PRESS. & TEMP: 30.24 in. Hg, 64.0 deg F
SLIT LOC. = 118 deg.
WIRE LOC. = 112 deg.
WIRE DIA. = 0.0125 in. Re_w = 43
SLIT DISTANCE FROM START OF CURVE (X) = 1.242 m
Re_x = 111,846
De = 167
Re_c = 1143 Re_h = 2231
KODAK RECORDING FILM ASA 1,000 (f2.8, B)

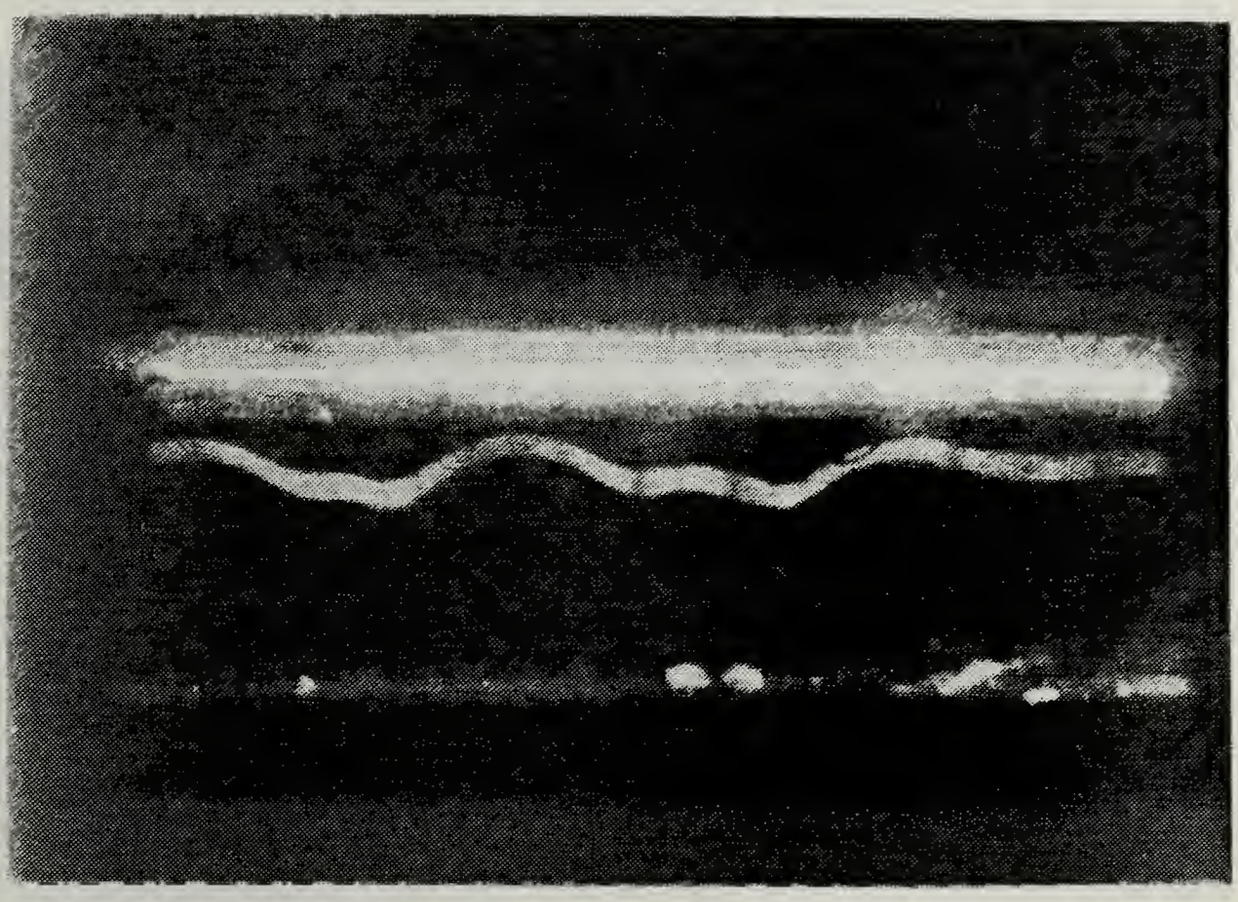

Figure C.33

IV-4 2100-2330 15 FEB 1987
8.0 % FLOW (rotameter)
MEAN AIR VELOCITY = 1.405 m/sec
VOLUMETRIC FLOW RATE = 0.00906 m^3/sec
MASS FLOW RATE = 0.01104 kg/sec
ATMOSPHERIC PRESS. & TEMP: 30.24 in. Hg, 64.0 deg F
SLIT LOC. = 118 deg.
WIRE LOC. = 112 deg.
WIRE DIA. = 0.0125 in. Re_w = 43
SLIT DISTANCE FROM START OF CURVE (X) = 1.242 m
Re_x = 111,846
De = 167
Re_c = 1143 Re_h = 2231
KODAK RECORDING FILM ASA 1,000 (f2.8, B)

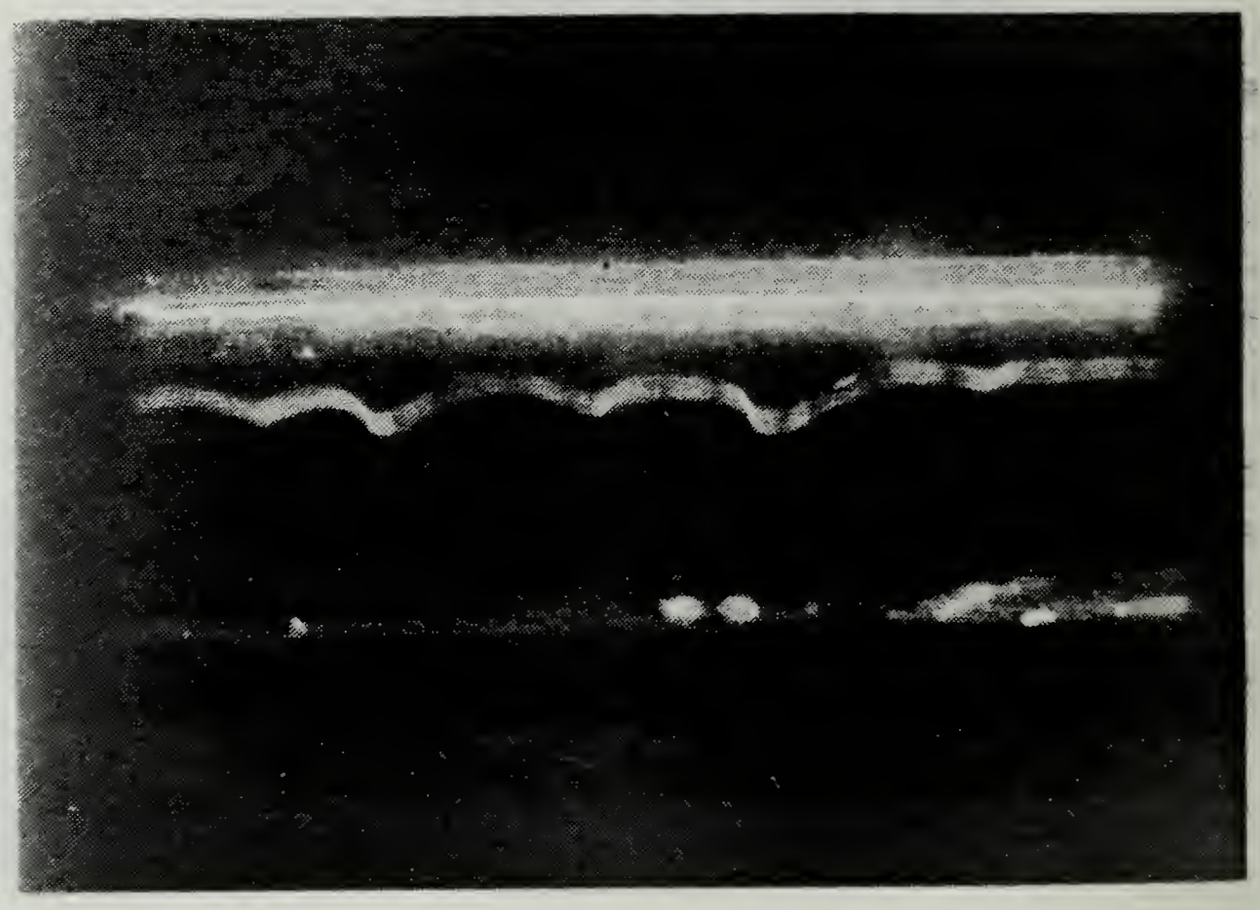

Figure C.34

IV-5 2100-2330 15 FEB 1987
9.0 % FLOW (rotameter)
MEAN AIR VELOCITY = 1.489 m/sec
VOLUMETRIC FLOW RATE = 0.00960 m^3/sec
MASS FLOW RATE = 0.01170 kg/sec
ATMOSPHERIC PRESS. & TEMP: 30.24 in. Hg, 64.0 deg F
SLIT LOC. = 118 deg.
WIRE LOC. = 112 deg.
WIRE DIA. = 0.0125 in. Re_w = 43
SLIT DISTANCE FROM START OF CURVE (X) = 1.242 m
Re_x = 118,546
De = 177
Re_c = 1212 Re_h = 2365
KODAK RECORDING FILM ASA 1,000 (f2.8, B)

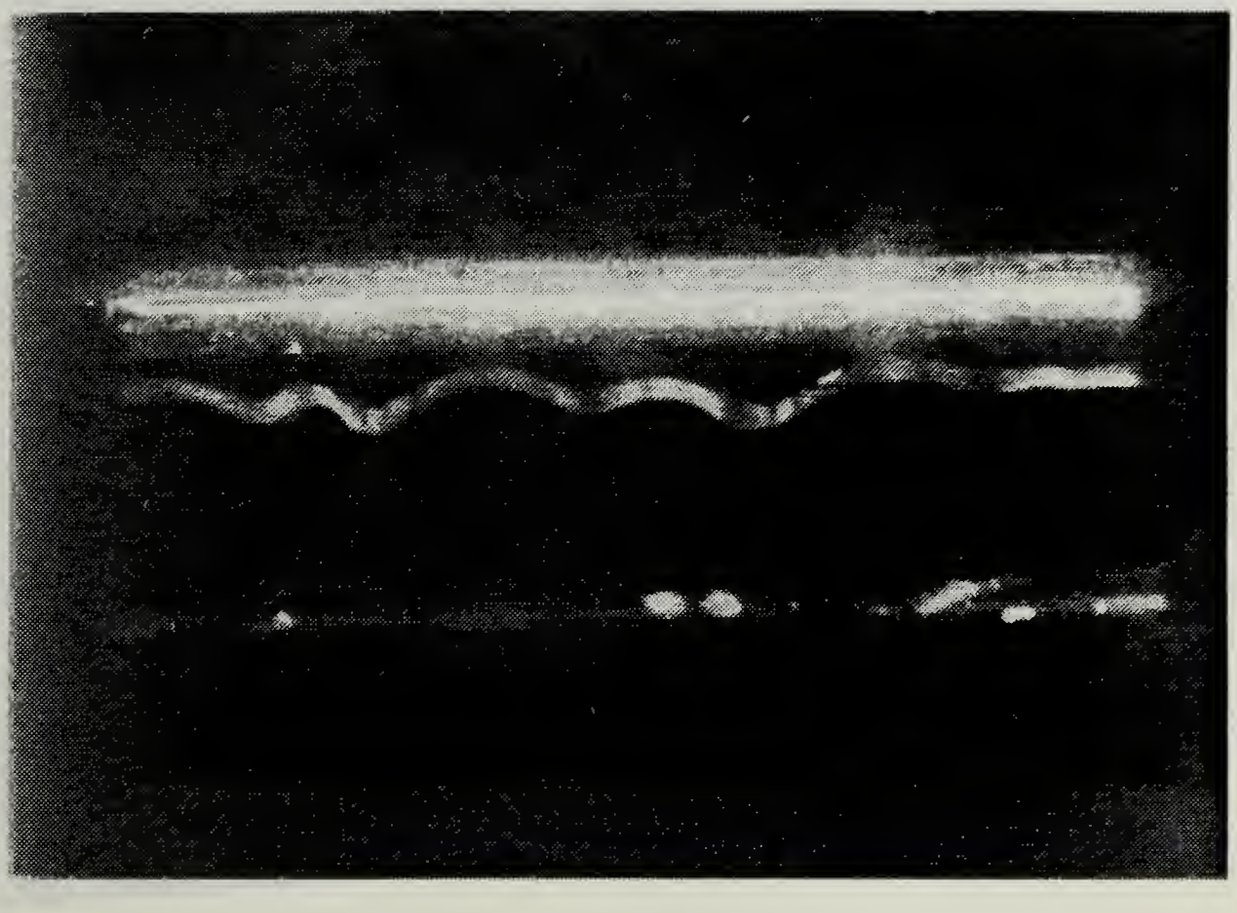

Figure C.35

IV-6 2100-2330 15 FEB 1987
9.0 % FLOW (rotameter)
MEAN AIR VELOCITY = 1.489 m/sec
VOLUMETRIC FLOW RATE = 0.00960 m^3/sec
MASS FLOW RATE = 0.01170 kg/sec
ATMOSPHERIC PRESS. & TEMP: 30.24 in. Hg, 64.0 deg F
SLIT LOC. = 118 deg.
WIRE LOC. = 112 deg.
WIRE DIA. = 0.0125 in. Re_w = 45
SLIT DISTANCE FROM START OF CURVE (X) = 1.242 m
Re_x = 118,546
De = 177
Re_c = 1212 Re_h = 2365
KODAK RECORDING FILM ASA 1,000 (f2.8, B)

Figure C.36

IV-7 2100-2330 15 FEB 1987
10.0 % FLOW (rotameter)
MEAN AIR VELOCITY = 1.573 m/sec
VOLUMETRIC FLOW RATE = 0.01015 m^3/sec
MASS FLOW RATE = 0.01236 kg/sec
ATMOSPHERIC PRESS. & TEMP: 30.24 in. Hg, 64.0 deg F
SLIT LOC. = 118 deg.
WIRE LOC. = 112 deg.
WIRE DIA. = 0.0125 in. Re_w = 48
SLIT DISTANCE FROM START OF CURVE (X) = 1.242 m
Re_x = 125,245
De^x = 187
Re_c = 1280 Re_h = 2487
KODAK RECORDING FILM ASA 1,000 (f2.8, B)

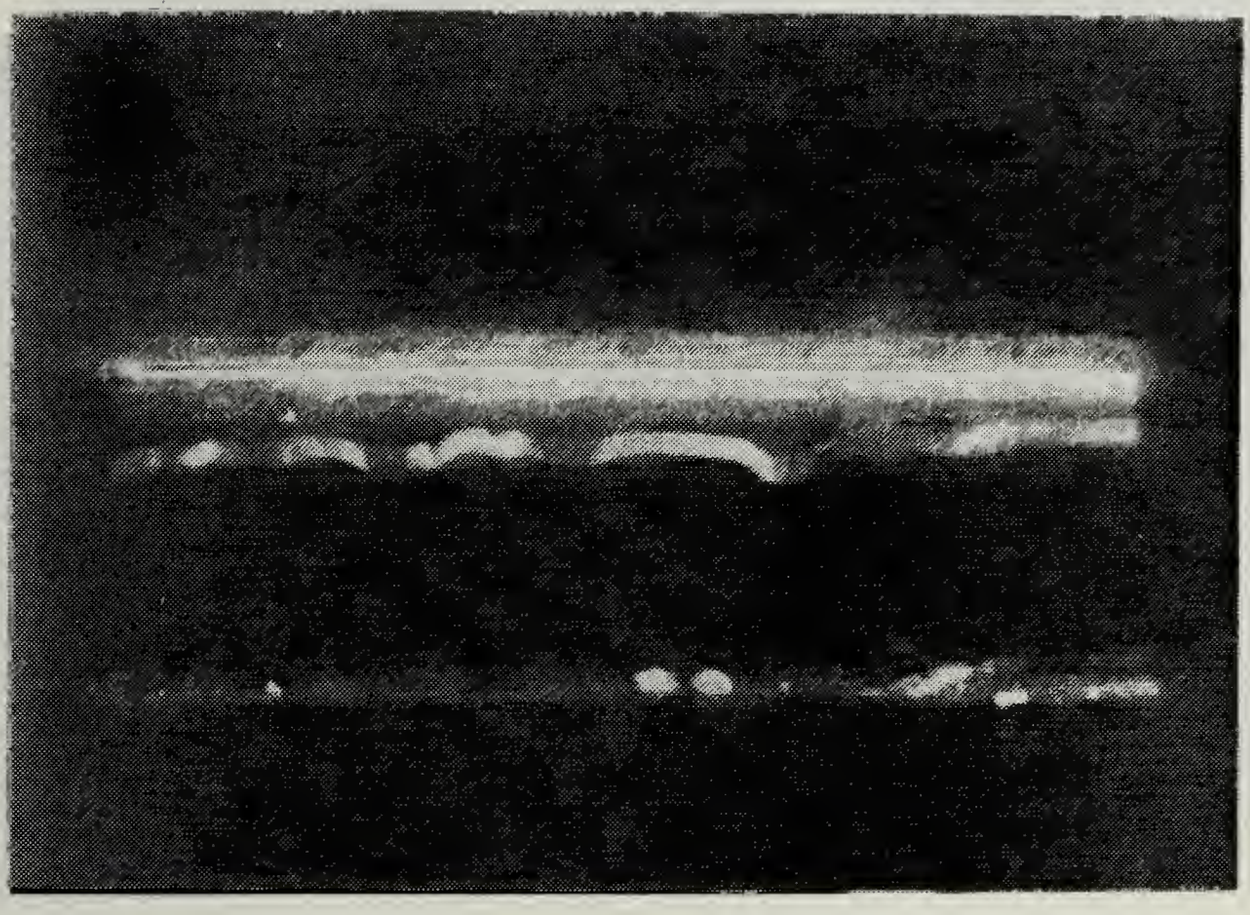

Figure C.37

IV-8 2100-2330 15 FEB 1987
10.0 % FLOW (rotameter)
MEAN AIR VELOCITY = 1.573 m/sec
VOLUMETRIC FLOW RATE = 0.01015 m^3/sec
MASS FLOW RATE = 0.01236 kg/sec
ATMOSPHERIC PRESS. & TEMP: 30.24 in. Hg, 64.0 deg F
SLIT LOC. = 118 deg.
WIRE LOC. = 112 deg.
WIRE DIA. = 0.0125 in. Re_w = 48
SLIT DISTANCE FROM START OF CURVE (X) = 1.242 m
Re_x = 125,245
De = 187
Re_c = 1280 Re_h = 2498
KODAK RECORDING FILM ASA 1,000 (f2.8, B)

Figure C.38

IV-9 2100-2330 15 FEB 1987
8.0 % FLOW (rotameter)
MEAN AIR VELOCITY = 1.405 m/sec
VOLUMETRIC FLOW RATE = 0.00906 m^3/sec
MASS FLOW RATE = 0.01104 kg/sec
ATMOSPHERIC PRESS. & TEMP: 30.24 in. Hg, 64.0 deg F
SLIT LOC. = 139 deg.
WIRE LOC. = 112 deg.
WIRE DIA. = 0.0125 in. Re_w = 43
SLIT DISTANCE FROM START OF CURVE (X) = 1.463 m
Re_x = 131,751
De = 167
Re_c = 1143 Re_h = 2231
KODAK RECORDING FILM ASA 1,000 (f2.8, B)

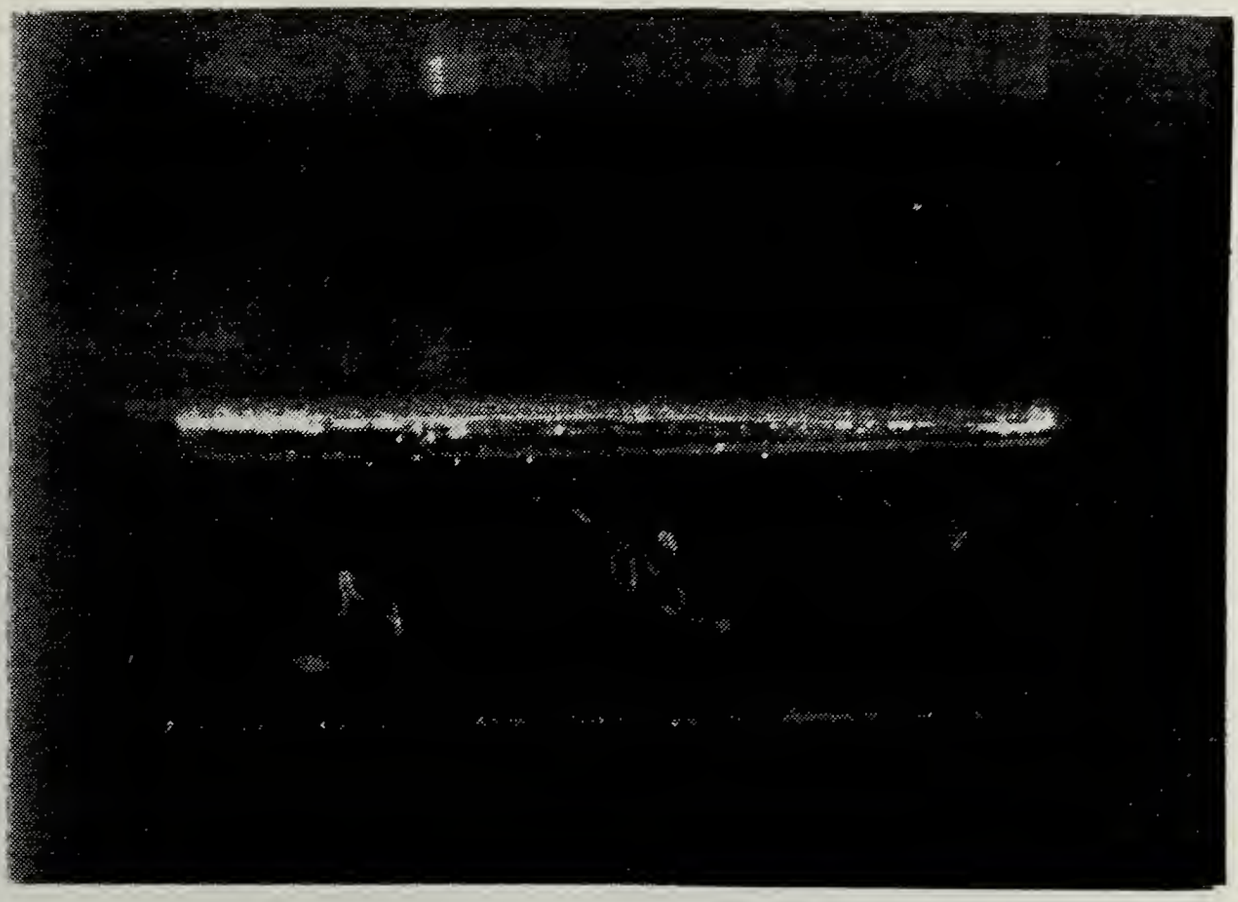

Figure C.39

IV-11 2100-2330 15 FEB 1987
8.0 % FLOW (rotameter)
MEAN AIR VELOCITY = 1.405 m/sec
VOLUMETRIC FLOW RATE = 0.00906 m^3/sec
MASS FLOW RATE = 0.01104 kg/sec
ATMOSPHERIC PRESS. & TEMP: 30.24 in. Hg, 64.0 deg F
SLIT LOC. = 139 deg.
WIRE LOC. = 112 deg.
WIRE DIA. = 0.0125 in. Re_w = 43
SLIT DISTANCE FROM START OF CURVE (X) = 1.463 m
Re_x = 131,751
De = 167
Re_c = 1143 Re_h = 2231
KODAK RECORDING FILM ASA 1,000 (f2.8, B)

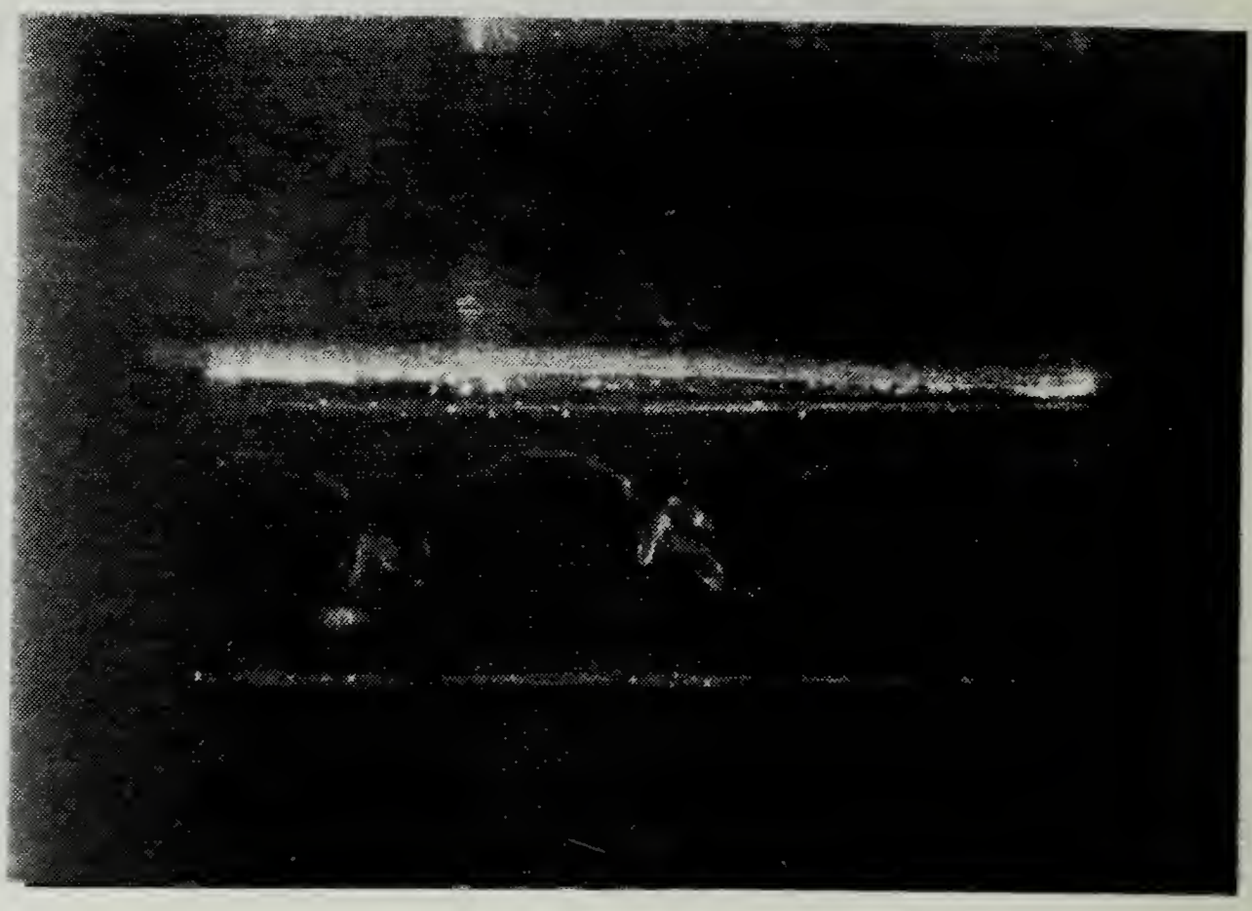

Figure C.40

IV-12 2100-2330 15 FEB 1987
8.0 % FLOW (rotameter)
MEAN AIR VELOCITY = 1.405 m/sec
VOLUMETRIC FLOW RATE = 0.00906 m^3/sec
MASS FLOW RATE = 0.01104 kg/sec
ATMOSPHERIC PRESS. & TEMP: 30.24 in. Hg, 64.0 deg F
SLIT LOC. = 139 deg.
WIRE LOC. = 112 deg.
WIRE DIA. = 0.0125 in. Re_w = 43
SLIT DISTANCE FROM START OF CURVE (X) = 1.463 m
Re_x = 131,751
De^x = 167
Re_c = 1143 Re_h = 2231
KODAK RECORDING FILM ASA 1,000 (f2.8, B)

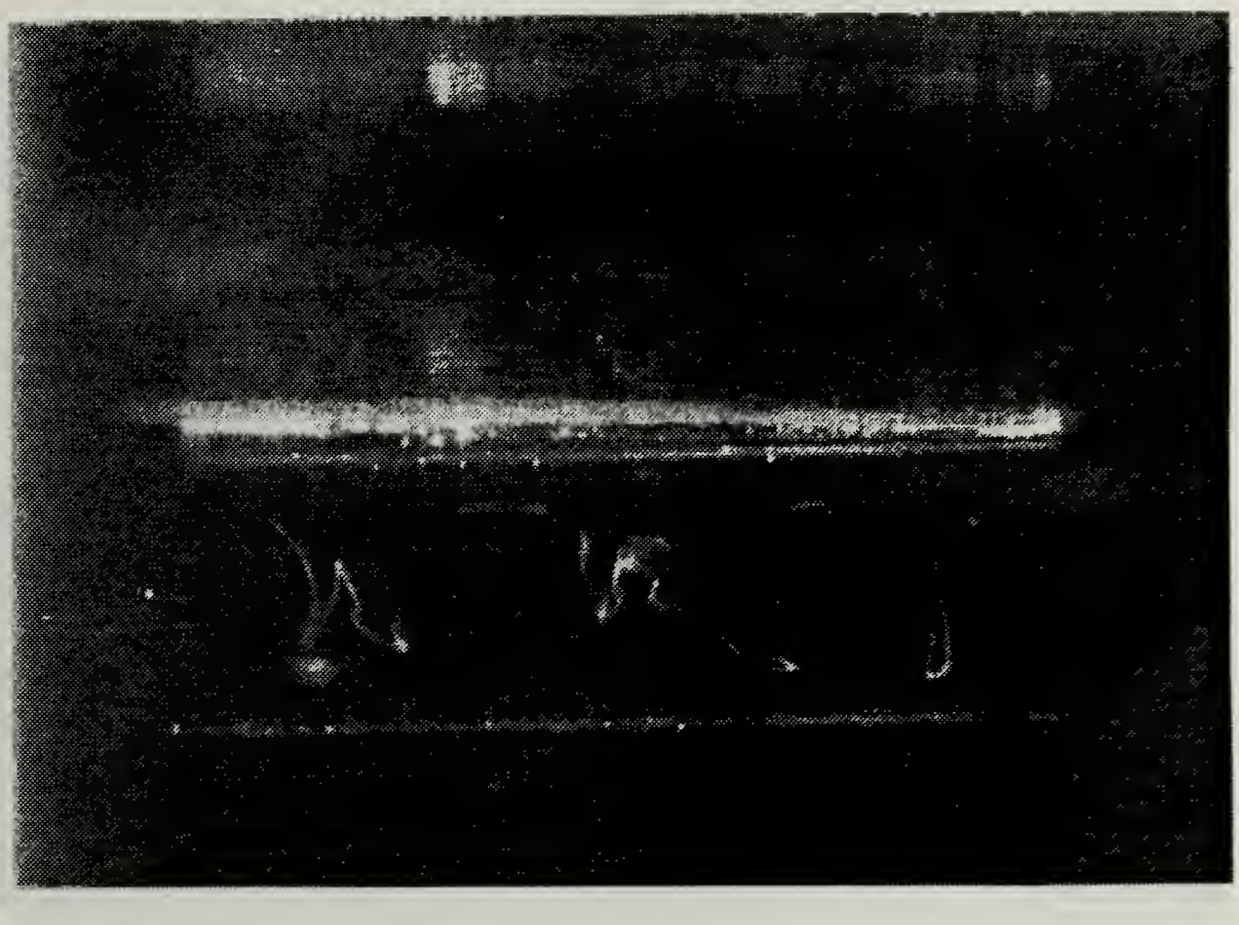

Figure C.41

IV-13 2100-2330 15 FEB 1987
9.0 % FLOW (rotameter)
MEAN AIR VELOCITY = 1.489 m/sec
VOLUMETRIC FLOW RATE = 0.00960 m^3/sec
MASS FLOW RATE = 0.01170 kg/sec
ATMOSPHERIC PRESS. & TEMP: 30.24 in. Hg, 64.0 deg F
SLIT LOC. = 139 deg.
WIRE LOC. = 112 deg.
WIRE DIA. = 0.0125 in. Re_w = 45
SLIT DISTANCE FROM START OF CURVE (X) = 1.463 m
Re_x = 139,643
De = 177
Re_c = 1212 Re_h = 2365
KODAK RECORDING FILM ASA 1,000 (f2.8, B)

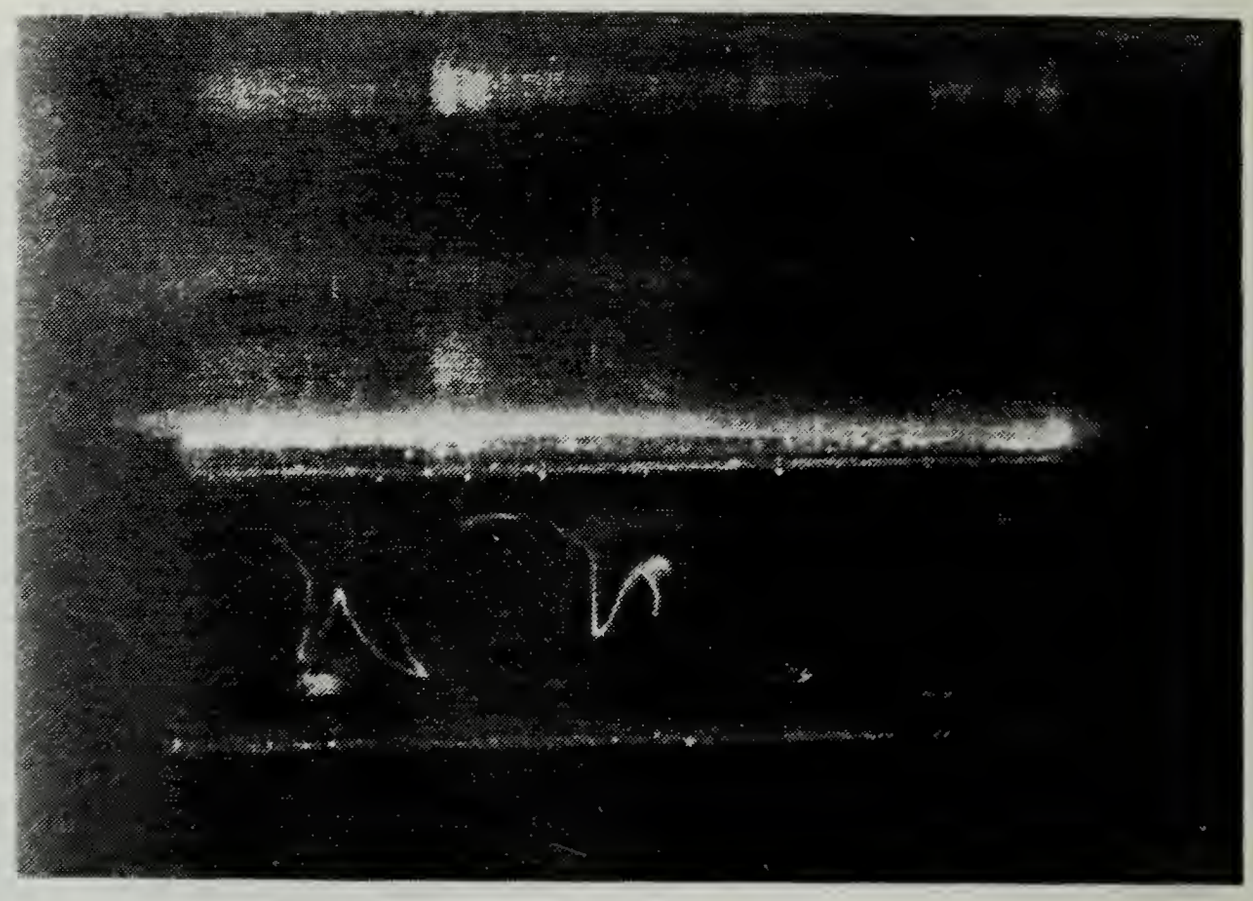

Figure C.42

IV-14 2100-2330 15 FEB 1987
9.0 % FLOW (rotameter)
MEAN AIR VELOCITY = 1.489 m/sec
VOLUMETRIC FLOW RATE = 0.00960 m^3/sec
MASS FLOW RATE = 0.01170 kg/sec
ATMOSPHERIC PRESS. & TEMP: 30.24 in. Hg, 64.0 deg F
SLIT LOC. = 139 deg.
WIRE LOC. = 112 deg.
WIRE DIA. = 0.0125 in. Re_w = 45
SLIT DISTANCE FROM START OF CURVE (X) = 1.463 m
Re_x = 139,643
De = 177
Re_c = 1212 Re_h = 2365
KODAK RECORDING FILM ASA 1,000 (f2.8, B)

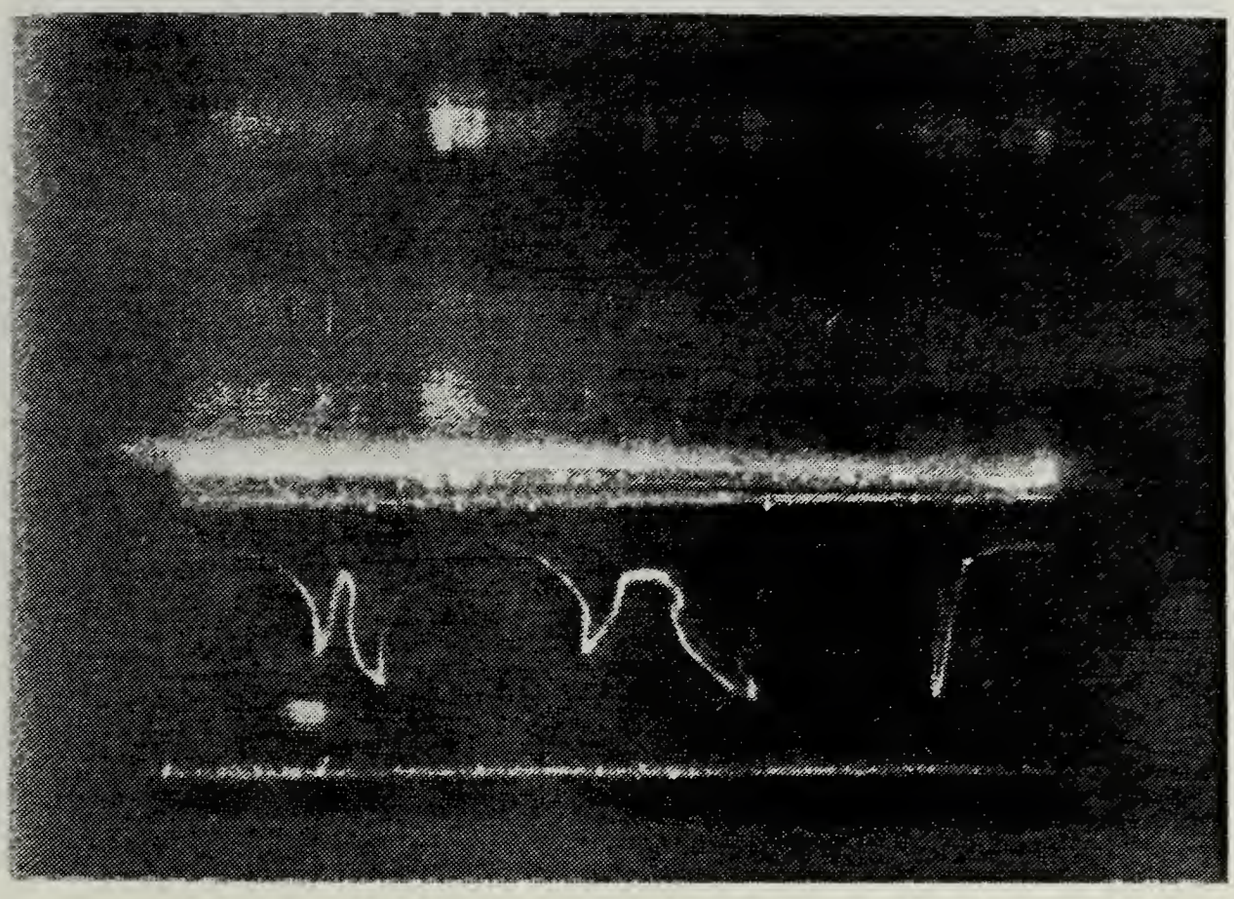

Figure C.43

IV-15 2100-2330 15 FEB 1987
10.0 % FLOW (rotameter)
MEAN AIR VELOCITY = 1.573 m/sec
VOLUMETRIC FLOW RATE = 0.01015 m^3/sec
MASS FLOW RATE = 0.01236 kg/sec
ATMOSPHERIC PRESS. & TEMP: 30.24 in. Hg, 64.0 deg F
SLIT LOC. = 139 deg.
WIRE LOC. = 112 deg.
WIRE DIA. = 0.0125 in. Re_w = 48
SLIT DISTANCE FROM START OF CURVE (X) = 1.463 m
Re_x = 147,534
De^x = 187
Re_c = 1280 Re_h = 2498
KODAK RECORDING FILM ASA 1,000 (f2.8, B)

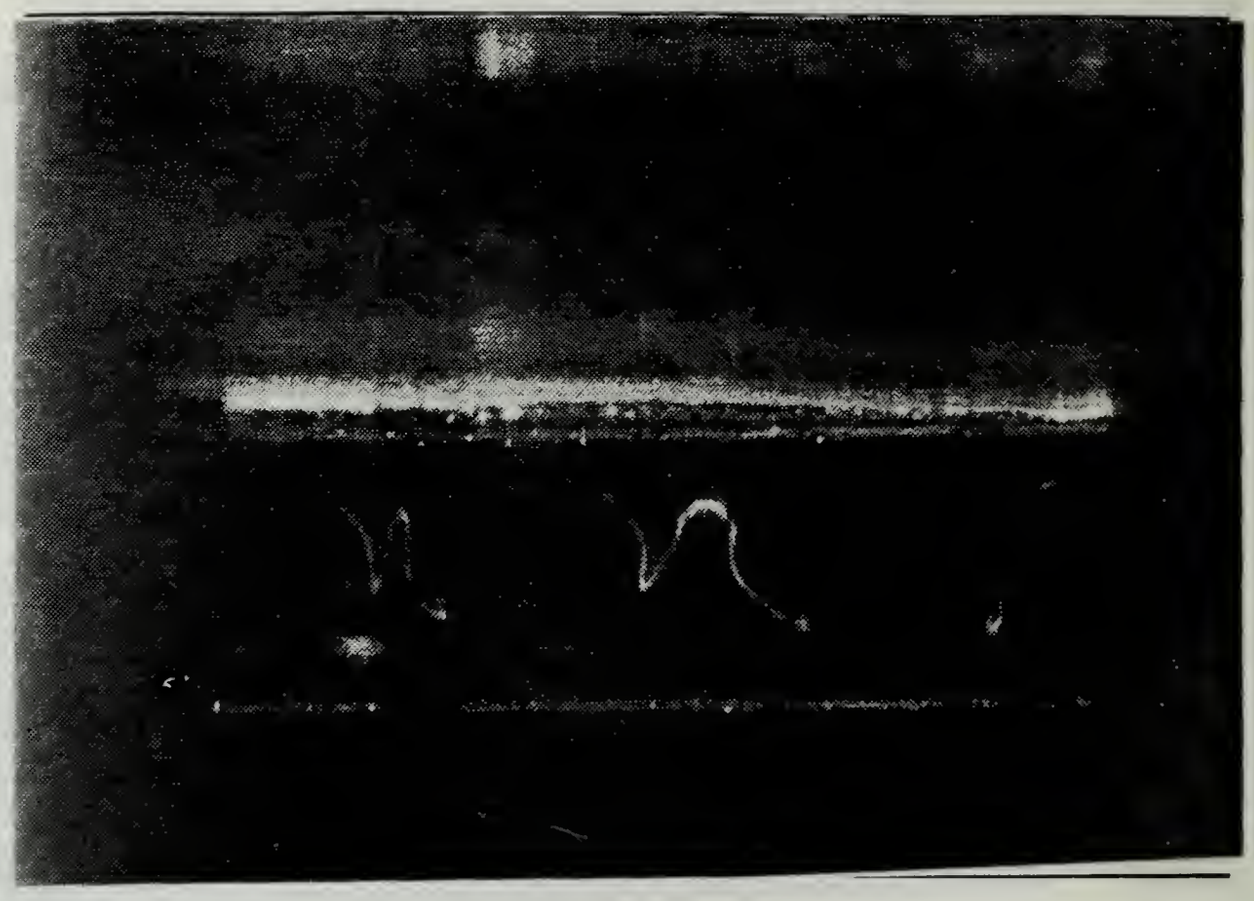

Figure C.44

IV-16 2100-2330 15 FEB 1987
10.0 % FLOW (rotameter)
MEAN AIR VELOCITY = 1.573 m/sec
VOLUMETRIC FLOW RATE = 0.01015 m^3/sec
MASS FLOW RATE = 0.01236 kg/sec
ATMOSPHERIC PRESS. & TEMP: 30.24 in. Hg, 64.0 deg F
SLIT LOC. = 139 deg.
WIRE LOC. = 112 deg.
WIRE DIA. = 0.0125 in. Re_w = 48
SLIT DISTANCE FROM START OF CURVE (X) = 1.463 m
Re_x = 147,534
De = 187
Re_c = 1280 Re_h = 2498
KODAK RECORDING FILM ASA 1,000 (f2.8, B)

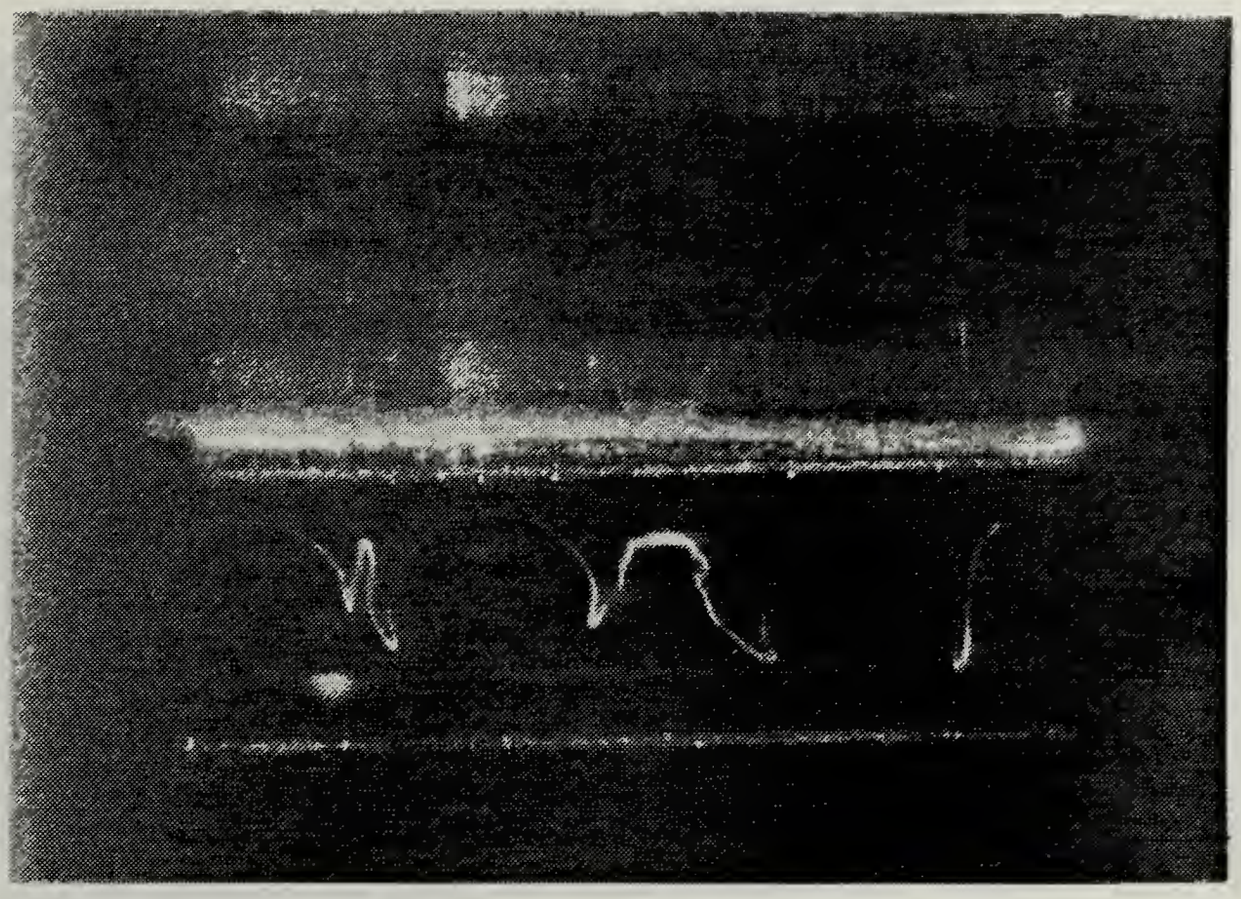

Figure C.45

IV-17 2100-2330 15 FEB 1987
11.0 % FLOW (rotameter)
MEAN AIR VELOCITY = 1.657 m/sec
VOLUMETRIC FLOW RATE = 0.01069 m^3/sec
MASS FLOW RATE = 0.01302 kg/sec
ATMOSPHERIC PRESS. & TEMP: 30.24 in. Hg, 64.0 deg F
SLIT LOC. = 139 deg.
WIRE LOC. = 112 deg.
WIRE DIA. = 0.0125 in. Re_w = 51
SLIT DISTANCE FROM START OF CURVE (X) = 1.463 m
Re_x = 155,425
De = 197
Re_c = 1349 Re_h = 2632
KODAK RECORDING FILM ASA 1,000 (f2.8, B)

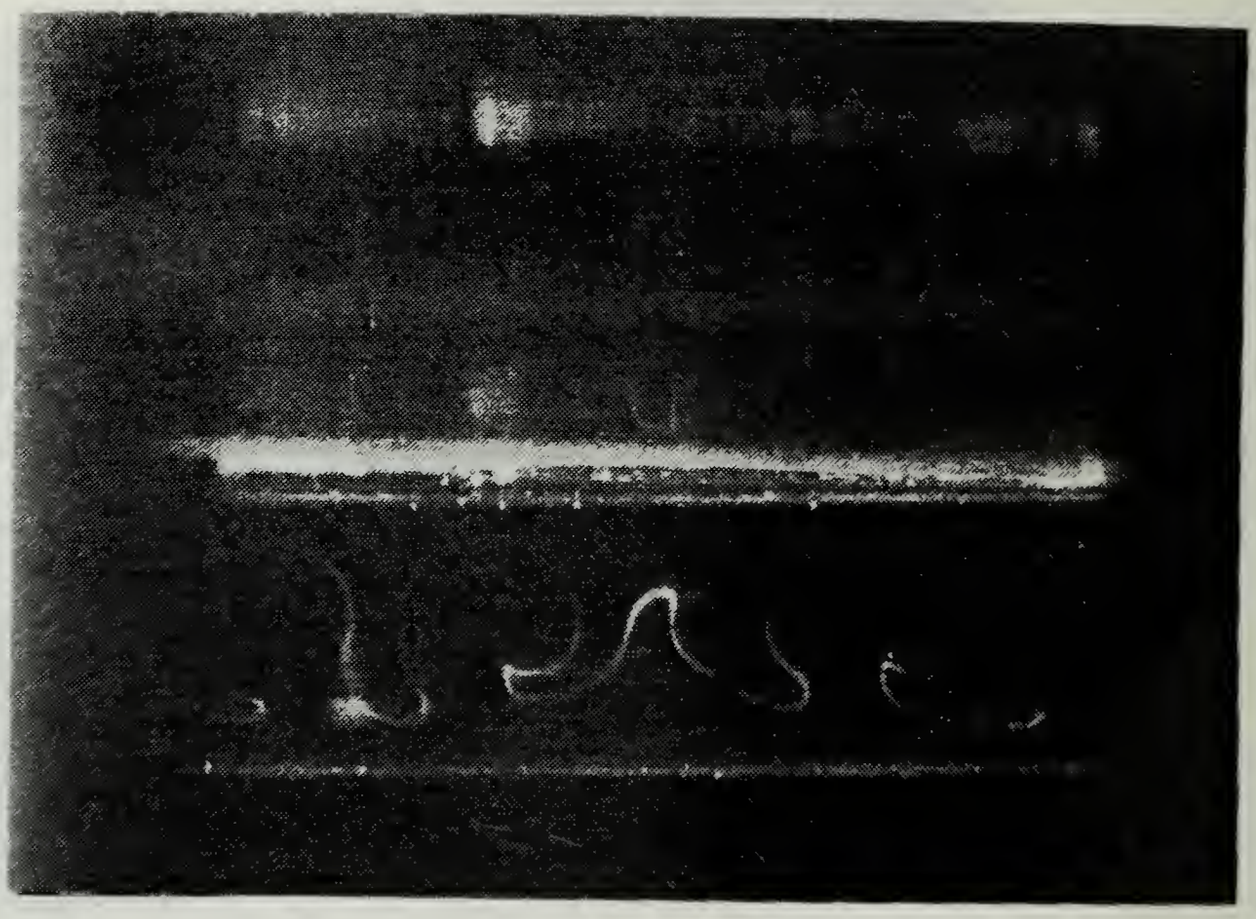

Figure C.46

IV-19 2100-2330 15 FEB 1987
12.0 % FLOW (rotameter)
MEAN AIR VELOCITY = 1.741 m/sec
VOLUMETRIC FLOW RATE = 0.01123 m^3/sec
MASS FLOW RATE = 0.01368 kg/sec
ATMOSPHERIC PRESS. & TEMP: 30.24 in. Hg, 64.0 deg F
SLIT LOC. = 139 deg.
WIRE LOC. = 112 deg.
WIRE DIA. = 0.0125 in. Re_w = 53
SLIT DISTANCE FROM START OF CURVE (X) = 1.463 m
Re_x = 163,317
De = 207
Re_c = 1417 Reh = 2766
KODAK RECORDING FILM ASA 1,000 (f2.8, B)

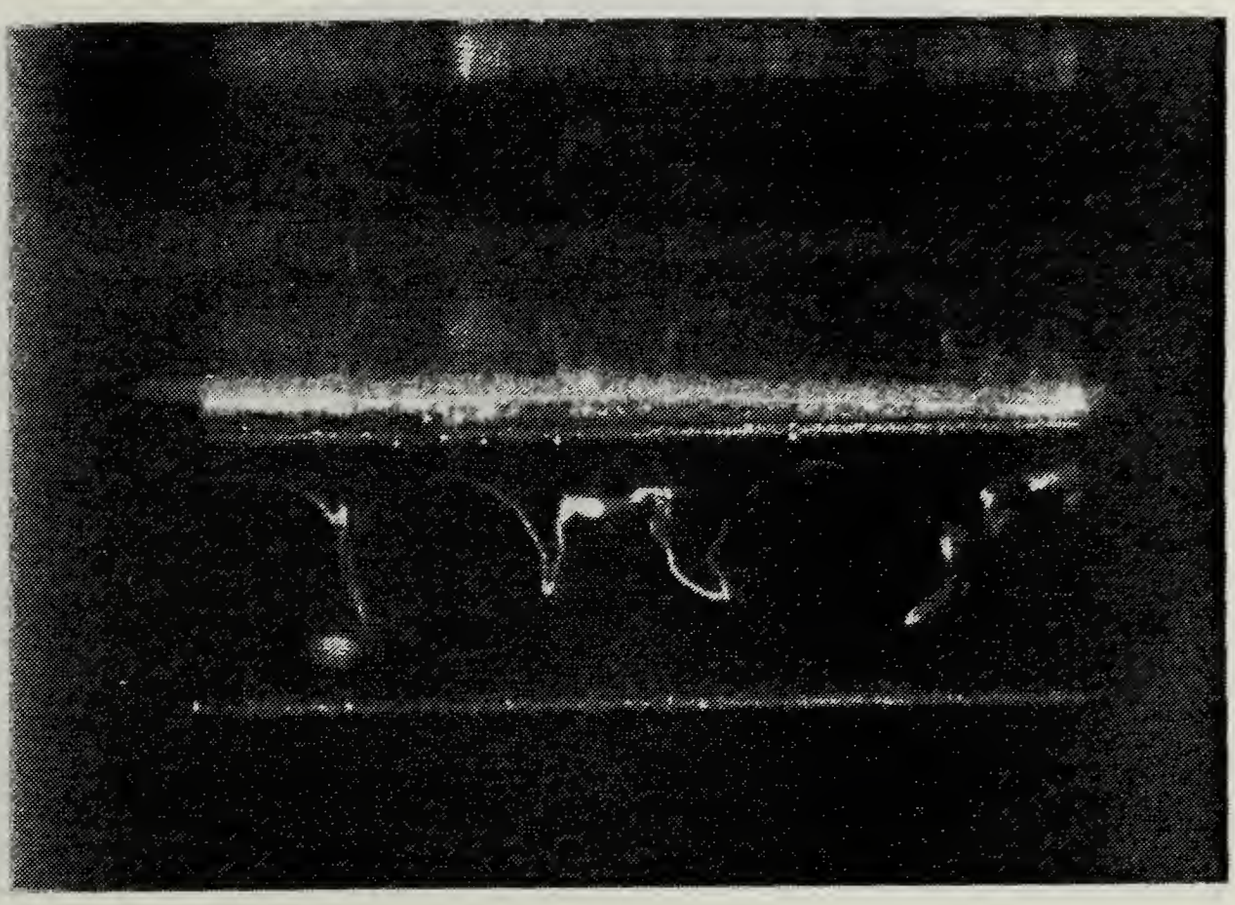

Figure C.47

IV-21 2100-2330 15 FEB 1987
13.0 % FLOW (rotameter)
MEAN AIR VELOCITY = 1.825 m/sec
VOLUMETRIC FLOW RATE = 0.01178 m^3/sec
MASS FLOW RATE = 0.01434 kg/sec
ATMOSPHERIC PRESS. & TEMP: 30.24 in. Hg, 64.0 deg F
SLIT LOC. = 139 deg.
WIRE LOC. = 112 deg.
WIRE DIA. = 0.0125 in. Re_w = 56
SLIT DISTANCE FROM START OF CURVE (X) = 1.463 m
Re_x = 171,208
De = 217
Re_c = 1486 Re_h = 2899
KODAK RECORDING FILM ASA 1,000 (f2.8, B)

Figure C.48

IV-23 2100-2300 15 FEB 1987
14.0 % FLOW (rotameter)
MEAN AIR VELOCITY = 1.909 m/sec
VOLUMETRIC FLOW RATE = 0.01232 m^3/sec
MASS FLOW RATE = 0.01501 kg/sec
ATMOSPHERIC PRESS. & TEMP: 30.24 in. Hg, 64.0 deg F
SLIT LOC. = 139 deg.
WIRE LOC. = 112 deg.
WIRE DIA. = 0.0125 in. Re_w = 58
SLIT DISTANCE FROM START OF CURVE (X) = 1.463 m
Re_x = 179,099
De = 227
Re_c = 1554 Re_h = 3033
KODAK RECORDING FILM ASA 1,000 (f2.8, B)

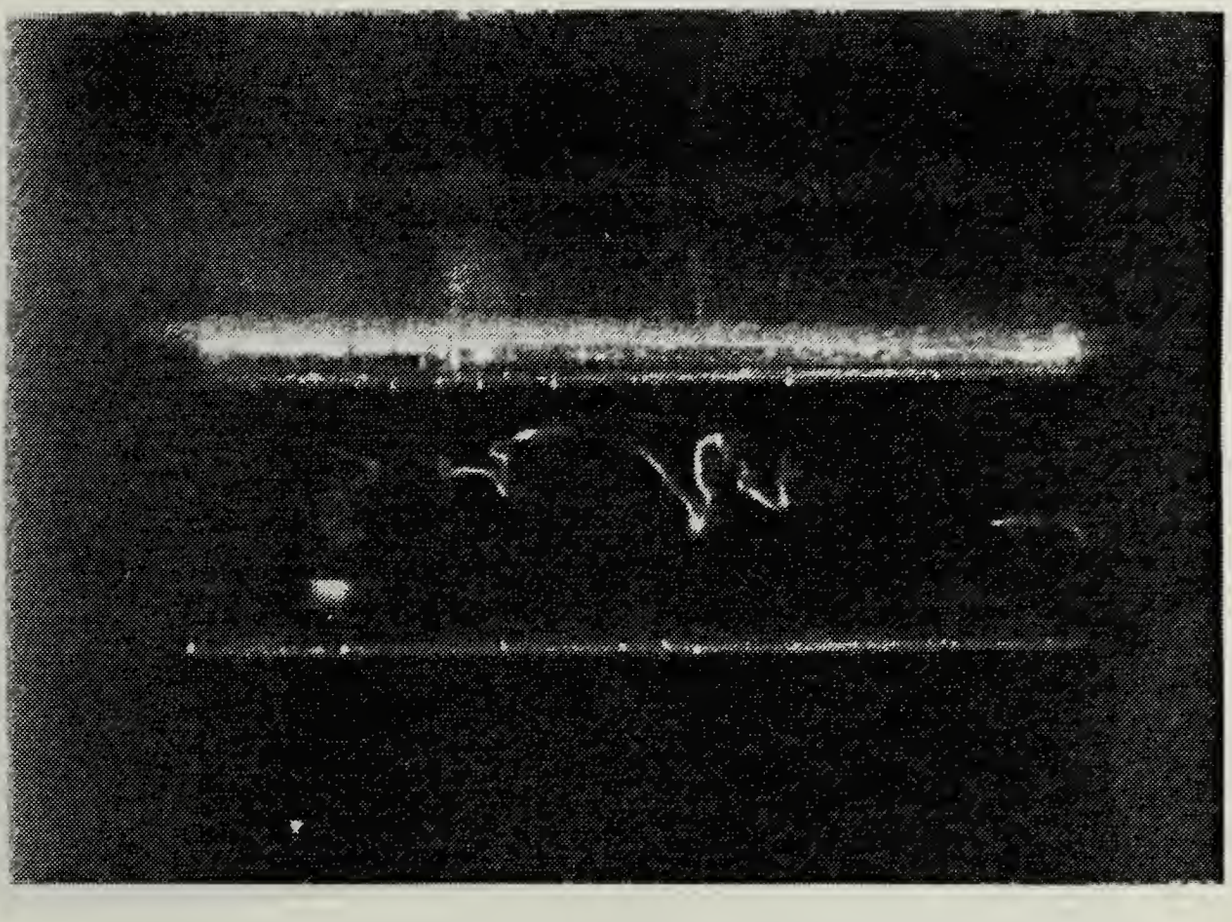

Figure C.49

IV-25 2100-2300 15 FEB 1987
15.0 % FLOW (rotameter)
MEAN AIR VELOCITY = 1.993 m/sec
VOLUMETRIC FLOW RATE = 0.01286 m^3/sec
MASS FLOW RATE = 0.01567 kg/sec
ATMOSPHERIC PRESS. & TEMP: 30.24 in. Hg, 64.0 deg F
SLIT LOC. = 139 deg.
WIRE LOC. = 112 deg.
WIRE DIA. = 0.0125 in. Re_w = 61
SLIT DISTANCE FROM START OF CURVE (X) = 1.463 m
Re_x = 186,99
De = 237
Re_c = 1623 Re_h = 3167
KODAK RECORDING FILM ASA 1,000 (f2.8, B)

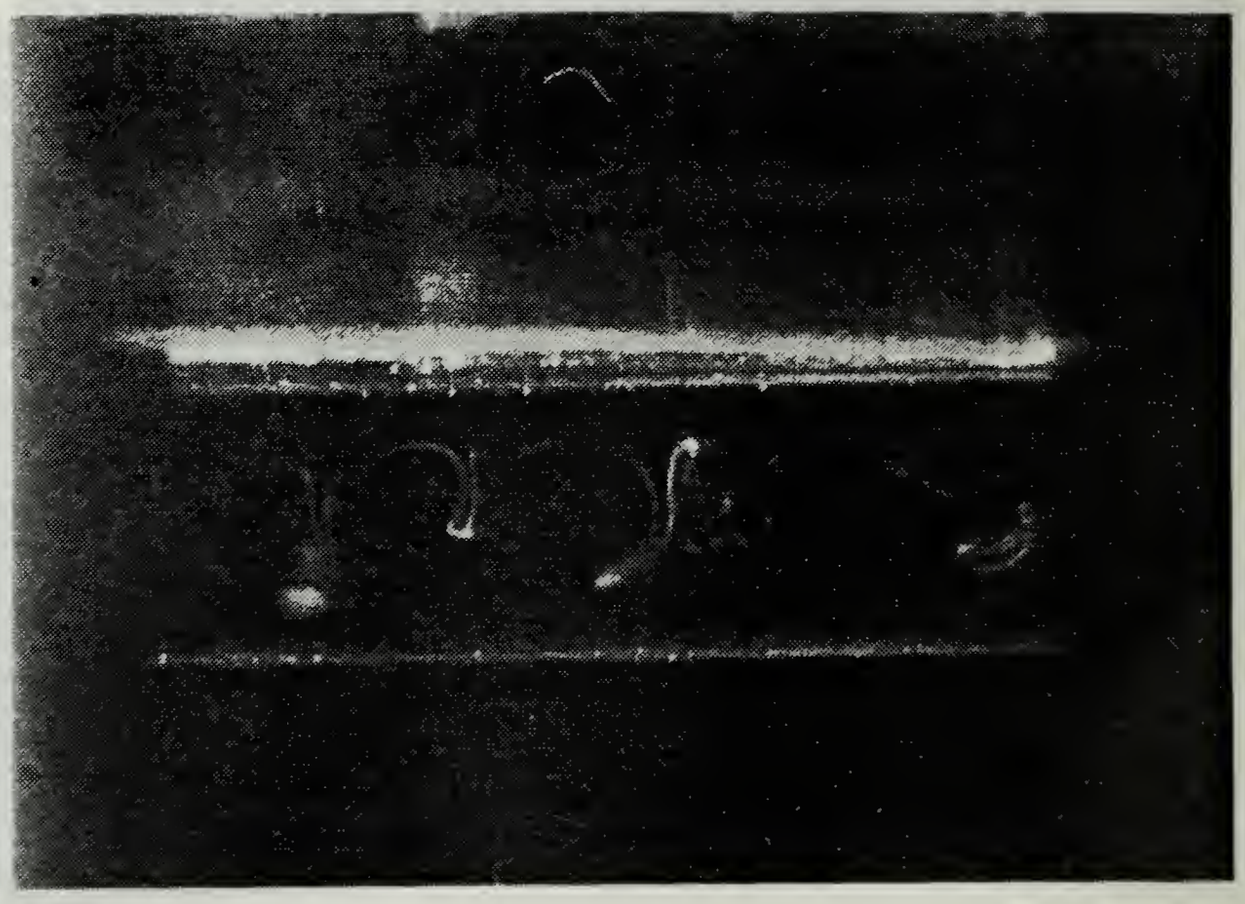

Figure C.50

IV-27 2100-2330 15 FEB 1987
15.0 % FLOW (rotameter)
MEAN AIR VELOCITY = 1.993 m/sec
VOLUMETRIC FLOW RATE = 0.01286 m^3/sec
MASS FLOW RATE = 0.01567 kg/sec
ATMOSPHERIC PRESS. & TEMP: 30.24 in. Hg, 64.0 deg F
SLIT LOC. = 139 deg.
WIRE LOC. = 112 deg.
WIRE DIA. = 0.0125 in. Re_w = 61
SLIT DISTANCE FROM START OF CURVE (X) = 1.463 m
Re_x = 186,991
De = 237
Re_c = 1623 Re_h = 3167
KODAK RECORDING FILM ASA 1,000 (f2.8, B)

LIST OF REFERENCES

1. Dean, W.R., "Fluid Motion in a Curved Channel," Proceedings of the Royal Society of London, Series A, Vol. 121, pp. 402-420, 1928.

2. Taylor, G.I., "Stability of a Viscous Liquid Contained Between Two Rotating Cylinders," Philosophical Transactions of the Royal Society of London, Series A, Vol. 223, pp. 289-343, 1923.

3. Göertler, H., "On the Three Dimensional Instability of Laminar Boundary Layers on Concave Walls," NACA TM 1375, 1942.

4. Holihan, R.G., Jr., Investigation of Heat Transfer in Straight and Curved Rectangular Ducts for Laminar and Transition Flows, Master's Thesis, Naval Postgraduate School, Monterey, California, June 1981.

5. McKee, R.J., An Experimental Study of Taylor-Göertler Vortices in a Rectangular Channel, Eng. Thesis, Naval Postgraduate School, Monterey, California, June 1973.

6. Durao, M. do Carmo, Investigation of Heat Transfer in Straight and Curved Rectangular Ducts Using Liquid Crystal Thermography, Eng. Thesis, Naval Postgraduate School, Monterey, California, June 1977.

7. Ballard, J.C. III, Investigation of Heat Transfer in Straight and Curved Rectangular Ducts, Master's Thesis, Naval Postgraduate School, Monterey, California, September 1980.

8. Daughety, S.F., Experimental Investigation of Turbulent Heat Transfer in Straight and Curved Rectangular Ducts, Master's Thesis, Naval Postgraduate School, Monterey, California, September 1983.

9. Wilson, J.L., Experimental Investigation of Turbulent Heat Transfer in Straight and Curved Rectangular Ducts, Master`s Thesis, Naval Postgraduate School, Monterey, California, December 1984.

10. Galyo, G.G., Experimental Investigation of Turbulent Heat Transfer in Straight and Curved Rectangular Ducts, Master's Thesis, Naval Postgraduate School, Monterey, California, December 1985.

11. Kelleher, M.D., Flentie, D.L., and McKee, R.J., "An Experimental Study of the Secondary Flow in a Curved Rectangular Channel," Journal of Fluids Engineering, Vol. 101, pp. 92-96, March 1980.

12. Finlay, W.H., Keller, J.B., and Ferziger, J.H., Finite Amplitude Vortices in Curved Channel Flow, Department of Mechanical Engineering, Stanford University, Stanford, California, 1986.

13. Mehta, R.D., and Bradshaw, P., "Design Rules for Small Low Speed Wind Tunnels," The Aeronautical Journal of the Royal Aeronautical Society, Vol. 83, pp. 443-449, November 1979.

14. Streeter, V.L., and Wylie, E.B., Fluid Mechanics, 8th edition, p. 189, McGraw Hill, 1985.

15. Han, L.S., "Hydrodynamic Entrance Lengths for Incompressible Laminar Flow in Rectangular Ducts," Journal of Applied Mechanics, Vol. 27, pp. 403-410, September 1960.

16. Fox, R.W., and Kline, S.J., "Flow Regime Data and Design Methods for Curved Subsonic Diffusers," Trans. ASME Journal of Basic Engineering, Ser. D., Vol. 84, pp. 303-312, 1962.

17. Schlichting, H., Boundary Layer Theory, 7th Edition, pp. 16-18, McGraw Hill, 1979.

18. Holman, J.P., and Gajda, W.J., Jr., Experimental Methods for Engineers, 4th Edition, pp. 238-247, McGraw Hill, 1984.

19. ASME Power Test Codes Committee, ASME Power Test Codes (Supplement on Instruments and Apparatus), part 5, Chapter 4, p. 25, American Society of Mechanical Engineers, 1959.

20. Westphal, R.V., Johnston, J.P., Eaton, J.K., Experimental Study of Flow Reattachment in a Single Sided Sudden Expansion, NASA Contractor Report 3765, pp. 187-194, January 1984.

INITIAL DISTRIBUTION LIST

		No. Copies
1.	Defense Technical Information Center Cameron Station Alexandria, Virginia 22304-6145	2
2.	Library, Code 0142 Naval Postgraduate School Monterey, California 93943-5002	2
3.	Department Chairman, Code 69 Department of Mechanical Engineering Naval Postgraduate School Monterey, California 93943	1
4.	Associate Professor P.M. Ligrani, Code 69Li Department of Mechanical Engineering Naval Postgraduate School Monterey, California 93943	6
5.	Mail Stop 5-11 Dr. Kestutis Civinskas Propulsion Directorate U.S. Army Aviation Research and Technology Activity - AVSCOM NASA - Lewis Research Center 21000 Brookpark Road Cleveland, Ohio 45433	4
6.	LCDR M. A. Siedband, USN 5821 Dorsett Dr. Madison, Wisconsin 53711	2

Thesis
S49334
c.1

Siedband
A flow visualization study of laminar/turbulent transition in a curved channel.